PURDUE UNIVERSITY

SCHOOL OF ELECTRICAL ENGINEERING

ELECTRONIC SYSTEMS RESEARCH LABORATORY

ANALOG COMMUNICATION OVER SELECTIVE FADING CHANNELS

by

John C. Lindenlaub, Principal Investigator

Dennis P. Murray

June, 1968

Lafayette, Indiana

Supported by

NATIONAL AERONAUTICS AND SPACE ADMINISTRATION

Washington, D. C.

Under

Grant NsG-553

FOREWORD

This report is an interim technical report which summarizes one phase of research being carried out at Purdue University in the area of communication theory under NASA Grant NsG-553.

The report deals with the problem of analog communication over a dispersive or multipath channel. This research is closely related to the studies of Lindenlaub and Bailey, "Digital Communication Systems Subject to Frequency Selective Fading," TR-EE67-17 and Hancock and Quincy, "Jointly Optimum Waveforms and Receivers for Channels with Memory," TR-EE66-7 which were also supported under this grant.

TABLE OF CONTENTS

		Page
LIST OF TABLES		vi
LIST OF FIGURES		vii
ABSTRACT		x
CHAPTER 1:	INTRODUCTION	1
1.1	Description of the Problem	1
1.2	The System Under Consideration	1
1.3	Channel Characterization	4
1.4	Known Dispersive Channels	5
1.5	Unknown Channels	7
1.6	Channel Measurement	8
1.7	Overall System Performance	9
1.8	Summary of the Report	10
CHAPTER 2:	OPTIMAL DEMODULATION FOR KNOWN DISPERSIVE CHANNELS	12
2.1	Mathematical Description of Selective Fading Channels	12
	Example Channels	15
	Single-Notch Selective Fading	18
2.2	Optimal Demodulation	19
	The MAP Estimate	21
2.3	The Mean Square Error Criterion	28
2.4	The Sampled-Data Formulation	31
2.5	Performance of Optimal Demodulators	35
	Analytical Results	38
	Numerical Results	43
CHAPTER 3:	SUBOPTIMAL DISPERSIVE CHANNEL DEMODULATORS	51
3.1	Optimal Demodulator Approximation	52
3.2	The Fourier Series Approximation	54
	Performance Analysis	59
3.3	The Minimum Mean-Square Equalizer	62

TABLE OF CONTENTS (Continued)

		Page
3.4	Approximate Demodulator Performance In the Presence of Noise	72
3.5	A Summary of Results for Known Dispersive Channel Demodulation	85
CHAPTER 4:	CHANNEL MEASUREMENT	92
4.1	Introduction	92
4.2	Channel Estimation Using the Information-Bearing Signal Alone	92
4.3	Channel Estimation Using Transmitted Reference Signals	99
4.4	Optimal Choice of Reference Signals	104
4.5	Design of Reference Signals	106
	Aperiodic Signals	108
	Periodic Reference Signals	113
4.6	Summary	117
CHAPTER 5:	DEMODULATOR PERFORMANCE FOR UNKNOWN DISPERSIVE CHANNELS	118
5.1	Assumptions	118
5.2	Exact Calculations of System Performance	121
5.3	Results of the Exact Calculations of System Performance	126
5.4	An Approximate Analysis of the Effect of Noisy Channel Measurements	143
5.5	The Infinite-Interval Approximation	148
5.6	Optimal Power Division	151
CHAPTER 6:	CONCLUDING REMARKS	155
6.1	Summary and Conclusions	155
6.2	Some Areas for Further Research	161
LIST OF REFERENCES		164
APPENDIX A:	DERIVATION OF THE MAP ESTIMATE	168
APPENDIX B:	THE EQUIVALENCE OF THE MAP AND MEAN SQUARE ERROR CRITERIA FOR LINEAR MODULATION	171
APPENDIX C:	EVALUATION OF THE OPTIMAL DEMODULATOR PERFORMANCE FOR SINGLE-NOTCH SELECTIVE FADING	174

TABLE OF CONTENTS (Continued)

Page

APPENDIX D: PN SEQUENCES WITH SMALL APERIODIC AUTOCORRELATION 182

LIST OF TABLES

Table		Page
2-1.	Impulse Responses for Example Channels	15
3-1.	System Performance for Single-Notch, Band-Edge Fading	80
3-2.	System Performance for Single-Notch, Center-Band Fading	81
3-3.	System Performance for Five Tap Example Channels	82
4-1.	Listing of Almost Uncorrelated Periodic Sequences	115
5-1.	System Performance Comparison for 7 dB Band-Edge Fading	134
5-2.	System Performance Comparison for 23 dB Band-Edge Fading	135
5-3.	System Performance Comparison for 7 dB Center-Band Fading	136
5-4.	System Performance Comparison for 23 dB Center-Band Fading	137

Appendix Table

C-1.	Parameter Definitions for the Matrix $\underline{\underline{Q}}$	176
D-1.	List of Aperiodic Pseudo-Noise Sequences	183
D-2.	Aperiodic Autocorrelation Functions for PN Sequences	184

LIST OF FIGURES

Figure		Page
1-1.	Dispersive Channel Communication System	2
2-1.	Frequency Response Functions for Example Channels	16
2-2.	Frequency Response Functions for Example Channels	17
2-3.	Transmitter and Channel Model	19
2-4.	Demodulator Block Diagram for Linear Modulation	24
2-5.	Demodulator Block Diagram for Angle Modulation	26
2-6.	Demodulator Performance for Single Notch Selective Fading	42
2-7.	Optimal Demodulator Performance for Single Notch Selective Fading	45
2-8.	Optimal Demodulator Performance for Example Channels 1, 3, and 5	46
2-9.	Optimal Demodulator Performance for Example Channels 2, 4, and 6	47
2-10.	Optimal Demodulator Performance for Example Channel 4	49
2-11.	Optimal Demodulator Performance for Example Channel 3	50
3-1.	Equalizer Performance for Single-Notch Selective Fading	68
3-2.	Optimal Equalizer Performance for Two-Root Channels	69

LIST OF FIGURES (Continued)

Figure		Page
3-3.	Equalizer Performance for Example Channels 1, 3, and 5	70
3-4.	Equalizer Performance for Example Channels 2, 4, and 6	71
3-5.	Equalizer Performance for Noisy, Single-Notch-Fading Channels	74
3-6.	Equalizer Performance for Noisy, Single-Notch Fading Channels	75
3-8.	Generalized Performance of Dispersive Channel Demodulators	88
4-1.	Autocorrelation Function of Optimal Reference Signal	106
4-2.	Channel Measurement System using Optimal Transmitted-Reference Signals	107
4-3.	Autocorrelation Function of Single Pulse	110
4-4.	Autocorrelation Function of Huffman Code	110
4-5.	Autocorrelation Function of Barker Code	110
4-6.	Autocorrelation Function of Generalized Barker Code	110
4-7.	Autocorrelation Function of Optimal, Periodic Ternary Sequence	114
4-8.	Autocorrelation Function of Periodic, Almost-Uncorrelated Binary Sequence	114
4-9.	Autocorrelation Function of Periodic, PN Sequence	114
5-1.	Optimal Demodulator Performance for 7 dB Band-Edge Fading	127
5-2.	Optimal Demodulator Performance for 23 dB Band-Edge Fading	128
5-3.	Optimal Equalizer Performance for 23 dB Band-Edge Fading (T_0=30 sec.)	129

LIST OF FIGURES (Continued)

Figure Page

5-4. Optimal Equalizer Performance for 23 dB Band-Edge Fading (T_0=10 sec.) 130

5-5. An Example of Transmitter Power Division 133

5-6. Overall Demodulator Performance Comparison for 7 dB Band-Edge Fading 139

5-7. Overall Demodulator Performance Comparison for 23 dB Band-Edge Fading 141

5-8. Overall Performance of Optimal Equalizers for 23 dB Band-Edge Fading 142

ABSTRACT

The purpose of this research has been to investigate the performance of demodulators for analog communication over slowly time-varying, frequency selective fading channels.

For known channels, demodulators optimal in the sense of maximum a-posteriori probability are derived for linear and angle modulation, but the resultant receiver structure for non-linear modulation is found to be impractical. A more fruitful approach considers optimal passband equalization of the transmitted signal based on minimum mean-square error. The performance of the demodulator optimal in this sense is investigated for certain examples of physical interest; it is found that selective fading causes an intrinsic loss in performance relative to non-fading channels, and that the length of the demodulator observation interval, directly related to system complexity, is a limiting factor whenever fading is severe.

Suboptimal approximations to the optimal demodulator consisting of a transversal equalizer followed by post-equalization filtering of various kinds are compared to the

optimal demodulator to determine whether these more easily implemented systems achieve near-optimal performance. It is concluded that the minimum mean-square error transversal equalizer with no post-equalization filtering is the most promising suboptimal system: it achieves near-optimal performance under low-noise conditions. For noisy channels, however, only the optimal demodulator performs well.

The investigation of channel equalization techniques leads to a simple method for estimating the effect of finite observation interval on system performance. An additional approximation based on the assymptotic behavior of the demodulator performance permits the effect of finite observation time to be isolated from effects due to noise, resulting in an approximate method for performance prediction which requires only simple calculations.

For unknown channels, methods for channel measurement are considered which use either the information-bearing signal alone to probe the channel or a transmitted reference signal multiplied with the message. In both cases optimal channel state estimates are presented, and in the latter case the optimization is carried out over the reference signal as well, including an extensive treatment of optimal and suboptimal signal design. It is found that the non-reference technique is impractical, but its consideration leads to a bound in the performance of any system subject to a constraint on transmitter power, a bound very nearly achieved by the optimal

transmitted reference system if the fading rate of the channel is much slower than the signalling bandwidth.

The effect of imperfect channel measurements on demodulator performance is investigated in an exact manner for the case of single-notch selective fading by means of a laborious numerical technique; this investigation includes a study of optimal transmitter power division. The results of these "exact" calculations point the way to a much simpler approximate technique for calculating, with reasonable accuracy, the effect of noisy channel measurements on system performance. This approximate analysis provides formulas which are the foundation of a simplified design procedure for predicting the overall performance of dispersive-channel communications systems in terms of some fundamental parameters of the channel and the system itself.

CHAPTER 1: INTRODUCTION

1.1 Description of the Problem

Many modern communications systems operate over channels which exhibit severe dispersive effects: transmitted waveforms are distorted in time and frequency by the channel. Dispersion might be caused by multiple transmission paths, as in H. F. ionospheric channels [1] or navigational satellite systems [3]. Reflection from an extended scatterer, such as lunar reflection [4], can cause dispersion, as can diffuse scatterers such as the ionosphere, troposphere, or meteor trials [2]. In any system of this sort the factor which fundamentally limits performance is distortion due to dispersion rather than additive fluctuation noise. The purpose of this research has been to analyze techniques for mitigating dispersion so that system performance may be improved. In particular, analog communications systems are considered. They are interesting in their own right for voice and telemetry communication, and they provide useful models for highly multiplexed digital systems as well.

1.2 The System Under Consideration

Figure 1-1 is a pictorial representation of the system investigated in this research. A message source, a(t), is

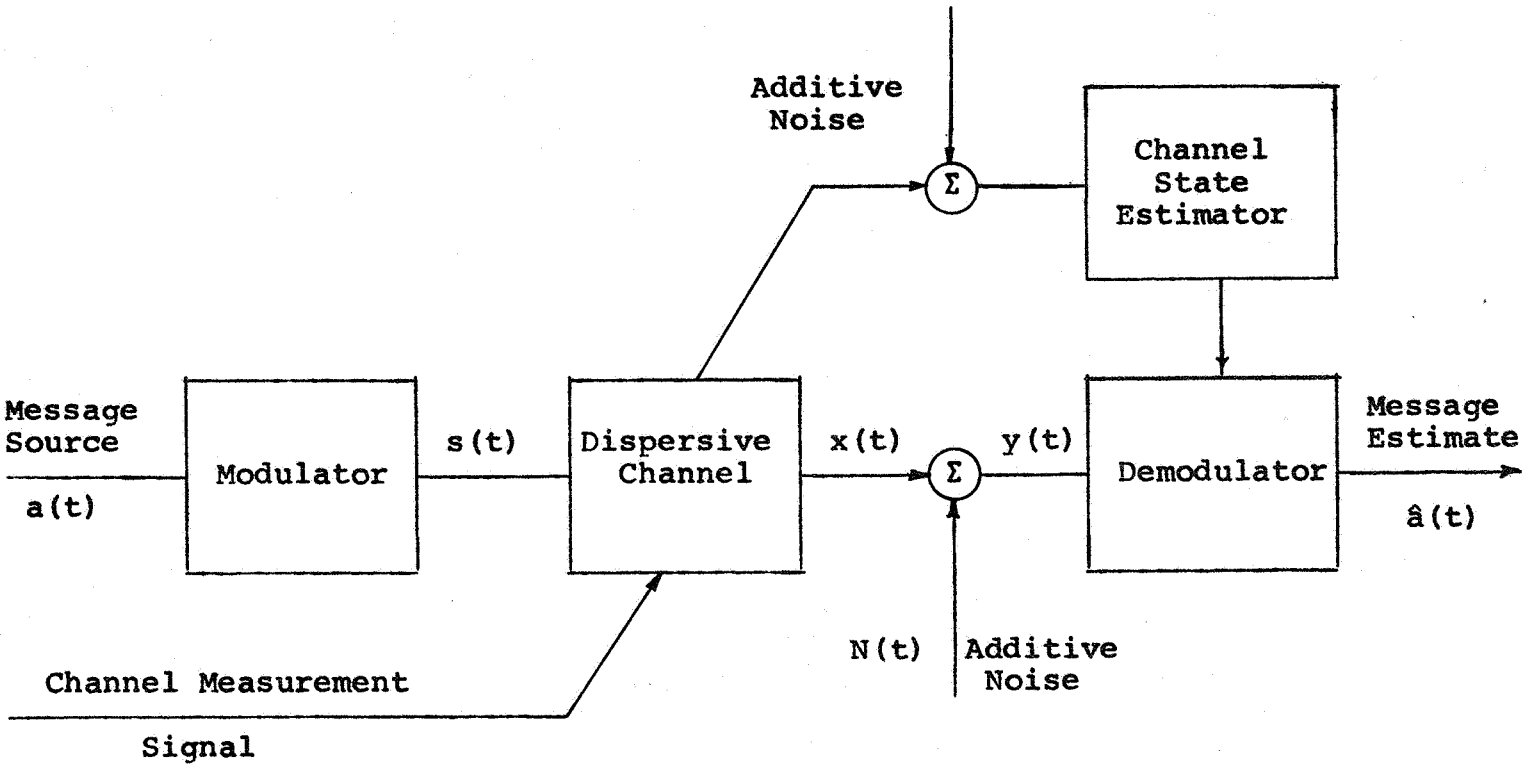

Figure 1-1. Dispersive Channel Communication System.

modeled by a stationary random process with known power spectrum. It is often convenient to assume also that this source is Gaussian. After modulation the resultant waveform, s(t), is passed through a dispersive channel and received in the presence of additive noise, N(t). The demodulator attempts to recover the message from the distorted channel output, y(t). If the state of the dispersive channel is unknown, it is necessary to measure it to demodulate efficiently. A measuring system is included for this purpose, the output of which controls channel-dependent parameters in the demodulator.

Many questions about this system are of interest:

1. How is the channel characterized?
2. For a given channel state, how is the received signal demodulated? Can an optimal demodulator be defined? If so, how well does it perform? How do practical, suboptimal demodulators compare to this performance? Can parameters which are fundamental to system performance be isolated?
3. If the channel is unknown, how can demodulation be performed? What is the performance of optimal methods? Does the use of a transmitted reference signal simplify the system? Can the channel measurement system and reference signal be jointly optimized? Are there simple schemes which are nearly optimal?

4. What is the effect of imperfect knowledge of the channel on demodulator performance? How can transmitter power be most profitably divided between message and reference signals?
5. What parameters are most important in characterizing overall system performance? Can the communication system be described by these parameters with sufficient accuracy to permit "first cut" system design using simplified methods?

This report is an attempt to answer these questions.

1.3 Channel Characterization

Dispersive communication channels, regardless of the physical origins of the dispersion, affect the signals passing through them in the same general way: an impulsive input will be dispersed in time, and a sinusoidal input will suffer spectral broadening. Since most channels used for communications (particularly electromagnetic channels) behave linearly [2], the channel is generally represented as a linear integral operation on its input, [1], [2], [5].

$$y(t) = \int_{-\infty}^{\infty} h(t,\xi)\, x(\xi)\, d\xi \qquad (1\text{-}1)$$

The channel is characterized by its time-varying impulse response, $h(t,\xi)$, or, equivalently, by its frequency response function, $H(\omega,t)$, [6].

$$H(\omega,t) = \int_{-\infty}^{\infty} h(t,\xi)\ e^{-j\omega\xi} d\xi \qquad (1\text{-}2)$$

In this research the time variation in the channel model is assumed to be slow with respect to the signalling bandwidth, usually the case in H. F. and troposcatter channels [1]. (If, as in orbital dipole channels [7], the rate of channel variation is greater than the signalling bandwidth, then the channel is not "measureable" [8] except in a statistical sense, and a waveform-dependent communication technique such as analog transmission would be useless.) This slow variation permits the use of a quasi-stationary channel model based upon a time-invariant impulse response valid in some time interval consistent with the channel fading rate. Channel time variations can then be accounted for by ensembles of time-invariant channel states, and the system will be independent of historical time.

For band-limited systems the tapped-delay-line approximation to the channel impulse response, [6], [9] through [13], is quite convenient and extensively used in this research.

1.4 Known Dispersive Channels

For channels modeled by known time-invariant impulse responses, the extension of well-known continuous estimation techniques, [14] through [17], to the case of complex random processes and post-nonlinearity system memory permits the derivation of analog demodulator structures optimal in the

sense of maximum a-posteriori probability. For linear modulation this criterion is shown to be equivalent to minimizing mean square error, and the resultant system is a form of Wiener-Hopf filter [18]. The performance of such a system in the case of an infinite observation interval bounds the performance of any physical demodulator. The dependence of this bound or parameters such as fading depth and SNR[1] is investigated for selective fading channels of physical interest. An interesting outcome of these calculations is that there is an intrinsic loss in performance which can be associated with selective fading channels relative to non-fading channels.

A sampled-data formulation of the problem permits investigation of the degradation of performance due to finite observation interval, an important parameter since it is directly related to system complexity. The resultant sampled data system is closely related in form to the equalization systems described by Tufts, [19] through [22], George [23], [24], and Niesson and Drouilhet [25] for digital communications. In the limit of high SNR these systems are equivalent to the minimum-mean-square error transversal equalizer of Lucky and Rudin [26]. Analysis of the performance of these closely related systems has led to some simple ways to predict the degradation due to finite observation time.

---

[1] Signal-to-Noise Ratio.

Simpler equalizers using a zero-forcing algorithm have been proposed by Lucky [27], [28], Ditoro [29], [30], and Schreiver [31]. These systems are compared to the optimal system to determine the conditions under which increased system complexity gives worthwhile performance gains.

1.5 Unknown Channels

When the selective fading channel is unknown, accuarate identification of the channel state is required to effectively demodulate the signal. This identification can in principle be made by observing the channel output when its input is a pure message-bearing signal, or the channel can be directly measured by transmitting a special reference signal for the purpose.

The first technique is desirable if the transmitter is power-limited since no transmitter power need be diverted to channel measurement. This no-reference method has been effectively applied to digital communications systems, [25] through [28], [31], in which decision feedback may be used to provide a virtually noise-free local reference equivalent to a transmitted reference. However, for analog communication the required feedback operations are quite complex, and the resultant local reference is not at all noise-free. Van Trees [32] has derived a feedback-type demodulator, but it has non-causal elements in the feedback loop which make its physical mechanization in feedback form impossible without the use of ideal predictors. A non-feedback system,

theoretically realizable, is investigated in this report; the system is very non-linear, and exact performance analysis has proved intractable. However, this system is the starting point for derivation of the Cramér-Rao bound [33] through [35] for simultaneous channel-state and message estimation, so it is of theoretical interest.

Use of a transmitted reference signal to make channel measurements independent of modulation greatly simplifies the construction and analysis of the demodulator; these measurements are used to control channel-dependent parameters in a receiver of "estimator-correlator" form [36]. This technique has been applied to digital communications by several authors [27], [30], [36] through [39]. Chesler [40] proposed an analog communication system using pilot tones for channel measurement but did not analyze the performance of the system.

It is shown in this research that if the reference system is optimized, and some reasonable assumptions on channel stationarity are made, then the performance of an adaptive transmitted reference demodulator very nearly achieves the Cramer-Rao bound.

1.6 Channel Measurement

Estimation of channel state using a transmitted reference signal and the optimization of the measurements have been studied using different problem formulations by Root [8], Kailath [41], [42], and Turin [43]. In this report the problem is reformulated with the tapped delay line channel model

explicitly accounted for. The resultant estimator is particularly convenient for implementation, and permits an easy derivation of a necessary and sufficient condition for optimal reference signals. The design of reference signals is extensively discussed; optimal signals are found and compared in performance to easily-generated suboptimal signals such as PN sequences [44].

1.7 Overall System Performance

Error at the output of an adaptive, dispersive-channel demodulator arises from three sources:

1. Additive noise at the receiver input.
2. Residual distortion due to incomplete "equalization" of the dispersive channel.
3. "Mismatch" between the channel and demodulator caused by imperfect channel measurements.

For a communication system subject to constraints on parameters such as transmitter power, system complexity, or bandwidth-to-fading-rate ratio, these sources of error cannot be independently minimized; but there usually exists a choice of design parameters for which the total error is a minimum. A large part of this research has been an investigation of the effect on system performance of this choice of parameters, and a comparison of suboptimal systems to the bounds provided by optimal systems.

Equations which exactly describe the performance of the adaptive demodulators considered in this report were derived for the case of noisy channel measurements, and evaluated numerically for several cases of physical interest to give insight into the problem. These "exact" calculations are extremely difficult; the equations are of non-linear matrix form and require numerical integration. However, an approximation technique which effectively eliminates the non-linearity, resulting in vast simplifications, has been found to be in good agreement with the "exact" results. This simplified form permits one to make rapid estimates of system performance as a function of gross channel parameters such as bandwidth, fading-rate, severity of fading, and delay spread, and of fundamental design parameters such as SNR and observation time. A consequence of this simplified analysis is an analytical expression for optimally dividing transmitter power between message and reference signals which closely fits the results obtained by numerical optimization.

1.8 Summary of the Report

This report is devoted to comparison of various techniques for analog communication over selective fading channels to provide a basis for the efficient overall design of systems for this purpose.

Chapter 2 describes optimal methods for analog communication over dispersive channels under the condition that the channel state is known. The performance of such systems is

studied to provide bounds on the performance of any simpler systems operating over the same channel. Chapter 3 is a discussion of some suboptimal methods which have been proposed for communicating over dispersive channels. Their performance is analyzed and compared to the results of Chapter 2. Chapter 4 considers the measurement of unknown channels. Both transmitted-reference and non-reference estimators are investigated and compared to the Cramér-Rao bound for simultaneous estimation of channel and message. Optimal and suboptimal reference signal designs are discussed. Chapter 5 treats the effect of noisy channel measurements on demodulator performance and treats the problem of optimal transmitter power division. The results of numerical evaluation of the exact performance equations are presented, and an approximate analytical technique of reasonable accuracy discussed. Chapter 6 summarizes the main conclusions of the research and includes some suggestions for additional work.

CHAPTER 2: OPTIMAL DEMODULATION FOR KNOWN DISPERSIVE CHANNELS

In this chapter we consider optimal techniques for communicating over known dispersive channels when the channel state is known (or has been measured without error). After a brief discussion of channel modeling, the optimality criterion of maximum a-posteriori probability is investigated; and receiver structures for linear and phase modulation derived. Consideration of these structures indicates that a more practical approach to the demodulation problem is to use linear passband equalizers under a mean square error optimality criterion. General expressions for system performance are derived using Wiener-Hopf techniques for the case of infinite observation intervals, and sampled-data techniques for finite intervals. These expressions are evaluated for certain examples of physical interest, leading to some general observations about the assymptotic behavior of optimal anti-dispersion systems.

2.1 Mathematical Description of Selective Fading Channels

In section 1.3 it was assumed that the time variation of the channel was sufficiently slow compared to the signalling bandwidth that the channel frequency response could be

modeled by a time-invariant transfer function,[1] $H(j\omega)$, valid over a time interval consistent with the quasi-stationary assumption. If the signals transmitted over the channel are essentially band-limited to the frequency band, $-\pi W \leq \omega \leq \pi W$, then $H(j\omega)$ need be represented only over this same band. An exponential Fourier series can thus be used to approximate $H(j\omega)$; the mean square error with respect to uniform frequency weighting will be minimized for a finite approximation.

$$H(j\omega) = \sum_{k=-\infty}^{\infty} h_k e^{-jk\frac{\omega}{W}} \quad , \ |\omega| \leq \pi W \tag{2-1}$$

$$h_k = \frac{1}{2\pi W} \int_{-\pi W}^{\pi W} H(j\omega) e^{jk\frac{\omega}{W}} \, d\omega \quad . \tag{2-2}$$

The impulse response of the equivalent bandlimited channel becomes

$$h(t) = \sum_{k=-\infty}^{\infty} h_k \delta\left[t - \frac{k}{W}\right] \quad , \tag{2-3}$$

resulting in the familiar tapped delay line channel model [6].

Since any physical channel will have an essentially time-limited impulse response, a nominal "delay spread," T_c, can be associated with the channel. T_c determines the number of terms in (2-1) or (2-3) required for adequate

---

[1] Throughout this report all signals, impulse responses, etc., will be assumed to be the pre-envelopes of the corresponding narrow band physical quantities (See reference [1], p. 285).

channel representation (i.e., $n_c \doteq WT_c$ delay elements are needed in the model).

All channels considered in this report will be assumed to be exactly represented by a finite number of terms, n_c. Thus,[1]

$$h(t) = \sum_{k=1}^{n_c} h_k \delta\left[t - \frac{k-1}{W}\right] \quad . \tag{2-4}$$

It is convenient to assume that all channels, regardless of the nature of their fading, are passive and dissipationless; this permits comparison of the effects due to different channel states independent of power considerations. The normalization condition

$$1 = \frac{1}{2\pi W} \int_{-\pi W}^{\pi W} |H(j\omega)|^2 \, d\omega = \sum_{k=1}^{n_c} |h_k|^2 \tag{2-5}$$

assures that signals with a flat spectrum have the same average power at both the input and output of the channel. It is also convenient to assume that time and frequency scaling has been performed to make the two-sided bandwidth of the system, 2W, equal to unity; the tap spacing in the channel model is then one second.

---

[1] It will be convenient at times to use a non-causal representation. Any fixed time advance required to make the channel causal will be lumped with the propagation delay.

Example Channels

The performance of demodulators for selective fading channels is quite sensitive to the state of the channel. It is impossible to consider all allowable channel states, so we are led to choose some examples of different channels on physical grounds, calculate performance, and then interpret the results as generally as possible on the basis of insight gained from the calculations.

The amount of fine-structure in frequency response which can be simulated by a delay line channel model depends upon the number of taps, n_c, used for representation. It has been found that five tap models generate reasonably realistic fading effects, so examples of this form were chosen to find the effect of various types of fading on demodulator performance. Six of these examples are referred to throughout the report: their impulse responses are given in Table 2-1, and Figure 2-1 and 2-2 show the corresponding frequency responses.

Table 2-1. Impulse Responses for Example Channels.

Channel No.	h_1	h_2	h_3	h_4	h_5
1	1.0	0.7	0.4	0.1	0.0
2	1.0	0.6	0.2	0.1	0.05
3	1.0	0.5	0.0	-0.5	-0.1
4	1.0	0.4	0.4	0.4	0.4
5	1.0	0.9	0.8	0.7	0.1
6	1.0	0.1	-0.5	0.2	-0.1

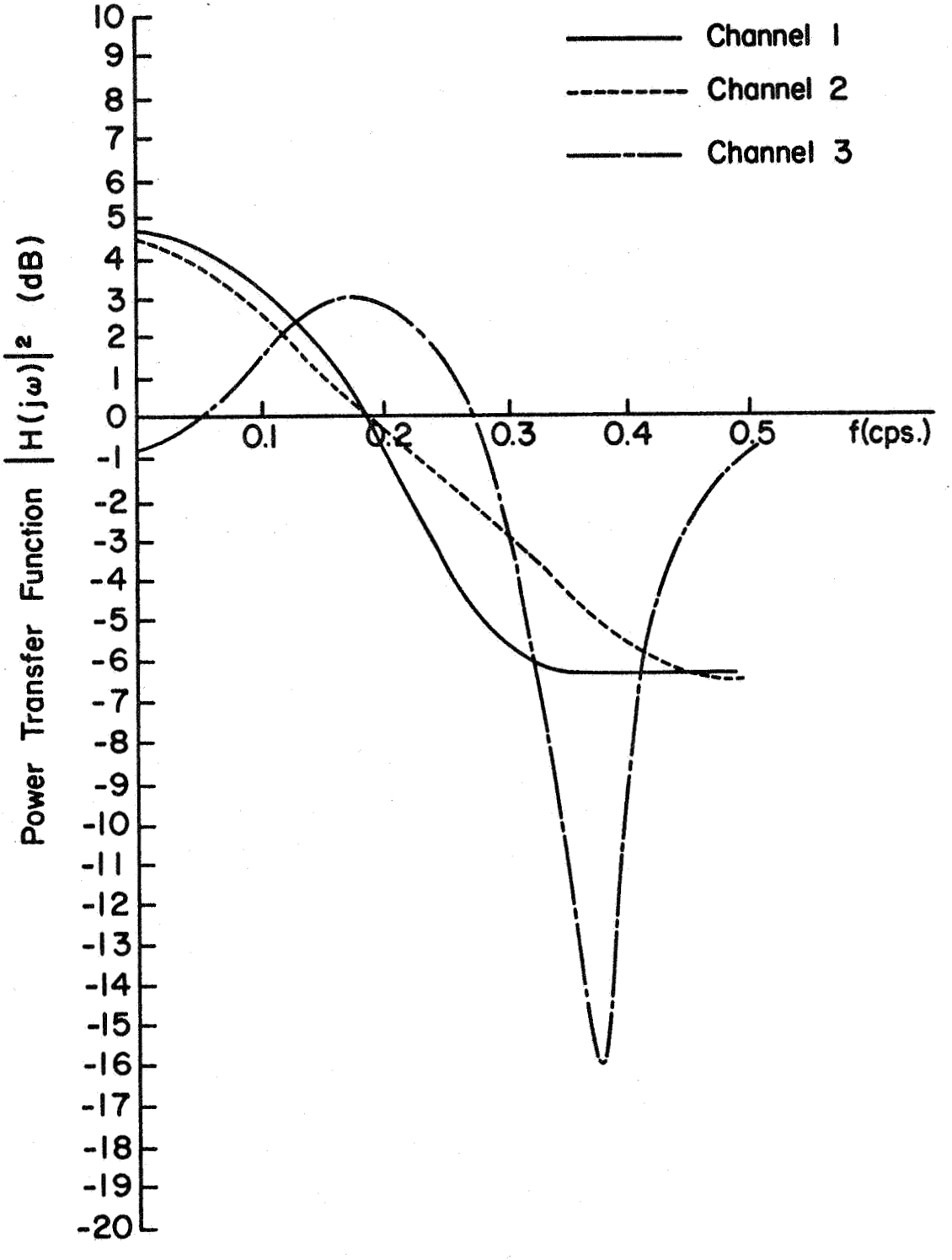

FIGURE 2-1. FREQUENCY RESPONSE FUNCTIONS FOR EXAMPLE CHANNELS (5 TAP).

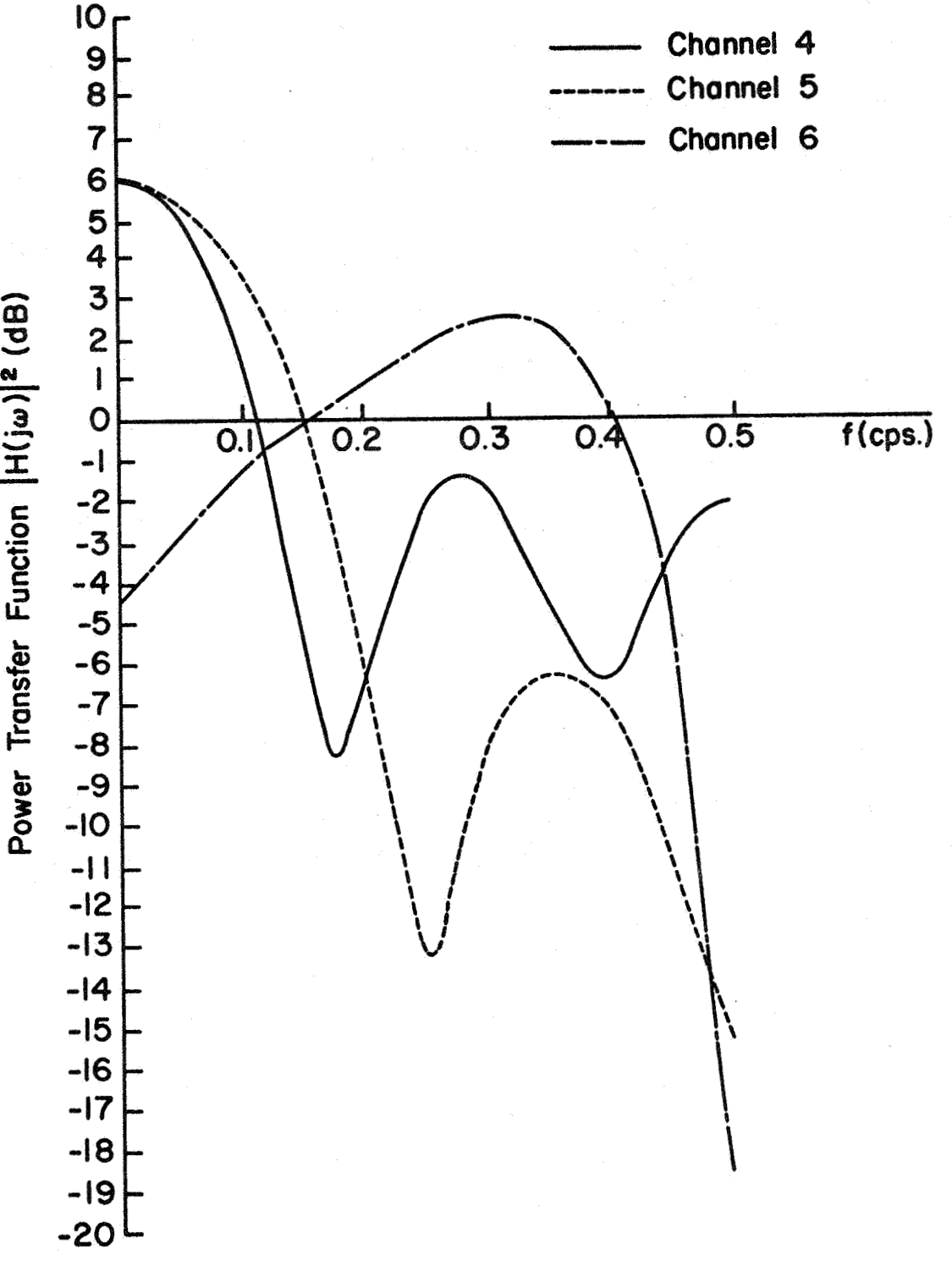

FIGURE 2-2. FREQUENCY RESPONSE FUNCTIONS FOR EXAMPLE CHANNELS (5 TAP).

For reasons of computational ease these examples have real tap-gain coefficients, which makes their bandpass frequency responses symmetrical about the carrier frequency. The loss in generality due to real coefficients is small because the Fourier series expansion for the bandpass channel could have been a one-sided one with the reference frequency taken at the lower edge of the passband; the resultant pre-envelope would then have been symmetrical.

Examination of Figures 2-1, 2-2, and Table 1-1 show channels 1 and 2 to be of the lowpass-filter variety, channel 1 having a sharper high-frequency cutoff than channel 2. Channel 3 has a single undershoot in its impulse response; and its spectrum exhibits a frequency-selective "notch." Channel 4 is an example of a channel with a long multipath-spread, its spectrum shows a double notch. Channel 5 illustrates the effect of severe, adjacent-multipath, and its frequency response has very deep fading. Channel 6 is an oscillatory channel; it shows a peaking effect in the passband, and an extreme fade at the band edge as well.

Examples such as these have provided a great deal of insight into effects caused by dispersive channels in general.

Single-Notch Selective Fading

The simplest possible model of selective fading consists of a single fading notch in the system passband. Only two taps in the channel model are required to simulate this effect. That is, if

$$H(j\omega) = 1 - \left[r\, e^{j\omega_0}\right] e^{-j\omega} \qquad (2\text{-}6)$$

then the channel frequency response has a single notch which appears at frequency ω_0 whose depth is controlled by the parameter, r. (As r→1 the fading depth goes to infinity; as r→0 the fading disappears.)

This simple model requires a minimum of computational complexity, and leads to satisfying physical interpretations of results which are not cluttered by second-order effects due to additional fine structure in the channel model.

2.2 Optimal Demodulation

The waveform observable by the demodulator, y(t), is produced by the system shown in Figure 2-3.

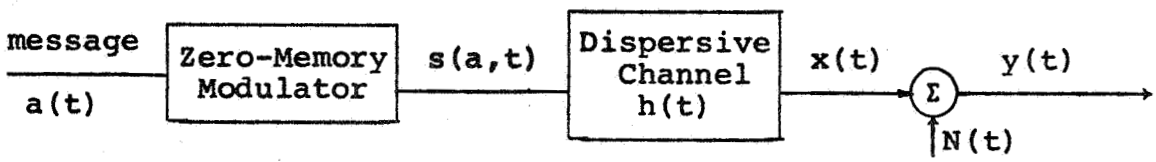

Figure 2-3. Transmitter and Channel Model.

The message, a(t), is assumed to be a zero-mean, stationary, Gaussian random process with known covariance. A zero-memory modulation step produces the signal s(a,t) which is transmitted over the dispersive channel, h(t). Additive, zero-mean, stationary Gaussian noise, N(t), perturbs the received signal; a(t) and N(t) are assumed to be statistically independent since they are generated by independent physical sources.

The purpose of the demodulator is to estimate the message given the observed channel output and any available a-priori statistical knowledge of the message. In finite dimensional estimation problems the technique of choosing the message estimate, $\hat{a}$, to be that value of a which maximizes the a-posteriori probability density function (the MAP criterion) is well known. Generalizations of this technique to the waveform estimation problem have been made by a number of authors, [14] through [16]. Their technique has been to reduce the random processes to coordinates using the Karhuren-Loéve expansion, find the MAP estimates based on a finite number of these coordinates, and generalize to the continuous case by formal limit-taking. The derivations are not rigorously justified, but the results are reasonable physically. A more straight forward approach is to use the notion of a probability density functional on a vector space of waveforms. Parzen[1] has shown that the vector space must be a reproducing kernel Hilbert space to make a valid definition of this functional, and considers several examples, one of which is directly applicable to the linear modulation case of this report. Although the extension to non-linear modulation is not obvious, this approach will be taken without proof to derive estimates in this section. The resultant estimator

---

[1]Parzen, E., "Probability Density Functionals and Reproducing Kernel Hilbert Spaces," Chapter 11 of Time Series Analysis, M. Rosenblatt, ed., John Wiley and Sons, New York, 1963.

agrees with the result obtained by applying Middleton's[1] orthogonal expansion for complex random processes to an extension of Williams' [16] work to the case of post-nonlinearity channel memory.

The MAP Estimate

If $\underline{a}$, $\underline{x}$, and $\underline{y}$ represent finite dimensional vectors whose components are time samples of the waveforms depicted in Figure 2-3, the a-posteriori density function $p(\underline{a}/\underline{y})$ can be written in the following way.[2, 3]

$$p(\underline{a}/\underline{y}) = \frac{p(\underline{y}/\underline{a})\ p_{\underline{a}}(\underline{a})}{p_{\underline{y}}(\underline{y})} = \frac{p_{\underline{N}}(\underline{y}-\underline{x})\ p_{\underline{a}}(\underline{a})}{p_{\underline{y}}(\underline{y})} \tag{2-7}$$

$$= K(\underline{y})\ \exp - \{(\underline{y}^*-\underline{x}^*)^T\ \underline{\underline{R}}_N^{-1}(\underline{y}-\underline{x}) +$$

$$+\ \underline{a}^{*T}\ \underline{\underline{R}}_a^{-1}\underline{a}\} \ .$$

$\underline{\underline{R}}_a$ and $\underline{\underline{R}}_N$ are the message and noise covariance operators, and $K(\underline{y})$ is a scalar function independent of the message, $\underline{a}$. The maximization of $p(\underline{a}/\underline{y})$ with respect to $\underline{a}$ is equivalent to minimizing the term in braces in (2-7). This term, call it ε^2, may be written in inner product form.

---

[1] Reference [5], p. 388.

[2] Notation: Vectors are denoted by single underscore, matrices by double underscore; transpose is denoted by superscript T, and complex conjugate by superscript *; lower case p stands for a probability density function.

[3] For a discussion of the density function for complex-envelope variables, see Wooding, R. A., "The Multivariate Distribution of Complex Normal Variables," Biometrika, Vol. 43, June, 1956.

$$\varepsilon^2 = \langle (\underline{y}-\underline{x}),\ \underline{\underline{R}}_N^{-1}\ (\underline{y}-\underline{x})\rangle + \langle a,\ \underline{\underline{R}}_a^{-1}\underline{a}\rangle \qquad (2\text{-}8)$$

The MAP criterion for the continuous case will be defined to be the formal extension of (2-8) to the vector space of continuous functions.

Suppose y(t) is observed over the time interval, T, of length T_0.

$$T = \{t:\ t_0 - T_0 \leq t \leq t_0\} \qquad (2\text{-}9)$$

Then, for a channel with delay spread T_c, y(t) depends upon a(t) for points of time in the interval T_a.

$$T_a = \{t:\ t_0 - T_0 - T_c \leq t \leq t_0\} \qquad (2\text{-}10)$$

Denoting the convolution operation by $\circledast$, ε^2 is written

$$\varepsilon^2 = \langle (y-x),\ R_N^{-1} \circledast (y-x)\rangle_T + \langle a,\ R_a^{-1} \circledast a\rangle_{T_a}$$

$$= \int_T \int_T R_N^{-1}(u-\tau)\,[y(u) - x(u)]\,[y(\tau) - x(\tau)]^*\,du\,d\tau$$

$$+ \int_{T_a} \int_{T_a} R_a^{-1}(\lambda-\tau)\ a(\lambda)\ a^*(\tau)\ d\lambda\,d\tau \quad . \qquad (2\text{-}11)$$

The functions $R_N^{-1}(.)$ and $R_a^{-1}(.)$ are the inverse covariance operators for noise and message, and they will be assumed to exist.[1] ε^2 can now be optimized with respect to

---

[1] For stationary random processes with rational power spectra, the inverse operator can be found in terms of generalized functions by the method in reference [5], Appendix E.

a(t) by the variational procedure of Appendix A. The resultant necessary condition on the estimate, $\hat{a}(t)$, of the message waveform is the integral equation

$$\hat{a}(t) = \int_T \{h^*(\tau) \circledast \left[\frac{\partial s^*}{\partial a}\bigg|_{a=\hat{a}} R_a^*(t-\tau)\right]\}d\tau$$

$$\cdot \int_T R_N^{*-1}(\tau-u)[y(u) - \hat{x}(u)]du, \qquad (2\text{-}12)$$

where

$$\hat{x}(t) = h(t) \circledast s(\hat{a},t) \quad . \qquad (2\text{-}13)$$

Equation (2-12) describes an estimation procedure which is physically unrealizable. However, it is possible to interpret this equation to give the structure of the demodulator or the type of operations required if we consider unrealizable filtering operations carried out over an infinite observation interval. Let us then assume that the set T of (2-9) is the entire real line, and also that the additive noise is essentially white with two-sided spectral density N_0, and examine the specific structure of the estimator, (2-12).

A. Linear Modulation, $s(t) = a(t)$. This case includes the possibilities of double-sideband A.M. (a(t) real), and single-sideband A.M. (the imaginary part of a(t) is the

Hilbert transform of the real part). Substituting into (2-12) we obtain[1]

$$\hat{a}(t) = \int_{-\infty}^{\infty} \{h^*(\tau) \circledast R_a^*(t-\tau)\} d\tau \int_{-\infty}^{\infty} \frac{1}{N_0} \delta(\tau-u)\,[y(u)-\hat{x}(u)]\,du$$

$$= \frac{1}{N_0} \int_{-\infty}^{\infty} R_{ax}(\tau-t)\,[y(\tau) - \hat{x}(\tau)]\,d\tau \qquad (2\text{-}14)$$

$$= \frac{1}{N_0} R_{xa}^*(t) \circledast [y(t) - \hat{x}(t)] \quad .$$

If $R_{xa}^*(t)$ is regarded as the impulse response of an unrealizable linear filter, the demodulator may be diagrammed as in Figure 2-4.

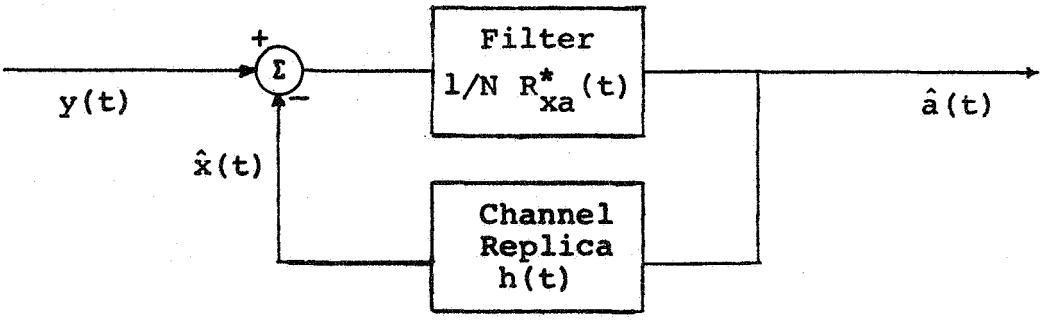

Figure 2-4. Demodulator Block Diagram for Linear Modulation.

Since most of this report is devoted to discussion of this system, it will not be treated in more detail here.

---

[1] $R_{xy}(t-\tau)$ denotes the crosscorrelation between two random processes, x(t) and y(t), i.e.

$$R_{xy}(t-\tau) = E[x(\tau)\, y^*(t)].$$

B. Angle Modulation, $s(t) = \sqrt{2A}\, e^{ja(t)}$. In this case a(t) may be assumed real, and, making use of the tapped delay line channel model, (2-4), the following relations are true.

$$\left.\frac{\partial s(a,t)}{\partial a}\right|_{a=\hat{a}} = j\sqrt{2A}\, e^{j\hat{a}(t)} \tag{2-15}$$

$$h^*(\tau) \circledast \left[\left.\frac{\partial s}{\partial a}(\tau)\right|_{a=\hat{a}} R_a(\tau-t)\right]^* =$$

$$= \int_{-\infty}^{\infty} \{\sum_{k=1}^{n_c} h_k^* \delta(\tau-\lambda-(k-1))\}\{\sqrt{2A}\, e^{-j\frac{\pi}{2}} e^{-j\hat{a}(\lambda)} R_a(\lambda-t)\}d\lambda$$

$$= \sqrt{2A}\, e^{-j\frac{\pi}{2}} \sum_{k=1}^{n_c} h_k^*\, e^{-j\hat{a}_k(\tau)}\, R_a(t-\tau+k-1) \tag{2-16}$$

$$\hat{a}_k(\tau) = \hat{a}(\tau - (k-1)) \tag{2-17}$$

Substituting into (2-12) we now obtain

$$\hat{a}(t) = \frac{1}{N_0}\int_{-\infty}^{\infty} \{\sqrt{2A}\, e^{-j\frac{\pi}{2}} \sum h_k^*\, e^{-j\hat{a}_k(\tau)} R_a(t-\tau+k-1)\}\{y(\tau)-\hat{x}(\tau)\}d\tau$$

$$= \sum_{k=1}^{n_c} f_k(t) \circledast \{e^{-j[\hat{a}_k(t)+\frac{\pi}{2}]}[y(t)-\hat{x}(t)]\}, \tag{2-18}$$

where

$$f_k(t) = \frac{\sqrt{2A}}{N_0} h_k^*\, R_a(t+k-1) \quad . \tag{2-19}$$

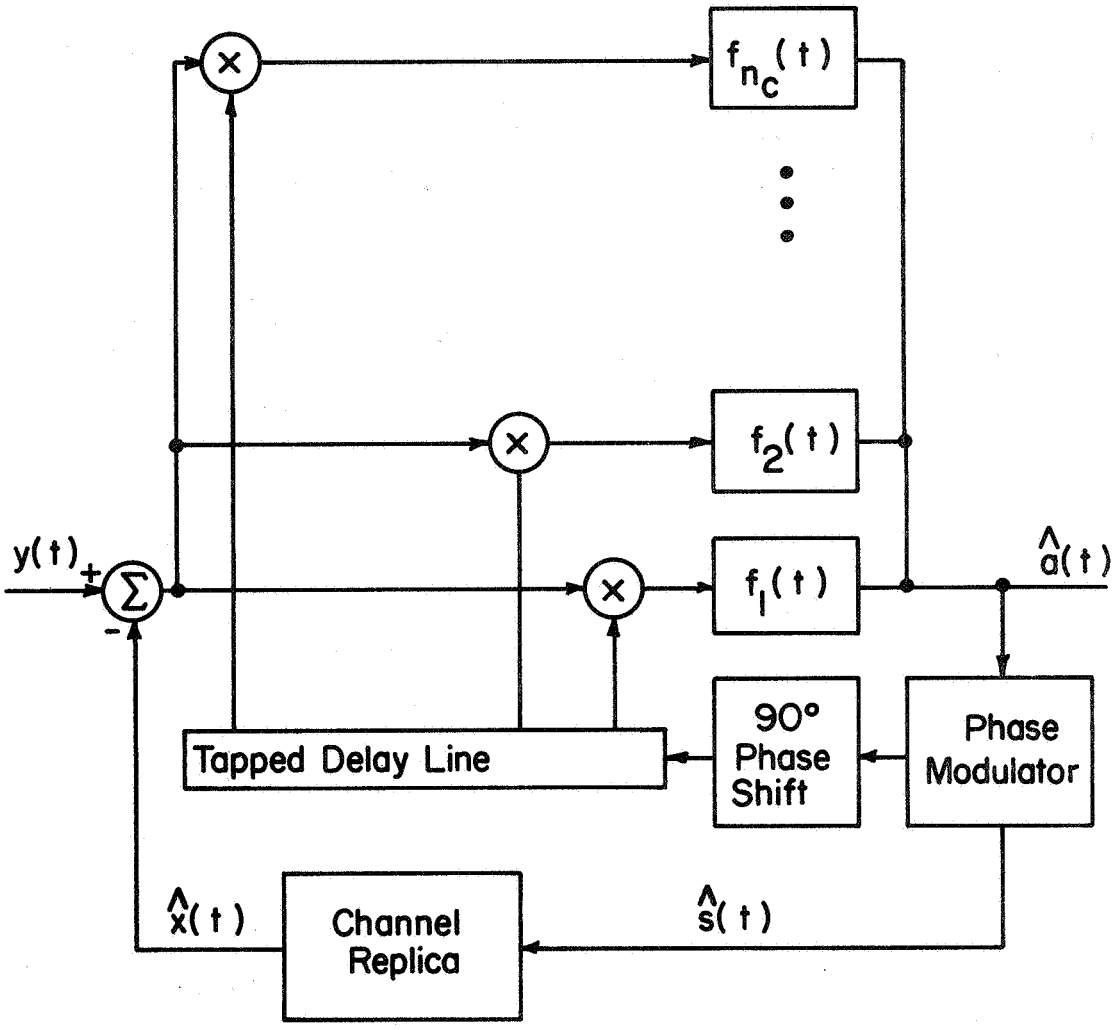

FIGURE 2-5. DEMODULATOR BLOCK DIAGRAM FOR ANGLE MODULATION.

Equation (2-18) can be block diagrammed as shown in Figure 2-5, a feedback demodulator differing from Van Trees' result [32] in that a bank of filters is required: Van Trees' needed only one filter because of his assumption of a zero-mean, purely random channel.

The structure of the receiver is seen to be in the form of a generalized phase-lock loop. The combinations of the multipliers and the 90°phase shifter give equivalent sinusoidal phase detectors. One input to each of the phase detectors is an appropriately delayed version of the receiver's estimate of what the transmitted signal s(t) is, so that the receiver is really trying to isolate each component of the incoming multipath, and to derive from this a correction signal to be applied to the phase modulator. This seems a logical thing to do.

However, the construction of such a receiver would be difficult because of the unrealizable nature of the block diagram. The feedback must be instantaneous in order to give the proper error signals from the phase detectors, but any physical delay line will cause a real delay of T_c seconds between the received signal and the estimate. This means we would have to build a system which predicts T_c seconds ahead of the input. Although it is possible to build predictors based on the statistical knowledge of the message, the prediction time in this case has to be n_c-1 times the nominal correlation time of the signal. Thus the prediction would be almost entirely statistical. Since the utility of the

phase-lock loop is based on precise, instantaneous phase correction, the very idea is negated when a predictor is used.

Another serious difficulty with this form of system is that of cross-modulation products. Since the input to each phase detector is a sum of delayed versions of the transmitted signal, there will, in general, be a non-zero phase detector output even though there might be a zero phase error between the estimate and a given multipath component of the received signal. This would lead to false correction signals, possibly with the wrong sign.

Although this receiver structure merits closer investigation, it does not appear to be practical as it stands. Fortunately, there is another technique for combating dispersion in the case of angle modulation: anti-dispersion measures can be taken before demodulation is attempted. That is, s(t) could be estimated (rather than a(t)) and standard, non-dispersive demodulation techniques applied to this estimate. Since this "equalization" procedure is linear, the case of non-linear, angle demodulation is not treated in detail in this research.

2.3 The Mean Square Error Criterion

If we are to restrict ourselves to equivalent linear demodulation techniques, then it is logical to use the criterion more easily interpreted in terms of conventional performance indices such as signal-to-noise ratio than is the criterion of maximum a-posteriori probability. It is easy

to show, using standard Wiener-Hopf techniques [45], that the minimum mean square linear estimate of the message a(t) is of the form

$$\hat{a}(t) = \int_T f(t-\lambda)\ y(\lambda)d\lambda \qquad (2\text{-}20)$$

where f(t) is the impulse response of linear filter satisfying the Wiener-Hopf integral equation,

$$\int_T R_y(\lambda_1-\lambda_2)\ f(t-\lambda_2)\ d\lambda_2 = R_{ax}(\lambda_1-t), \lambda_1 \varepsilon T. \qquad (2\text{-}21)$$

Appendix B shows that, for the linear demodulation case, the MAP estimate of the preceding section is fully equivalent to the estimate given by (2-20) and (2-21), so distinction between the two criteria need no longer be made.

Equation (2-21) is well known to have a solution for physically reasonable correlation functions, [46], but the ease of finding explicit solutions is greatly dependent upon assumptions regarding the observation "window," T (See Equation (2-9). A finite interval makes explicit solutions quite difficult to obtain: the only systematic method of solution applies to problems in which the correlation functions of (2-21) have rational Fourier transforms (see Appendix A of [18]), which is not true for this problem due to the pure delay in the channel model. Also, this technique is not amenable to efficient solution by computer. For this reason

the case of finite observation intervals has been treated by taking advantage of the bandlimited nature of the signals and using a sampled-data formulation of this problem, discussed in a later section.

If the observation interval is infinite, then (2-21) can be solved using Fourier transform methods. Consideration of this case provides a bound on the performance of any communication system operating over a given selective fading channel. It is not difficult to solve (2-21) under those conditions; the resultant frequency response function, $F(j\omega)$, for the optimal demodulator is of the form

$$F(j\omega) = \left[\frac{S_{xa}(-\omega)}{S_y(-\omega)}\right]^* \quad , \tag{2-22}$$

where $S_{xa}(\omega)$ and $S_y(\omega)$ are spectral densities corresponding to the correlation functions $R_{xa}(\tau)$ and $R_y(\tau)$. Noting the input-output relations of Figure 2-3, and using properties of random signals passed through linear systems, (2-22) can be written as

$$F(j\omega) = \frac{H^*(j\omega)\ S_a(-\omega)}{S_N(-\omega) + |H(j\omega)|^2 S_a(-\omega)} \quad . \tag{2-23}$$

Note that in the absence of noise the frequency response of the optimal, infinite observation interval demodulator is just the inverse of the frequency response function of the channel.

The mean square error associated with this system is calculated using standard Wiener-Hopf methods.

$$\varepsilon^2 = E[|\hat{a}(t) - a(t)|^2] =$$

$$= R_a(o) - \int_{-\infty}^{\infty}\int_{-\infty}^{\infty} R_y(\lambda_1-\lambda_2)\ f(\lambda_1)\ f^*(\lambda_2)\ d\lambda_1 d\lambda_2$$

$$= \frac{1}{2\pi}\int_{-\infty}^{\infty} [S_a(\omega) - |F(-j\omega)|^2 S_y(\omega)]d\omega$$

$$= \frac{1}{2\pi}\int_{-\infty}^{\infty} \frac{S_a(\omega)\ S_N(\omega)}{S_N(\omega) + |H(-j\omega)|^2 S_a(\omega)}\ d\omega \qquad (2\text{-}24)$$

Equation (2-24) provides a bound on the performance attainable using any physical communication system operating over the dispersive channel, $H(j\omega)$, and is consequently useful for comparing with the actual performance of the system to see if it is nearly optimal. However, before evaluating this bound let us consider the case of a finite observation interval by formulating the demodulation problem in discrete time-sample form.

2.4 The Sampled-Data Formulation

In the preceding section the difficulty of finding explicit solutions to the Wiener-Hopf integral equation, (2-21), for finite observation intervals was discussed. Because the length of this interval, T_0, can be related to the complexity of the required demodulator, as is shown in

Chapter 3, and because the magnitude of T_0 is limited by the rate of fading in the channel, this case is of crucial importance. A sampled-data approach to the problem automatically incorporates the length of this interval and provides results which are theoretically useful and computationally efficient.

In Section 2.1 it was assumed that the system was essentially bandlimited to a normalized frequency interval, $-\pi \leq \omega \leq \pi$, so that samples taken at the Nyquist rate (once per second) are a sufficient representation for the random processes involved.

Suppose the dispersive channel is represented by n_c taps in the delay line model (thus the channel delay spread is $T_c = n_c - 1$) and that the channel output is observed for an integral number of seconds, T_0, starting at $t = 0$. Then, referring to Figure 2-3, the observed waveform can be written

$$y(t) = h(t) \circledast a(t) + N(t)$$

$$= h_1 a(t) + \ldots + h_{n_c} a(t-T_c) + N(t). \qquad (2\text{-}25)$$

Let $\underline{y}$, $\underline{N}$, and $\underline{a}$ be vectors of time samples of the corresponding waveforms with the k^{th} component defined to be

$$y_k = y(t)\Big|_{t = k-1}, \quad k = 1,2, \ldots T_0$$

$$N_k = N(t)\Big|_{t = k-1}, \quad k = 1,2, \ldots T_0$$

$$a_k = a(t)\Big|_{t = k - 1 - T_c}, \quad k = 1,2, \ldots (T_0+T_c).$$

Then, if we define a $T_0 x (T_0+T_c)$ channel matric $\underline{\underline{H}}$ to be

$$\underline{\underline{H}} = \begin{bmatrix} h_{n_c} \cdots h & 0 \cdots 0 \\ 0 \; h_{n_c} \cdots h \; 0 \cdots 0 \\ \vdots \qquad \ddots \qquad \vdots \\ 0 \qquad h_{n_c} \cdots h_1 \end{bmatrix} , \tag{2-26}$$

the time-sampled channel output can be expressed as

$$\underline{y} = \underline{\underline{H}} \, \underline{a} + \underline{N} \quad . \tag{2-27}$$

By assumption, $\underline{a}$ and $\underline{N}$ are statistically independent, zero-mean, Gaussian random vectors with stationary covariance matrices given by

$$E[\underline{a} \, \underline{a}^{*T}] = \sigma_a^2 \, \underline{\underline{\Phi}}_a \quad , \quad E[\underline{N} \, \underline{N}^{*T}] = \sigma_N^2 \, \underline{\underline{\Phi}}_N \quad .$$

The a-posteriori density function for $\underline{a}$ given $\underline{y}$ can then be expressed as follows.

$$p(\underline{a}/\underline{y}) = \frac{p(\underline{y}/\underline{a})\,p(\underline{a})}{p(\underline{y})} = \frac{p(\underline{y}, \underline{a})}{\int p(\underline{y},\underline{a})\,d\underline{a}} \tag{2-28}$$

$$= \frac{\exp\left[-\frac{1}{\sigma_N^2} \{(\underline{y}^* - \underline{\underline{H}}^* \, \underline{a}^*)^T \, \underline{\underline{\Phi}}_N^{-1} (\underline{y} - \underline{\underline{H}}\underline{a})\} - \frac{1}{\sigma_a^2} \, \underline{a}^{*T} \underline{\underline{\Phi}}_a^{-1} \underline{a} \right]}{\int \exp\,[.]\; d\,\underline{a}}$$

A procedure analogous to "completing the square" in the exponents of (2-28) leads to the form below.

$$p(\underline{a}/\underline{y})=(2\pi\sigma_N^2)^{-\frac{T_0+T_c}{2}} |\underline{\underline{Q}}|\exp -\frac{1}{\sigma_N^2}\{(\underline{a}-\underline{\underline{Q}}^{-1}\underline{\underline{H}}^T\underline{\underline{\Phi}}_N^{-1}\underline{y})^{*T}\ \underline{\underline{Q}}(\underline{a}-\underline{\underline{Q}}^{-}\ \underline{\underline{H}}^T\underline{\underline{\Phi}}_N^{-1})\} \tag{2-29}$$

$$\underline{\underline{Q}} = \left[\underline{\underline{H}}^{*T}\ \underline{\underline{\Phi}}_N^{-1}\underline{\underline{H}} + \frac{1}{\eta}\ \underline{\underline{\Phi}}_a^{-1}\right] \tag{2-30}$$

$$\eta = \frac{\sigma_a^2}{\sigma_N^2} \tag{2-31}$$

The quantity $\underline{\underline{Q}}^{-1}\underline{\underline{H}}^{*T}\ \underline{\underline{\Phi}}^{-1}\underline{y}$ is the mean value of the a-posteriori density function for $\underline{a}$, so this quantity must be the minimum mean square Bayes estimate for the message vector $\underline{a}$.[1] That is,

$$\hat{\underline{a}} = \underline{\underline{Q}}^{-1}\underline{\underline{H}}^{*T}\ \underline{\underline{\Phi}}_N^{-1}\ \underline{y} = \left[\underline{\underline{H}}^{*T}\ \underline{\underline{\Phi}}_N^{-1}H+\ \frac{1}{\eta}\ \underline{\underline{\Phi}}_a^{-1}\right]^{-1}\underline{\underline{H}}^{*T}\ \underline{\underline{\Phi}}_N^{-1}\ \underline{y} \tag{2-32}$$

is the estimator of $\underline{a}$ which minimizes the mean square demodulation error; from (2-29) the normalized error covariance matrix is seen to be

$$\underline{\underline{\Lambda}} = \frac{1}{\sigma_a^2}\ \mathrm{Cov}(\hat{\underline{a}}-\underline{a}) = \frac{1}{\eta}\ \underline{\underline{Q}}^{-1} \quad . \tag{2-33}$$

---

[1] See reference [2], Chapter 5.

The parameter η is seen to be the input SNR (signal-to-noise power ratio) for the system; and, since the error variance is equal to the noise power at the demodulator output, the diagonal elements of $\underline{\Lambda}$ can be interpreted as the reciprocal of the output SNR's for each message component. Thus (2-33) may be used for computing the effect of finite observation interval on system performance.

2.5 Performance of Optimal Demodulators

Equation (2-24) determines the ultimate performance of any physical demodulator. Equation (2-33) gives a similar bound for a finite observation interval. It is of great interest to examine the way in which selective fading channels affect these measures of ultimate system performance.

The equations for mean square error depend upon the channel state and the power spectra, or covariance matrices, of both the message and noise random processes. Since these quantities can take on an endless number of possible forms, it is necessary to consider idealizations of actual channels and spectra which retain only the most important, basic parameters which affect system performance. These simplified forms are discussed below.

A. Channel State. The modeling of the channel was treated in Section 2.1. The five-tap example channels have frequency responses which are so complex that their main usefulness is to show that nothing catastrophic happens to performance when fine detail is present in the channel model.

Examples of single-notch selective fading permit simplified interpretation of the results in terms of fading depth and placement of the fading notch, the most important parameters describing selective fading.

B. The Message Spectrum. In this report two examples of message power spectrum are considered: messages with a flat spectrum over the frequency band $-\pi \leq \omega \leq \pi$, and messages with a power spectrum

$$S_a(\omega) = \frac{2\alpha\ \sigma_a^2}{\omega^2+\alpha^2} \quad ,\alpha = 0.75 \quad . \tag{2-34}$$

The first case makes all portions of the frequency band equally important and can be regarded as the zeroth order idealization for message spectra. The second case gives non-uniform weighting across the frequency band, and the results are sensitive to the frequency at which fading occurs. This case has some useful analytical properties: a Gaussian random process with power spectrum (2-34) is a first order Markov process; the inverse of the normalized covariance matrix of this process is the simple tridiagonal form shown below, for arbitrary order.

$$\underline{\underline{\Phi}}_a^{-1} = \begin{bmatrix} \frac{1}{1-x^2} & \frac{-x}{1-x^2} & 0 & \cdots & 0 \\ \frac{-x}{1-x^2} & \frac{1+x^2}{1-x^2} & & & \vdots \\ 0 & \cdot & \cdot & \cdot & 0 \\ \vdots & & \cdot & \frac{1+x^2}{1-x^2} & \frac{-x}{1-x^2} \\ 0 & \cdots & 0 & \frac{-x}{1-x^2} & \frac{1}{1-x^2} \end{bmatrix} , \qquad (2\text{-}35)$$

where $x = e^{-\alpha}$.

Choosing $\alpha = 0.75$ insures that 85 percent of the message power is contained in the frequency band $-\pi \leq \omega \leq \pi$, so the message is essentially bandlimited.

C. The Noise Spectrum. The additive noise will be assumed to be white and bandlimited, a situation typically true in practice. However, in some calculations it is convenient to have a rational noise spectrum, and in these cases the form of the noise spectrum will be assumed to be

$$S_N(\omega) = \frac{2b\sigma_N^2}{\omega^2 + b^2} \quad , b = 2 \quad . \qquad (2\text{-}36)$$

The bandwidth parameter b is chosen to be b = 2 to make the equivalent white noise bandwidth, Weq, defined as

$$Weq = \frac{\int_0^\infty S_N(f)\ df}{S_N(0)} \quad , \tag{2-37}$$

equal to $\frac{1}{2}$, the assumed channel bandwidth. This makes the noise power, σ_N^2, equal to the noise spectral density, $S_N(0)$.

Analytical Results

Using the above assumptions about the signal and noise spectra one can numerically evaluate (2-24) or (2-33) for the mean square demodulation error for any channel state. However, it is possible to develop some relatively simple analytical expressions for demodulator performance for the case of single-notch selective fading which provide insight into the general problem.

Let us assume a channel frequency response,

$$H(j\omega) = \frac{1-r\ e^{j\omega_0}e^{-j\omega}}{\sqrt{1+r^2}} \quad , \tag{2-38}$$

with power transfer function

$$|H(j\omega)|^2 = 1 - 2\rho Cos(\omega - \omega_0) \quad , \tag{2-39}$$

$$\rho = \frac{r}{1+r^2} \leq \frac{1}{2} \quad . \tag{2-40}$$

Then, for the case of a flat message spectrum,

$$S_a(\omega) = \sigma_a^2 \quad , \ |\omega| \leq \pi \quad ,$$

and an infinite observation interval, Equation (2-24) can be immediately evaluated.[1]

$$\frac{\varepsilon^2}{\sigma_a^2} = \frac{1}{\sigma_a^2} \frac{1}{2\pi} \int_{-\pi}^{\pi} \frac{S_a(\omega)\ S_N(\omega)\ d\omega}{S_N(\omega)+|H(-j\omega)|^2 S_a(\omega)} \tag{2-41}$$

$$= \frac{1}{\eta} \cdot \frac{1}{2\pi} \int_{-\pi}^{\pi} \frac{d\omega}{(1+\frac{1}{\eta})^2 - 2\rho \cos(\omega+\omega_0)}$$

$$= \frac{1}{\eta} \cdot \frac{1}{\sqrt{(1+\frac{1}{\eta})^2 - 4\rho^2}} \quad , \tag{2-42}$$

where

$$\eta = \frac{\sigma_a^2}{\sigma_N^2} = \text{input SNR} \quad . \tag{2-43}$$

For the Markov message process of (2-34) the integration is not so straightforward, but it is possible to approximate the transcendental channel frequency response function by a rational, Padé approximant[2] to obtain an analytical result in essentially perfect agreement with results calculated numerically. The (1,1) Padé approximant to the unit delay function, $e^{-j\omega}$, is

---

[1] Dwight, H. B., Tables of Integrals and Other Mathematical Data, to Macmillan, 1961, p. 218.

[2] Truxal, J. G., Control System Synthesis, McGraw Hill, New York, 1955, p. 548.

$$e^{-j\omega} \cdot \frac{-j\omega + 2}{j\omega + 2} \quad . \tag{2-44}$$

When this approximation is used in (2-38) and the rational signal spectrum, (2-34), and rational noise spectrum, (2-36), are assumed, then the integral for mean square error, (2-24), may be evaluated using residue calculus to obtain the following result.

$$\frac{\varepsilon^2}{\sigma_a^2} \quad \frac{1}{\eta} \quad \frac{1}{\sqrt{1-4\rho^2+\frac{1}{\eta}[(q+q^{-1})-2\rho\cos\omega_0(q-q^{-1})]+\frac{1}{\eta 2}}} \tag{2-45}$$

$$q = \frac{b}{\alpha} = \frac{2}{0.75} = 2.67 \quad . \tag{2-46}$$

Since ε^2 is the output noise power of the demodulator, the quantity σ_a^2/ε^2 can be regarded as the output SNR. Thus, for uniform frequency weighting (flat message spectrum),

$$SNR_0 = \eta\sqrt{1 - 4\rho^2 + \frac{2}{\eta} + \frac{1}{\eta^2}} \quad , \tag{2-47}$$

while for a Markov message source

$$SNR_0 = \eta\sqrt{1-4\rho^2+\frac{1}{\eta}[(q+q^{-1})-2\rho\cos\omega_0(q-q^{-1})]+\frac{1}{\eta 2}} \tag{2-48}$$

Examination of (2-47) and (2-48) shows that the placement of the selective fading notch (ω_0) makes no difference in the case of a flat message spectrum, while it does affect performance at low input SNR's for the Markov message source.

The parameter ρ in these equations may be related to the depth of the selective fading notch using Equation (2-39). Letting D denote the fading depth in dB, we find that

$$10^{\frac{-D}{10}} = |H(j\omega_0)|^2 = 1 - 2\rho \quad , \tag{2-49}$$

$$4\rho^2 = \left[1 - 10^{\frac{-D}{10}}\right]^2 \quad . \tag{2-50}$$

Figure 2-6 shows the effects of various parameters on system performance for a Markov message source, given by (2-48). On the scale of Figure 2-6, the performance for a white message source is virtually indistinguishable from the case of mid-band fading ($\omega_0=\pi/2$) and the Markov source. Note that as fading depth increases it becomes more and more difficult to improve system performance by merely increasing the input SNR (or transmitter power): performance is increasingly limited by dispersion rather than by additive noise. Note also that the placement of the fading notch is more important for low-performance systems than for high-performance ones. The worst case occurs when the notch is at the peak of the signal spectrum, and performance improves as the notch approaches the band edge. Increasing reliance must be placed upon a-priori statistical knowledge of the message as the input SNR gets small; and, since there is more observable message information at the center of the frequency band than at the band edge, center-band fading must be the most severe.

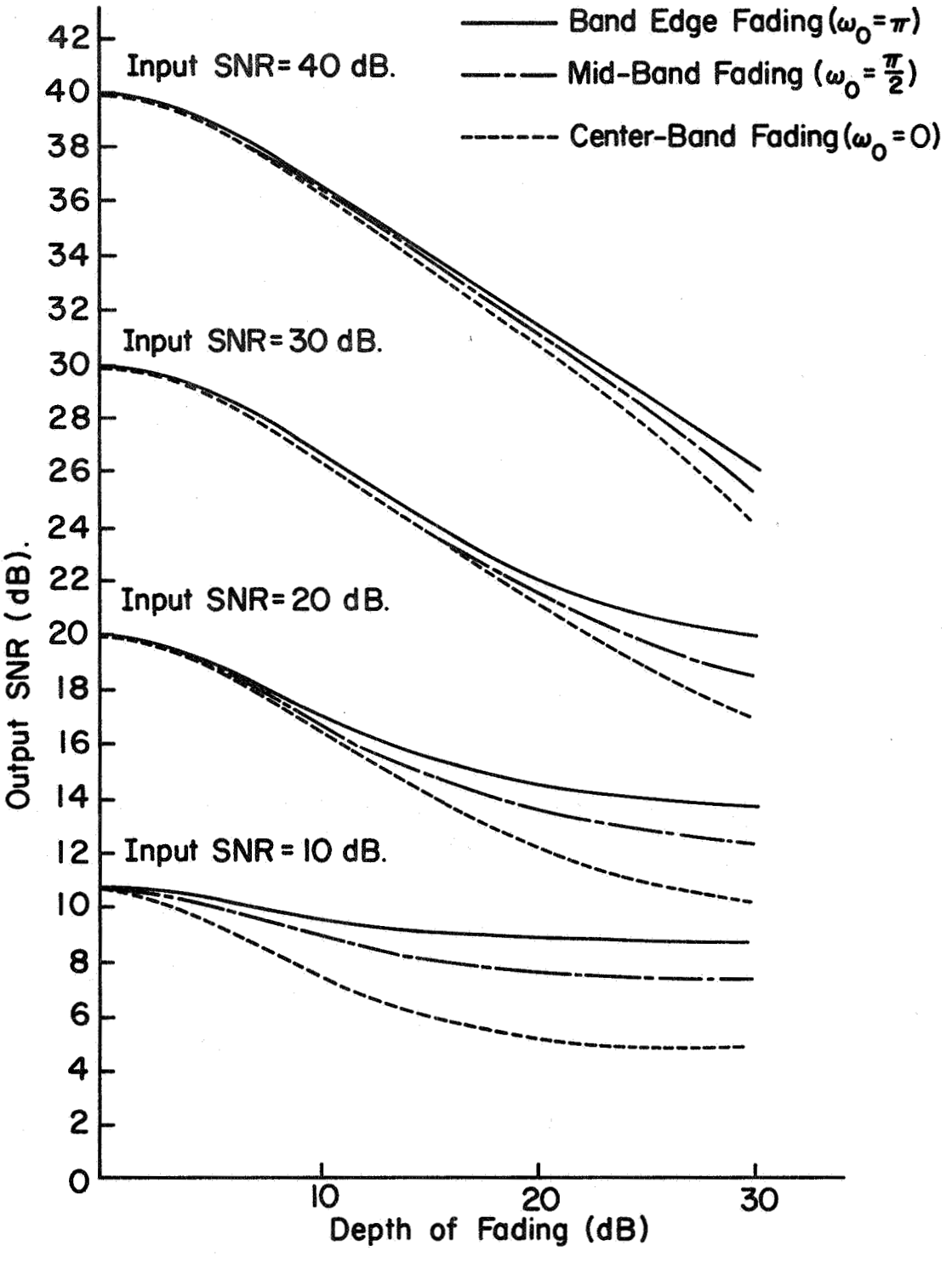

FIGURE 2-6. DEMODULATOR PERFORMANCE FOR SINGLE NOTCH SELECTIVE FADING.

As the input SNR gets large the output SNR becomes independent of the message spectrum. That is,

$$SNR_0 \longrightarrow \sqrt{1-4\rho^2}\ \eta \quad . \tag{2-51}$$

For $\rho=0$, the non-dispersive channel, the output SNR goes up as the input SNR, which is well known to be the dependence observed in practice. However, in the selective fading case there is a distinct degradation in performance compared to the non-fading case, <u>despite</u> the fact that the channel was normalized to assure no power gain or loss regardless of the fading depth, (passive and dissipationless channel). This result is quite significant, for it means that no amount of sophisticated receiver design can ever completely overcome the deleterious effects of channel dispersion. The actual amount of this irreducible loss depends on the exact nature of the channel, and could be regarded as a measure of the degradation in "channel capacity" caused by selective fading.

Numerical Results

If the case of finite observation intervals is to be considered, or we wish to examine the effects of higher-order channels, then numerical methods must in general be used to evaluate equations (2-24) and (2-33). However, for the case of single-notch selective fading it is possible to analytically invert the matrix (2-33), which vastly reduces the numerical effort required. This matrix inversion is described in Appendix C.

Figure 2-7 shows the effect of a finite observation interval on optimal demodulator performance for single-notch selective fading and a flat message spectrum. The Markov message source gives similar results except that the curves are shifted up or down depending on the placement of the fading notch. These results were computed using Equation (2-33), using that point estimator of the message which gives the smallest diagonal element of (2-33). (We estimate one point in time of the continuous waveform and "slide" the incoming data through the resultant demodulator.) Note that for deep fading channels system performance is primarily limited by the observation interval rather than additive noise, i.e., there is severe degradation compared to the infinite observation interval case when the fading is deep and the observation interval small. Recalling that the observation interval is limited by the rate of fading, it is apparent that systems operating over channels exhibiting severe, rapid fading will fall far short of the performance given by the infinite observation interval case.

Figure 2-8 and Figure 2-9 show the results of computing (2-24) for the five-tap example channels of Section 2.1. These examples show the same irreducible loss in performance due to selective fading as do the single-notch fading examples. The exact amount of this loss depends upon the channel state and, as $\eta \to \infty$, is given by the expression

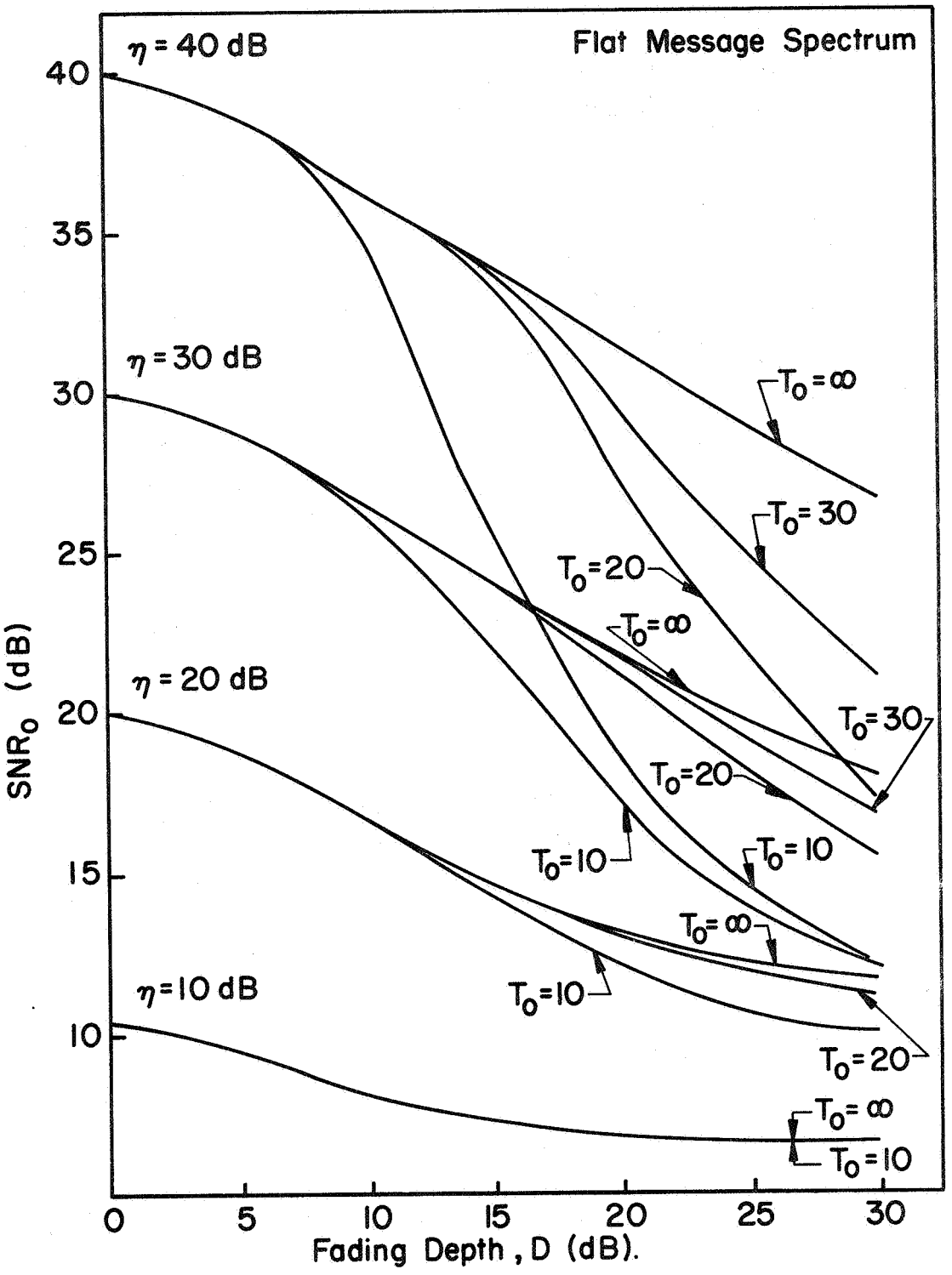

FIGURE 2-7. OPTIMAL DEMODULATOR PERFORMANCE FOR SINGLE NOTCH SELECTIVE FADING.

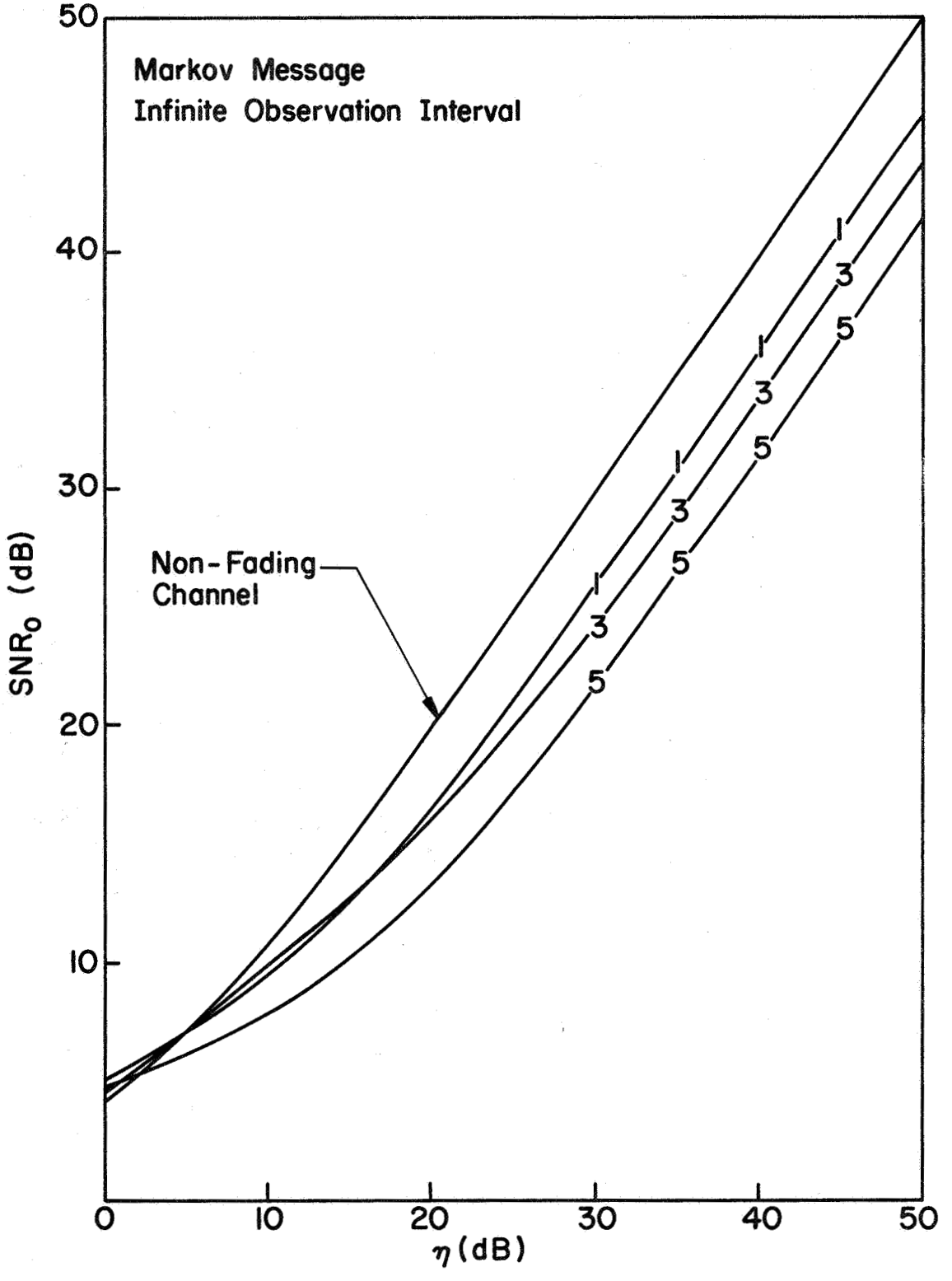

FIGURE 2-8. OPTIMAL DEMODULATOR PEFORMANCE FOR EXAMPLE CHANNELS 1, 3, AND 5.

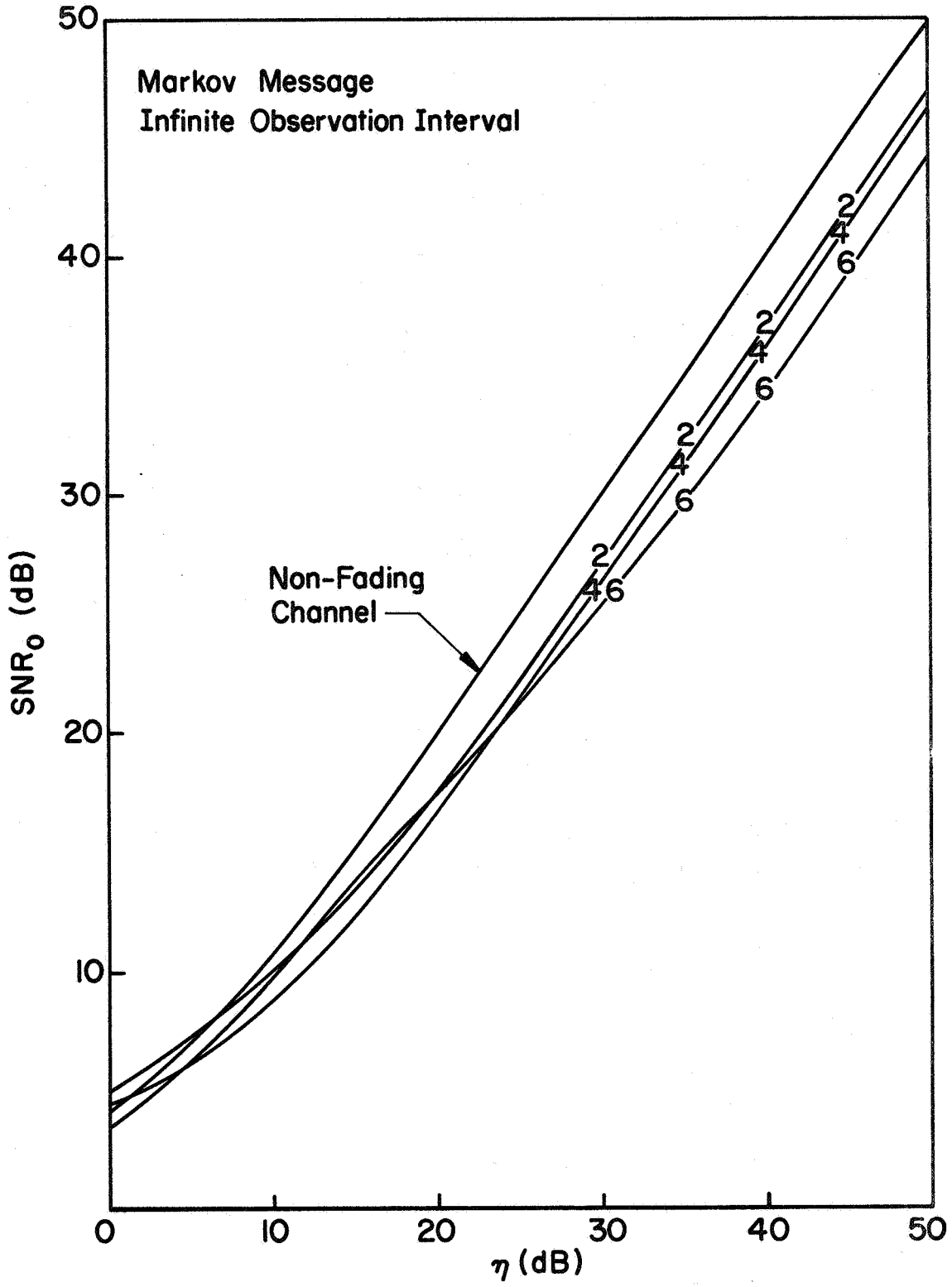

FIGURE 2-9. OPTIMAL DEMODULATOR PERFORMANCE FOR EXAMPLE CHANNELS 2, 4, AND 6.

$$10 \log \left[\frac{1}{2\pi} \int_{-\pi}^{\pi} \frac{d\omega}{|H(-j\omega)|^2} \right] \qquad (2\text{-}52)$$

Figure 2-10 and 2-11 illustrate the effect of finite observation interval, T_0, on demodulator performance. Only two examples are shown, but the trends are the same for all examples if the scales for input and output SNR are extended or contracted: there is an upper limit on performance due to the finite observation interval, and the numerical value of this limit depends upon the exact state of the channel; the performance of the system approaches the case of an infinite observation interval as the input SNR decreases; selective fading alone causes a performance degradation relative to a non-fading channel.

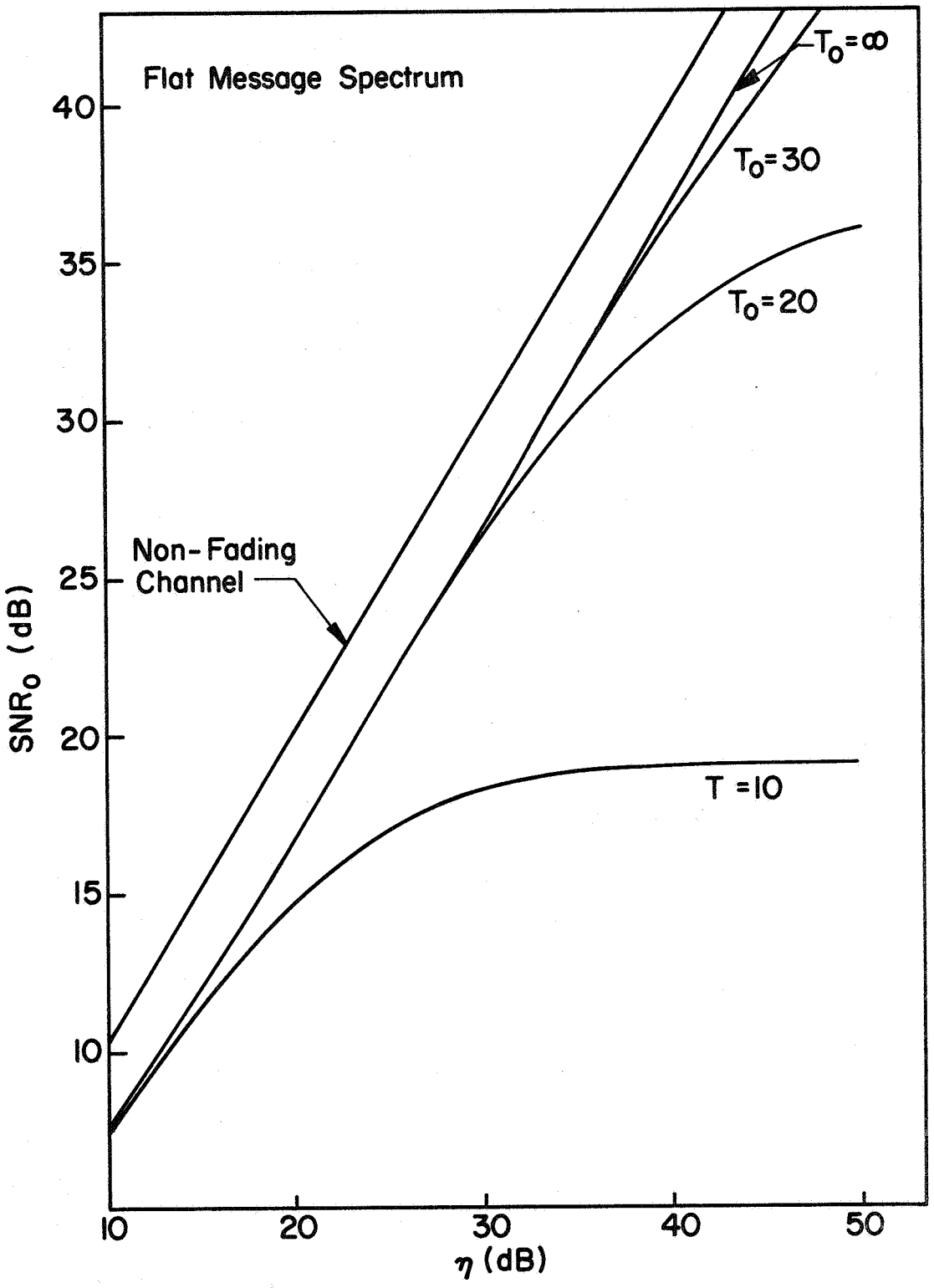

FIGURE 2-10. OPTIMAL DEMODULATOR PERFORMANCE FOR EXAMPLE CHANNEL 4 (5 TAPS).

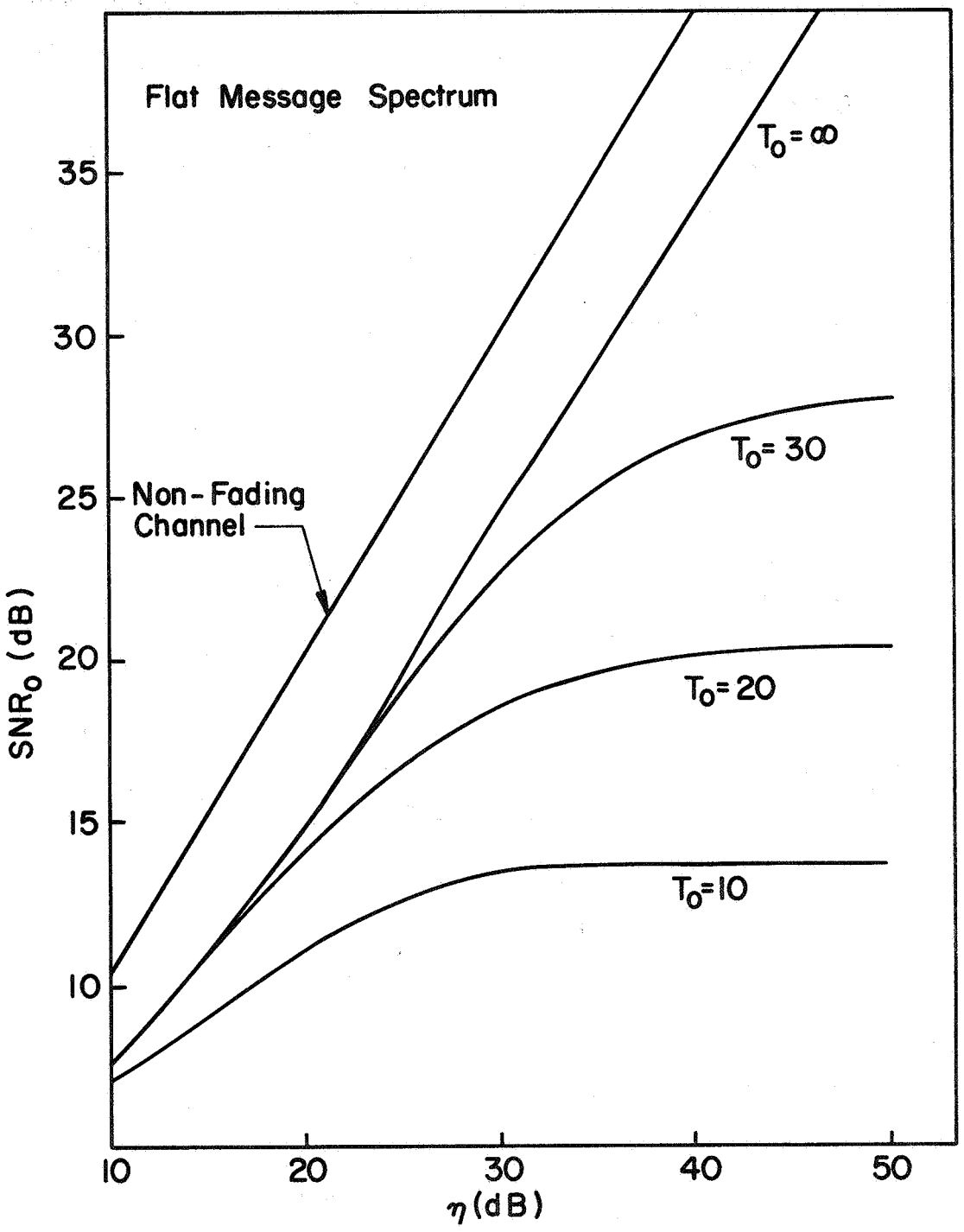

FIGURE 2-11. OPTIMAL DEMODULATOR PERFORMANCE FOR EXAMPLE CHANNEL 3 (5 TAPS).

CHAPTER 3: SUBOPTIMAL DISPERSIVE CHANNEL DEMODULATORS

In this chapter approximations to the optimal demodulator for known dispersive channels are considered to see the conditions under which simple suboptimal systems are nearly optimal. It is shown that the optimal filtering operation may be regarded as the cascade of two operations - channel inversion and post-inversion filtering. The inversion (equalization) operation may be implemented with relative ease in the cases of two different equalization algorithms discussed. An analysis and comparison of the performance of these equalizers leads to a simple method for predicting the dependence of the equalization error on the length of the observation interval, a parameter related to system complexity.

When the channel is noisy, post-inversion filtering is required to give near-optimal performance. Various approximations to the ideal filter are analyzed for performance, leading to some general conclusions concerning the effectiveness of different suboptimal demodulators. Finally, an approximate technique for rapid prediction of the performance of demodulation schemes for known dispersive channels is developed. This method requires only simple computations of assymptotes.

3.1 Optimal Demodulator Approximation

The minimum mean-square error demodulator was given, for infinite observation intervals, by (2-23),

$$F(j\omega) = \frac{H^*(j\omega)\ S_a(-\omega)}{S_N(-\omega) + S_a(-\omega)\,|H(j\omega)|^2} \quad , \tag{3-1}$$

and for finite intervals by (2-32).

$$\underline{\hat{a}} = \left[\underline{\underline{H}}^{*T}\underline{\underline{\Phi}}_N^{-1}\underline{\underline{H}} + \frac{1}{\eta}\,\underline{\underline{\Phi}}_a^{-1}\right]^{-1}\underline{\underline{H}}^{*T}\underline{\underline{\Phi}}_N^{-1}\underline{Y} \tag{3-2}$$

Equation (3-2) is actually the estimator for the entire set of message samples; in practice one would choose that point estimator of the message which minimizes the mean-square error; that is, if $\hat{a}_k$ is that message sample estimate with minimum error, then

$$\hat{a}_k = \underline{c}^T\underline{Y} \quad , \tag{3-3}$$

where $\underline{c}^T$ is the k^{th} row of the matrix of (3-2). The vector $\underline{c}$ can be interpreted as the set of tap-gain coefficients of a transversal filter[1] operating on the observed waveform. Note that as the observation interval is increased there is a proportionate increase in the number of delay elements and tap gain computers of the transversal filter, so that system complexity is at least proportional to the length of this

---

[1]Bennett, W. R., J. R. Davey, Data Transmission, McGraw-Hill, New York, 1965, p. 269.

interval. Note also that the channel state appears in a very complex way (a matrix inverse) in computing $\underline{c}$, so this optimal system is not easily adapted to changing channel states. Consequently, it is of interest to consider suboptimal demodulator algorithms which are more easily adapted to changing channel states than the optimal system, hence more amenable for construction.

Let us rewrite (3-1) as follows:

$$F(j\omega) = \frac{1}{H(j\omega)} \cdot \frac{1}{1 + \frac{1}{\eta} \frac{G(\omega)}{|H(j\omega)|^2}} , \qquad (3\text{-}4)$$

$$G(\omega) = \frac{S_N(-\omega)/\sigma_N^2}{S_a(-\omega)/\sigma_a^2} , \quad \eta = \frac{\sigma_a^2}{\sigma_N^2} . \qquad (3\text{-}5)$$

$G(\omega)$ is an a-priori determined filter function independent of the channel. Examination of (3-4) reveals that the optimal filter may be regarded as two successive operations on the data: channel inversion and post-inversion filtering. Since we are assuming dispersion-limited communications, it is apparent that the channel inversion operation is the more significant of the two operations in improving performance. That is, the input SNR, η, might be large enough that $F(j\omega)$ could be approximated by a few terms in the expansion

$$(F(j\omega \triangleq \frac{1}{H(j\omega)} \cdot \left[1 - \frac{1}{\eta} \frac{G(\omega)}{|H(j\omega)|^2} + \frac{1}{\eta^2} \frac{G^2(\omega)}{|H(j\omega)|^4} + \cdots\right] . \qquad (3\text{-}6)$$

Suppose then that $C(j\omega)$ is some approximation to the channel inverse,

$$C(j\omega) \triangleq \frac{1}{H(j\omega)} \tag{3-7}$$

Then

$$F(j\omega) \triangleq C(j\omega) \left[1 - \frac{1}{\eta} G(\omega)|C(j\omega)|^2 + 0(\frac{1}{\eta^2})\right]. \tag{3-8}$$

The higher order terms in (3-8) may be realized by cascading stages of channel inversion, so the crux of the realization of dispersive channel demodulators lies in finding approximations, $C(j\omega)$, to the channel inverse which can be mechanized with reasonably simple systems.

Later in the chapter the post-inversion filtering operation is investigated, but for the moment let us consider the inversion ("equalization") operation alone. In particular, let us consider the easily implemented transversal filter approximation,

$$C(j\omega) = \sum_k c_k e^{-jk\omega} \quad . \tag{3-9}$$

3.2 The Fourier Series Approximation

The most obvious way to approximate the channel inverse is to use an exponential Fourier series, since (3-9) is an expansion of this form. That is, choose the $\{c_k\}$ such that

$$c_k = \frac{1}{2\pi} \int_{-\pi}^{\pi} \frac{e^{jk\omega}}{H(j\omega)}\, d\omega \quad , \tag{3-10}$$

which assures that the norm error ε^2 is a minimum.

$$\varepsilon^2 = \frac{1}{2\pi} \int_{-\pi}^{\pi} \left| \frac{1}{H(j\omega)} - C(j\omega) \right|^2 d\omega \tag{3-11}$$

It is convenient at this point to introduce the z transform,[1] $z = e^{j\omega}$, and inner product notation.

$$C(z) = \sum_k c_k z^{-k} \quad , \tag{3-12}$$

$$c_k = \left\langle \frac{1}{H(z)} , z^{-k} \right\rangle \quad , \tag{3-13}$$

$$\varepsilon^2 = \left\| \frac{1}{H(z)} - C(z) \right\|^2 \quad , \tag{3-14}$$

where

$$\langle f(z), g(z) \rangle \triangleq \frac{1}{2\pi j} \oint f(z) g^*(z^{-1}) \frac{dz}{z} \tag{3-15}$$

The notation $g^*(z^{-1})$ refers to the reciprocal polynomial[2] of $g(z)$; the polynomial obtained by replacing z by z^{-1} and using the complex conjugate coefficients. The contour of

---

[1] Truxal, J. G., Control System Synthesis, McGraw-Hill, New York, 1955.

[2] Grenander, U. and G. Szego, Toeplitz Forms and Their Applications, University of California Press, Berkeley, California, 1958, p. 3.

integration is around the unit circle in the positive sense. When the channel is represented by a delay line model,

$$H(z) = \sum_{k=1}^{n_c} h_k z^{-(k-1)} \tag{3-16}$$

then the inner products of (3-12) - (3-15) involve only polynomials in z, and may be calculated by straightforward residue calculus.[1] This algorithm would appear at first glance to be difficult to implement, but it turns out that the Fourier series approximation has the property of forcing zeros in the "sidelobes" of the equalized channel output, C(z) H(z). (Sidelobes are defined to be the coefficients of all the terms of C(z) H(z) except the constant term.) This is the algorithm used by Lucky [27], [28], DiToro [29], [30], and Schreiver [31] in mechanizing their transversal equalizers. The Fourier series approach taken here is far more convenient for calculating performance, however, than the formulations used by the above authors.

This zero-forcing property is demonstrated as follows. Suppose that

$$C(z) = \sum_{k=-\eta}^{m} c_k z^{-k} \tag{3-17}$$

Then the overall response of the channel and equalizer is H(z) C(z), ideally equal to unity.

---

[1] Churchhill, R. V., Complex Variables and Applications, McGraw-Hill, New York, 1960.

$$H(z)\ C(z) = \sum_{\ell=1}^{n_c} h_k z^{-(k-1)} \cdot \sum_{k=-\eta}^{m} c_k z^{-k}$$

$$= \sum_{r=-\eta}^{m+n_c-1} \alpha_r z^{-r} \quad , \tag{3-18}$$

where

$$\alpha_r = \begin{cases} \sum_{k=1}^{n_c+r+1} h_k c_{r-k+1} \ , & -\eta \le r \le -(\eta-n_c+2) \\ \sum_{k=1}^{n_c} h_k c_{r-k+1} \ , & -(\eta-n_c+1) \le r \le m \\ \sum_{k=r-m+1}^{n_c} h_k c_{r-k+1} \ , & m+1 \le r \le m+n_c-1 \end{cases} \tag{3-19}$$

For $-(\eta-n_c+1) \le r \le m$ we may substitute (3-13) into (3-19) to obtain

$$\alpha_r = \sum_{k=1}^{n_c} h_k c_{r-k+1} = \sum_{k=1}^{n_c} h_k \left\langle \frac{1}{H} , z^{r-k+1} \right\rangle$$

$$= \frac{1}{2\pi j} \oint \frac{\sum_{k=1}^{n_c} h_k z^{r-k+1}}{H(z)} \frac{dz}{z} = \frac{1}{2\pi j} \oint \frac{H(z) z^r}{H(z)} \frac{dz}{z}$$

$$= \begin{cases} 1 \ , & r = 0 \\ 0 \ , & r \neq 0 \end{cases} \tag{3-20}$$

Thus this algorithm forces zeros in the overall response for the first m positive sidelobes and $m+n_c-1$ negative sidelobes.

Another useful property of this inversion algorithm is that the equalizer is causal if H(z) is minimum-phase (no zeros outside the unit disc). Suppose that (3-16) is factored into the form

$$H(z) = h_1 \prod_{\ell=1}^{n_c-1} (1-r_\ell z^{-1}) \quad , \tag{3-21}$$

so that H(z) is minimum-phase if $|r_\ell| < 1$, $\ell = 1,\ldots,n_c-1$. Substituting into (3-13) we obtain

$$c_k = \frac{1}{2\pi j} \oint \frac{z^k}{H(z)} \frac{dz}{z} = \frac{1}{2\pi j} \oint \frac{z^{-k}}{H(z^{-1})} \frac{dz}{z}$$

$$= \frac{1}{2\pi j} \oint \frac{z^{-k}}{h_1 \prod_{\ell=1}^{n_c-1} (1-r_\ell z)} \frac{dz}{z} \quad . \tag{3-22}$$

For a minimum-phase channel the integrand of (3-22) is analytic on the unit disc if k<0, making $c_k=0$ for $k < 0$, a causal equalizer. (It is also apparent that if H(z) is analytic on the unit disc, then $c_k=0$ for k<0, a completely non-causal system.) This makes good sense since we would expect a channel with no zeros outside the unit circle to have an inverse with no poles outside the unit circle (no negative time response).

The above remarks show that the equalizer, (3-17), is one-sided if the roots of the channel, H(z), are all either inside or outside the unit circle. When there is a mixture of roots inside and outside, the equalizer will be two-sided, so that there will be an optimum choice of the number of positive and negative taps, subject to a constraint on the total number of taps (observation interval). The required juggling of the number of positive and negative taps to achieve this optimum is not amenable to analysis. However, the experience of many examples indicates that the performance of this fully optimized system is essentially the same as the performance for a channel whose zeros outside the unit disc have been reflected into the unit disc; this "equivalent" channel has a one-sided equalizer requiring no optimization. Consequently, there appears to be little loss of generality in considering only minimum-phase channels in evaluating performance.

Performance Analysis

The index of performance for the channel inversion approximation will be the mean-square equalization error,

$$\varepsilon^2 = \left|\left|1 - H(z)\ C(z)\right|\right|^2 \quad , \qquad (3\text{-}23)$$

rather than the approximation norm of (3-14). Equation (3-23) has more physical meaning than (3-14) and is easily calculated if use if made of (3-18) through (3-20).

As in Chapter 2, simple examples of selective fading channels lead to analytical results which provide insight

into the more general cases. First consider single-notch selective fading,

$$H(z) = 1 - re^{j\omega_0} z^{-1} \quad , \quad r \leq 1 \quad , \tag{3-24}$$

for which (3-23) is quite simple to evaluate using residue calculus:

$$\varepsilon^2 = (r^2)^{T_0} \quad , \tag{3-25}$$

where T_0 is the length of the observation interval. The magnitude of the channel zero, r, is related to the depth of selective fading by (2-49). Note that on a decibel scale the equalizer error is proportional to the observation interval, the constant of proportionality depending upon the fading depth.

For higher-order channel models the trends are generally the same: to see this consider a channel with two zeros.

$$H(z) = (1-r_1 z^{-1})(1-r_2 z^{-1}) \quad , \quad |r_2| \leq |r_1| \quad . \tag{3-26}$$

The equalization error for this channel may be shown to be

$$\varepsilon^2 = |r_1|^{2T_0} \cdot \frac{\left|1-\left[\frac{r_2}{r_1}\right]^{T_0+1}\right|^2 + |r_2|^2 \left|1-\left[\frac{r_2}{r_1}\right]^{T_0}\right|^2}{\left|1-\frac{r_2}{r_1}\right|^2} \tag{3-27}$$

If the channel roots are well separated (in radius), i.e.

$$\left|\frac{r_2}{r_1}\right|^{T_0} << 1 \quad ,$$

then

$$\varepsilon^2 \doteq \left|r_1\right|^{2T_0} \cdot \frac{1 + \left|r_2\right|^2}{\left|1 - \frac{r_2}{r_1}\right|^2} \quad . \tag{3-28}$$

This result is quite similar to (3-25): the error is <u>dominated</u> by that root closest to the unit circle, and there is a multiplicative factor (intercept on decibel scale) which causes a degradation in performance relative to (3-25).

To see what happens when the channel roots are not well separated, consider the case of two conjugate channel roots:

$$r_1 = re^{j\omega_0} \quad , \quad r_2 = re^{-j\omega_0} \tag{3-29}$$

Substituting into (3-27) we obtain

$$\varepsilon^2 = (r^2)^{T_0} \cdot \left\{\left[\frac{\mathrm{Sin}\omega_0(T_0+1)}{\mathrm{Sin}\omega_0}\right]^2 + r^2\left[\frac{\mathrm{Sin}\omega_0 T_0}{\mathrm{Sin}\omega_0}\right]^2\right\} . \tag{3-30}$$

Now there is an oscillatory multiplicative factor, but the dependence upon T_0 is still dominated by the channel root radius.

The degenerate case of multiple channel zeros is obtained by setting $\omega_0 = 0$ in (3-30).

$$\varepsilon^2 = (r^2)^{T_0} \cdot [(T_0+1)^2 + r^2 T_0^2] \quad . \qquad (3\text{-}31)$$

In this case the dependence upon T_0 is not basically linear (on a dB scale); however, multiple channel zeros would be unlikely to occur physically.

Calculations of the equalization error for higher-order channels gets algebraically complicated, and are best done numerically. These calculations show that the performance trends are similar to those of the preceding examples; in particular, the dependence upon T_0 is basically linear and the rate of improvement depends upon that channel zero closest to the unit circle. This point will be discussed more fully in the next section, where the performance of the Fourier series equalizer is compared to a somewhat different equalizer.

3.3 The Minimum Mean-Square Equalizer

Although the criterion used to evaluate the performance of the Fourier series equalizer was the mean square equalization error, that algorithm was not optimal in this sense. It is thus logical to consider the optimal transversal equalizer, successfully mechanized for telephone channels by Lucky and Rudin [26], to see whether this more complex system performs significantly better than the zero-forcing equalizer.

Let us assume a causal equalizer of the form

$$C(z) = \sum_{k=1}^{m} c_k z^{-(k-1)} \quad , \qquad (3\text{-}32)$$

where any required non-causality is realized by delay. That is, if n seconds of delay are required, the equalization error is

$$E(z) = z^{-n} - H(z)\ C(z) \quad . \tag{3-33}$$

Then the most general form for mean square error is

$$\varepsilon^2 = \langle R_a(z)E(z), E(z)\rangle = \frac{1}{2\pi j}\oint R_a(z)E(z)E^*(z^{-1})\frac{dz}{z}\ , \tag{3-34}$$

where $R_a(z)$ is a weighting function, typically the z transform of the message autocorrelation function.[1] This error may be written as

$$\varepsilon^2 = \frac{1}{2\pi j}\oint R_a(z)H(z)H^*(z^{-1})\left[\frac{z^{-n}}{H(z)} - C(z)\right]\left[\frac{z^n}{H^*(z^{-1})} - C^*(z^{-1})\right]\frac{dz}{z}\ , \tag{3-35}$$

which can be interpreted as the channel inversion error with respect to the non-uniform weighting function

$$W(z) = R_a(z)H(z)H^*(z^{-1}) \quad . \tag{3-36}$$

Defining the new, weighted inner-product

---

[1] For a flat message spectrum, $R_a(z) = 1$, while for the Markov message source of section 2.5,

$$R_a(z) = \frac{-2z\ \mathrm{Sinh}\alpha}{(z-e^{-\alpha})(z-e^{\alpha})}$$

$$\langle f(z), g(z) \rangle_W = \frac{1}{2\pi j} \oint W(z) f(z) g^*(z^{-1}) \frac{dz}{z} \quad , \tag{3-37}$$

we may use the Gram-Schmidt procedure[1] to find a sequence of basis functions $\{\psi_k(z)\}$, such that

$$\langle \psi_k(z), \psi_\ell(z) \rangle_W = \delta_{k\ell} \tag{3-38}$$

The required orthogonal basis functions are given explicitly by the recursion formula below.

$$\psi_k(z) = \frac{z^{-k} - \sum_{i=0}^{k-1} \langle z^{-k}, \psi_i \rangle_W \psi_i(z)}{\left|\left| z^{-k} - \sum_{i=0}^{k-1} \langle z^{-k}, \psi_i \rangle_W \psi_i(z) \right|\right|} \quad . \tag{3-39}$$

Then the equalizer which minimizes (3-35) is just the expansion

$$C(z) = \sum_{k=0}^{m-1} \left\langle \frac{z^{-n}}{H(z)}, \psi_k(z) \right\rangle_W \psi_k(z) \quad , \tag{3-40}$$

with corresponding equalization error given by

$$\begin{aligned} \varepsilon^2 &= \left|\left| \frac{z^{-n}}{H(z)} - C(z) \right|\right|_W^2 = \left\langle \frac{z^{-n}}{H(z)}, \frac{z^{-n}}{H(z)} \right\rangle_W - \langle C(z), C(z) \rangle_W \\ &= \left\langle \frac{z^{-n}}{H(z)}, \frac{z^{-n}}{H(z)} \right\rangle_W - \sum_{k=0}^{m-1} \left| \left\langle \frac{z^{-n}}{H(z)}, \psi_k(z) \right\rangle_W \right|^2 , \end{aligned} \tag{3-41}$$

---

[1] Ref. [46], p. 50.

where (3-40) has been substituted for C(z) in the last step. The evaluation of the various inner products in Equations (3-39) through (3-41) requires only the simple manipulation of polynomials of z to find residues of poles within the unit circle, an efficient computational technique which was used to perform all the calculations in this section except the case of single-notch fading, a special case which will be treated shortly.

In the discussion of the Fourier series equalizer it was shown that equalizer is causal for minimum-phase channels, a reasonable result since a channel with no zeros outside the unit disc in the z plane would be expected to have no corresponding poles in its approximate inverse (the equalizer). This was a useful property because it eliminated the need for juggling the number of positive and negative tap gains in an equalizer of given length to find the best combination. It is conjectured that this property is also true for the minimum mean square error equalizer. This conjecture has been borne out in all the examples considered, but a proof could not be found. However, its truth will be assumed in the discussion to follow.

An analytical expression for the minimum mean-square equalizer performance can be obtained for the case of single-notch selective fading by noting that the optimal message estimator given by Equations (3-2) and (3-3) must reduce to the optimal equalizer in the limit as the noise goes to zero. Both systems are transversal filters which minimize the mean

square error under identical conditions, so the truth of the statement should be apparent. The formal proof of equivalence is omitted for the sake of brevity. We can thus obtain the minimum mean square equalization error by letting $\eta \to \infty$ in the expression for the error covariance of the optimal demodulator, Equation (2-33).

$$\lim_{\eta \to \infty} \frac{1}{\eta} \left[\underline{\underline{H}}^{*T} \underline{\underline{H}} + \frac{1}{\eta} \underline{\underline{\Phi}}_a^{-1} \right]^{-1} \tag{3-42}$$

The diagonal elements of this matrix are the mean-square errors associated with all possible equalizers of length $T_0 = m$ seconds. The lower right-hand corner element of (3-42) corresponds to the causal transversal filter which operates only on the present and past values of the channel output. In accordance with our previous conjecture on causality, this will be assumed to be the best choice of equalizer tap gains for a minimum-phase channel.

For single-notch selective fading channels,

$$H(z) = h_1 + h_2 z^{-1} = \frac{1 - re^{j\omega_0} z^{-1}}{\sqrt{1 + r^2}}, \quad 0 \leq r \leq 1, \tag{3-43}$$

the matrix (3-42) was evaluated in Appendix C. Its lower right-hand corner element is given by Equation (C-24), for a flat message spectrum.[1]

---

[1]The Markov message case is also given in Appendix C but will not be discussed in this section because it is not directly comparable to the Fourier series equalizer, for which an unweighted performance index, (3-23), was used.

$$\varepsilon^2 = (r^2)^m \frac{1 - r^2}{1 - (r^2)^{m+1}}$$

$$= (r^2)^{T_0} \cdot \frac{1 - r^2}{1 - (r^2)^{T_0+1}} \qquad (3\text{-}44)$$

(3-44) is the equalization error for the optimal equalizer, valid for $0 \leq r \leq 1$, the condition for minimum phase. Comparing this result with the corresponding result for the Fourier series channel inverter, (3-25), we see that the optimal equalizer performs significantly better for severe fading channels, as illustrated by Figure 3-1. (D denotes the fading depth in decibels, related to r by (2-49).) Note that the two equalizers have assymptotically parallel error curves, but that the "y intercept" for the optimal equalizer can be much higher.

Figure 3-2 shows the performance of the optimal equalizer for the two-root channel defined by (3-26) and (3-28) for various angular separations of the roots. The dashed line gives the performance of an optimal equalizer for a single-notch fading channel with the same root radius, r. As was the case for the Fourier series equalizer, the performance is dominated by the root radius, but there are oscillatory deviations in the error curve similar to (3-30). The case of multiple channel roots ($\omega_0 = 0$) is degenerate in that the performance dependence is not purely exponential.

Figures 3-3 and 3-4 show equalizer performance for the five-tap example channels of section 2-1. The dashed lines

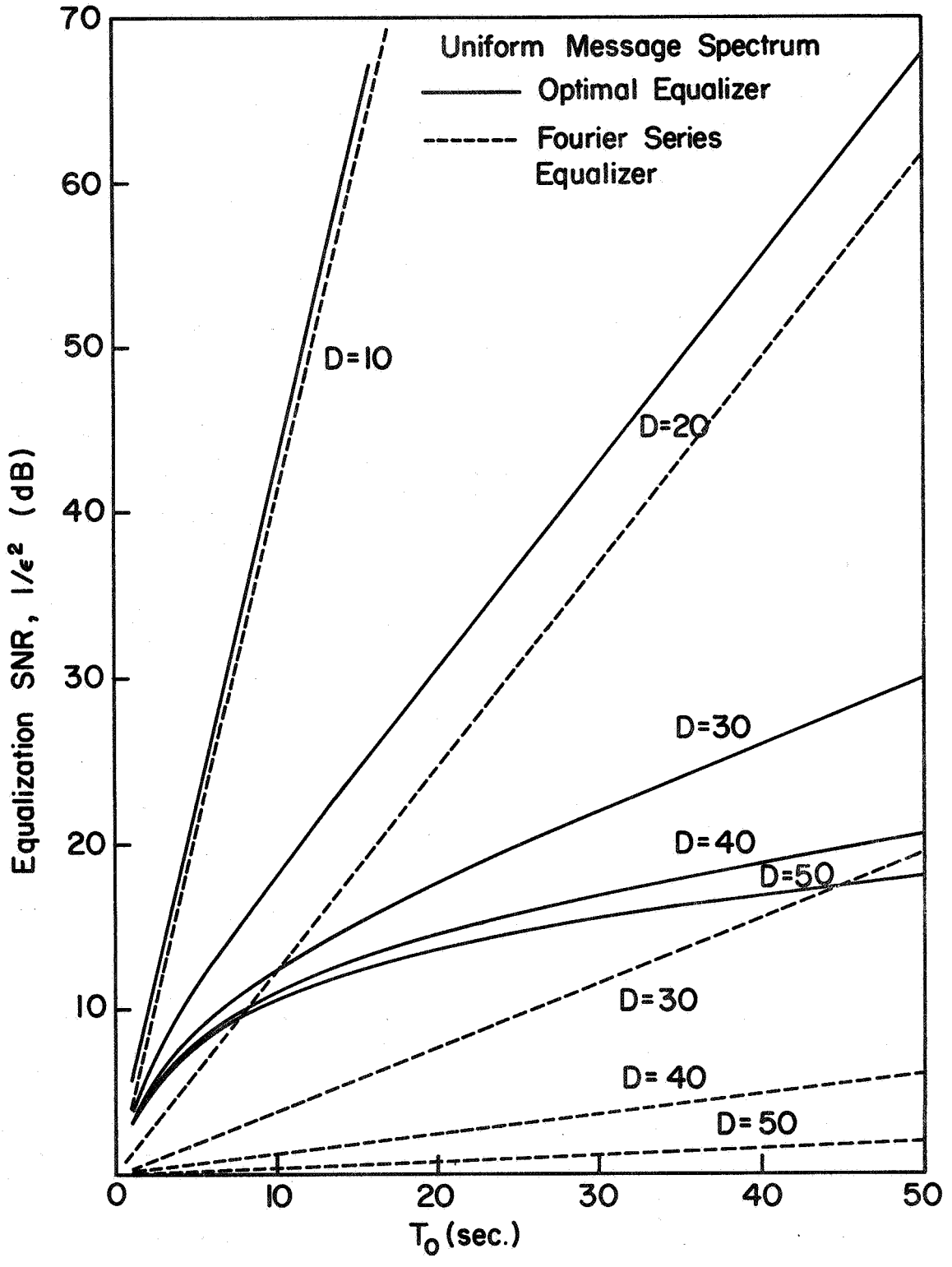

FIGURE 3-1. EQUALIZER PERFORMANCE FOR SINGLE-NOTCH SELECTIVE FADING.

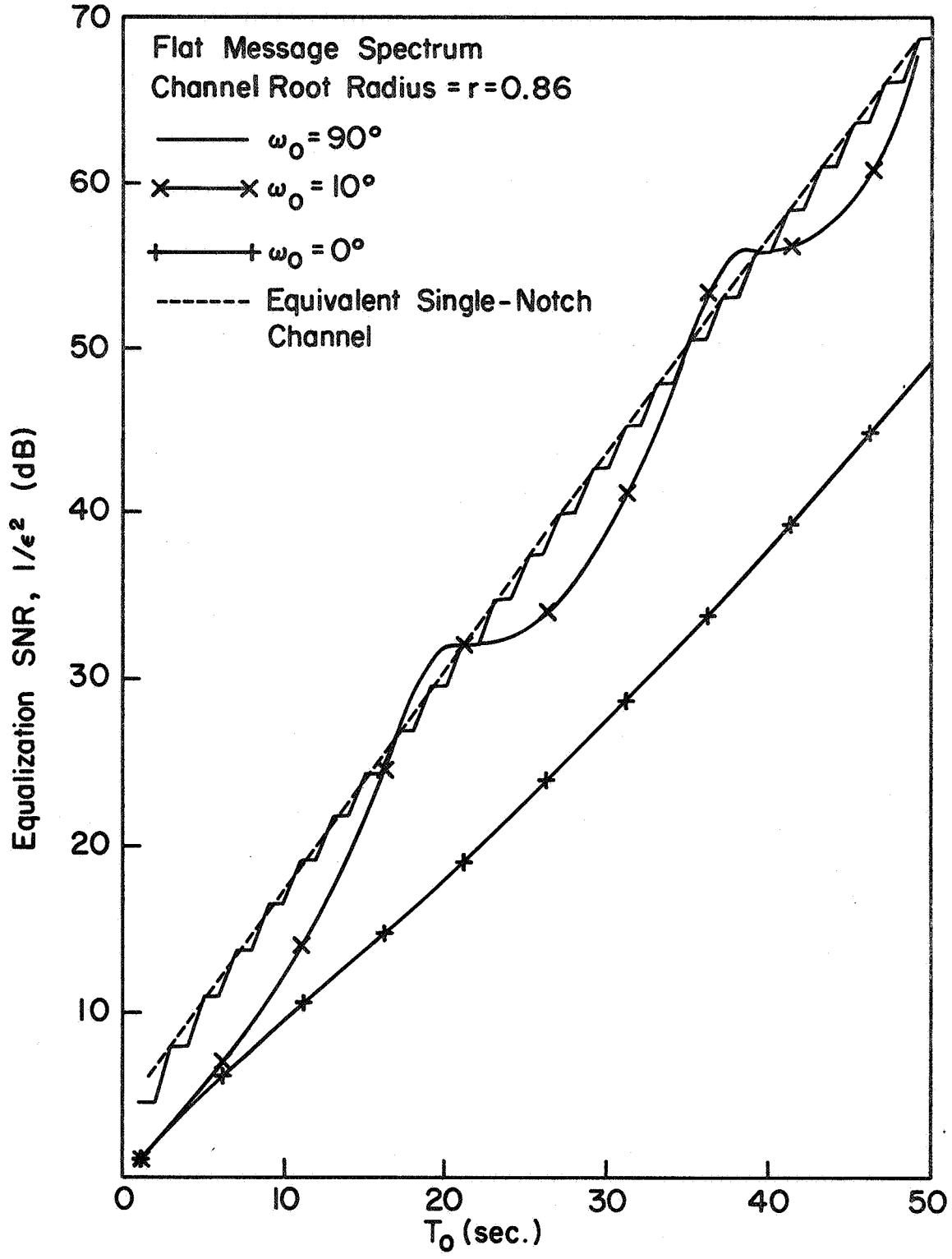

FIGURE 3-2. OPTIMAL EQUALIZER PERFORMANCE FOR TWO-ROOT CHANNELS.

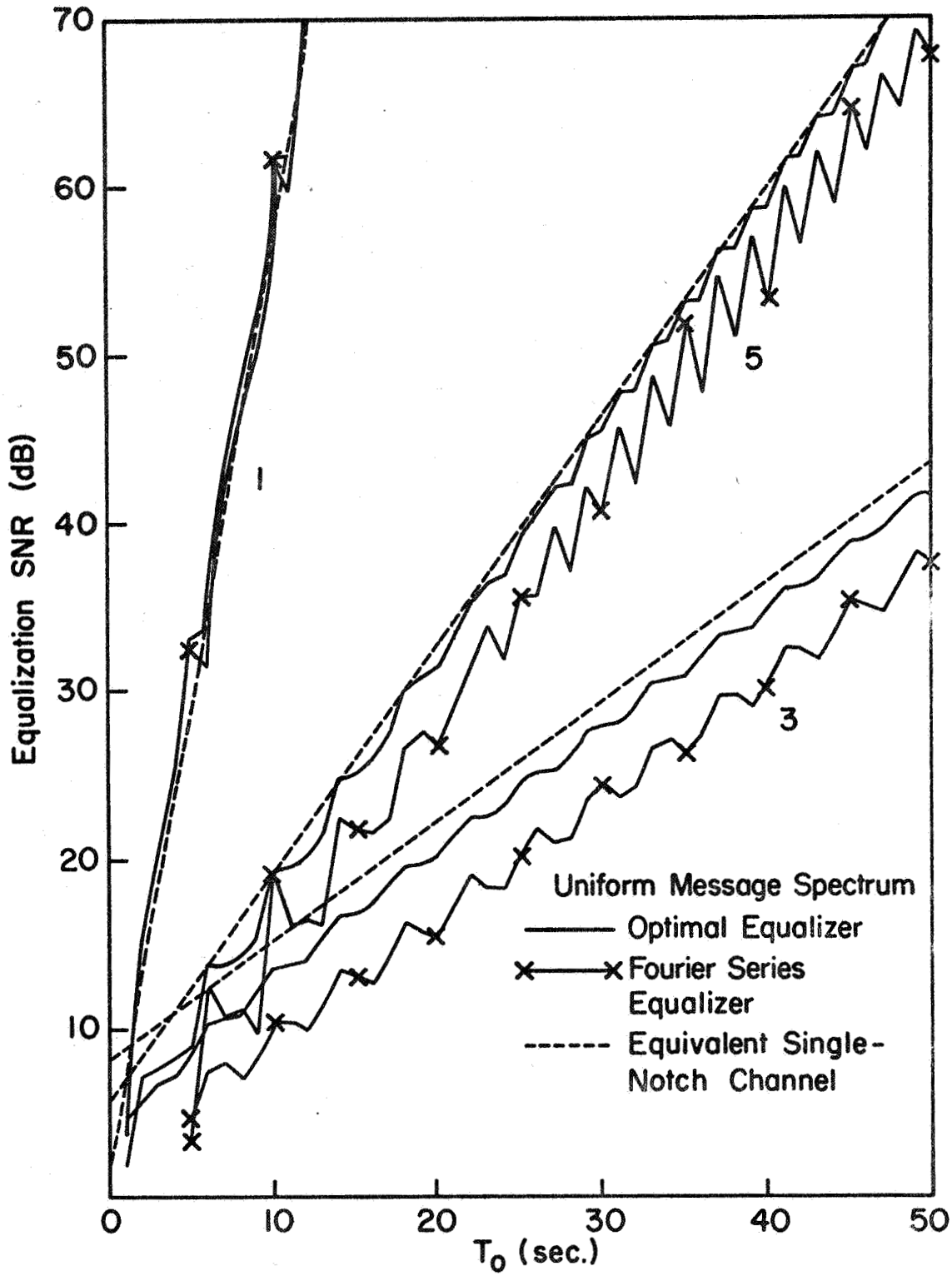

FIGURE 3-3. EQUALIZER PERFORMANCE FOR EXAMPLE CHANNELS 1, 3, AND 5.

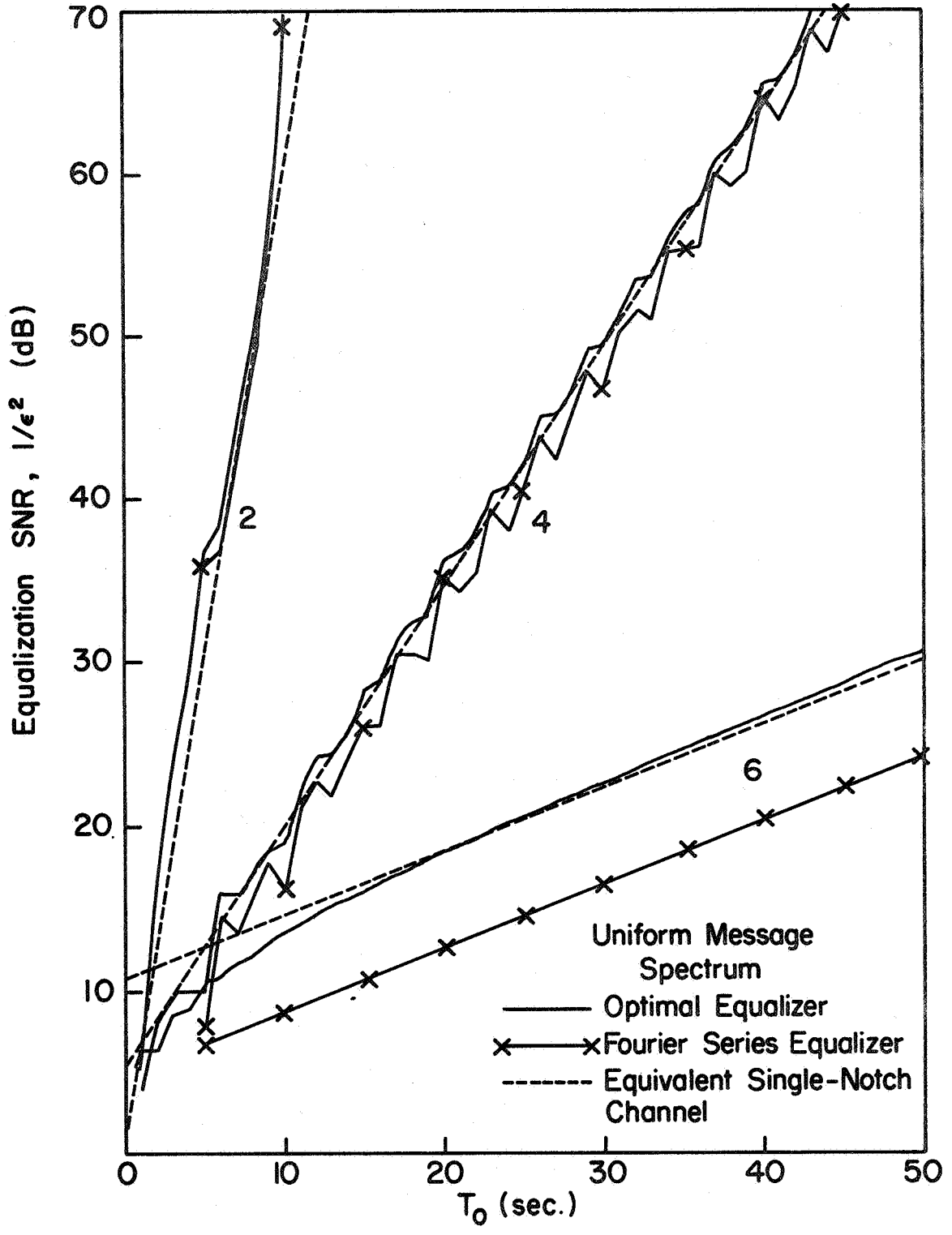

FIGURE 3-4. EQUALIZER PERFORMANCE FOR EXAMPLE CHANNELS 2, 4, AND 6.

give the performance of an optimal equalizer for a single-notch fading channel with its root taken to be that root of the five-tap channel closest to the unit circle. Note that the optimal equalizer performance is rather well described by the "equivalent" single notch channel performance; i.e., the additional channel roots with smaller radii add only fine-grain detail to the error curves. Again, the optimal equalizer is far superior to the Fourier series equalizer in cases of severe selective fading (channels 3 and 6). This behavior has been borne out by many more example channels which were randomly selected; equalizer performance is basically determined by the channel root closest to the unit circle, and Equation (3-51) may be used to roughly predict the number of optimal equalizer taps required for channel inversion.

These results for mean-square equalization error may be regarded as the performance of dispersive channel demodulators when there is no noise. Let us now go back to the case of noisy channels considered in section 3.1.

3.4 Approximate Demodulator Performance In the Presence of Noise

When the additive noise is bandlimited and white, and independent of the message it is easy to show that the performance of either equalizer is given by

$$\frac{1}{\sigma_a^2}\,\mathrm{Var}(\hat{a}-a) = \varepsilon^2 + \frac{1}{n}\sum_{k=1}^{m}\left|c_k\right|^2 , \qquad (3\text{-}45)$$

where ε^2 is the mean-square equalization error, η is the input SNR, and $\{c_k\}$ is the set of equalizer tap gains. This performance is illustrated in Figures 3-5 and 3-6 for single-notch fading channels and for two different observation intervals. Also included for purposes of comparison is the performance of the exact optimal demodulator (Figure 2-7). Some general observations may be made:

1. The optimal equalizer performs very nearly as well as the optimal demodulator when η is large (i.e., no post-equalization filtering is required).
2. The Fourier series equalizer is much inferior to the optimal equalizer if deep fades are expected.
3. When the demodulator is noise-limited (i.e., if ε^2 is much smaller than $1/\eta$) increasing the observation interval actually degrades performance if no post-equalization filtering is employed.
4. For systems with low input SNR, additional noise filtering is required to make the performance near-optimal, as can be seen by looking at the case η = 10 dB.

The poor performance of the equalizers at low input SNR's, compared to the optimal demodulator, brings us back to the post-equalization filter approximations of Equations (3-7)

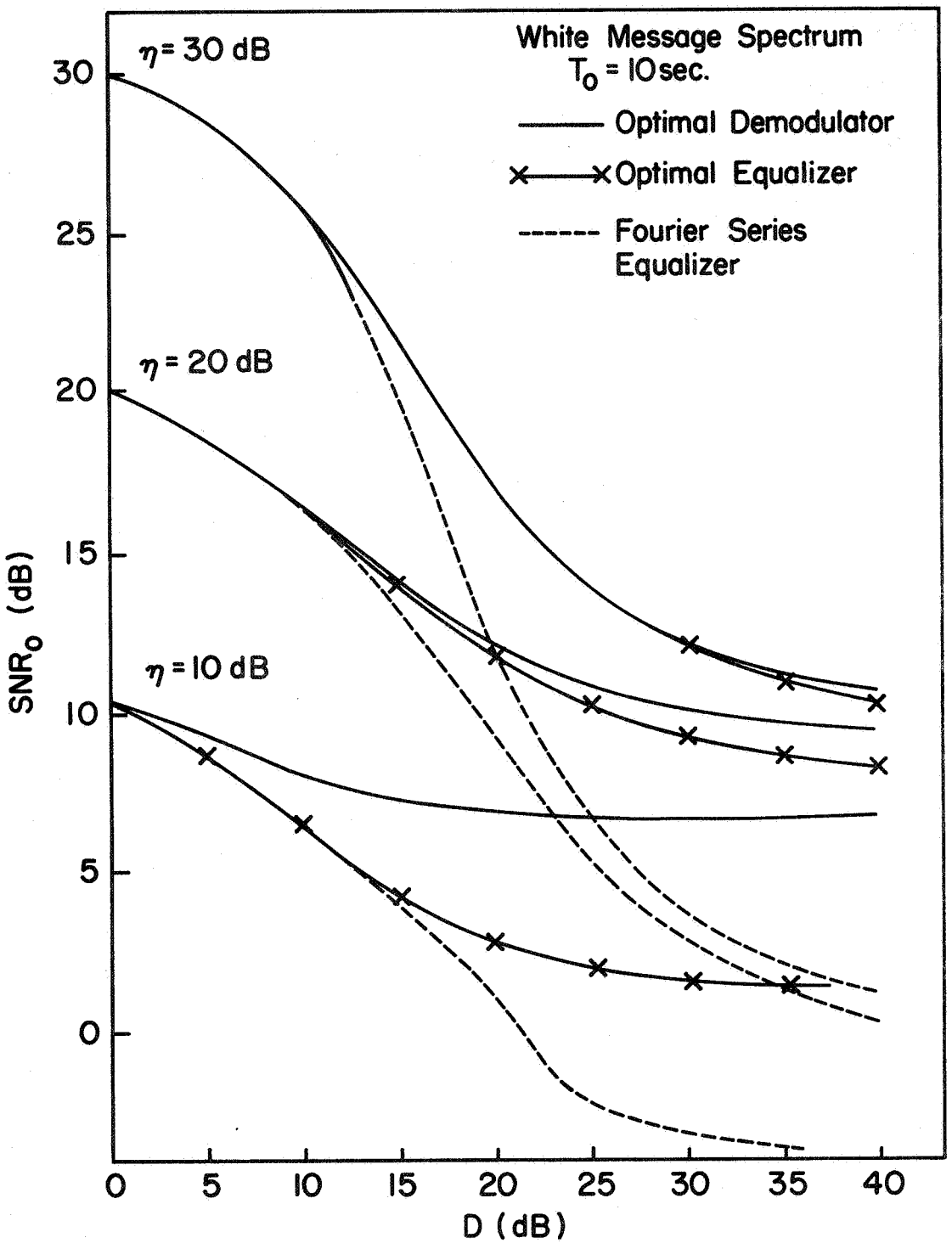

FIGURE 3-5. EQUALIZER PERFORMANCE FOR NOISY, SINGLE-NOTCH-FADING CHANNELS.

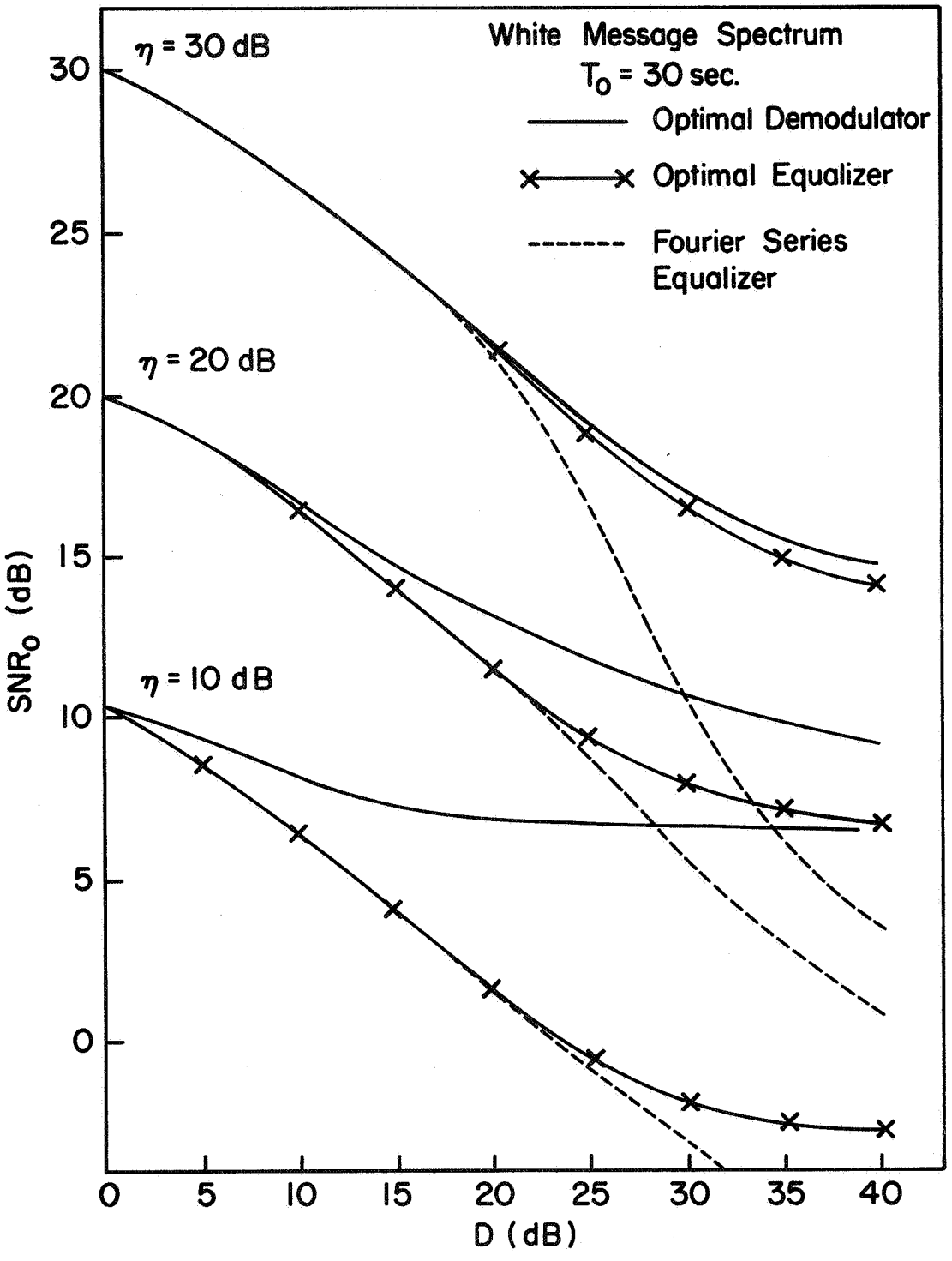

FIGURE 3-6. EQUALIZER PERFORMANCE FOR NOISY, SINGLE-NOTCH FADING CHANNELS.

and (3-8). Will a low order filter approximation of the form shown in (3-8) significantly improve system performance?

We will consider three cases of approximation of the form (3-8):

1. The zeroth order approximation,

$$F_0(j\omega) = C(j\omega) \quad . \tag{3-46}$$

2. The first order approximation,

$$F_1(j\omega) = C(j\omega)\left[1 - \frac{1}{\eta} G(\omega)|C(j\omega)|^2\right] \quad . \tag{3-47}$$

3. The exact post-equalization filter,

$$F_\infty(j\omega) = C(j\omega)\left[1 + \frac{1}{\eta} G(\omega)|C(j\omega)|^2\right]^{-1} \quad . \tag{3-48}$$

This last case could not be easily implemented, but gives a useful assymptotic result; it tells how much degradation in performance is due to imperfect channel inversion (equalization) alone.

The estimation error for the nth order approximate demodulator may be calculated using the expression

$$\mathrm{Var}(\hat{a}-a) = \frac{1}{2\pi}\int_{-\pi}^{\pi} \{|1 - F_n(j\omega)H(j\omega)|^2 S_a(\omega) + |F_n(j\omega)|^2 S_N(\omega)\}d\omega, \tag{3-49}$$

or by the analogous formulations using z transforms or matrices. However, before giving the results of such calculations it is interesting to consider the optimal demodulator

approximation from a discrete data viewpoint; this approach lends some theoretical insight into the nature of this approximation.

Equation (3-2) for the vector message estimate $\hat{\underline{a}}$ may be manipulated into the form

$$\hat{\underline{a}} = \underline{\underline{\Phi}}_a \underline{\underline{H}}^{*T} \left[\underline{\underline{H}} \underline{\underline{\Phi}}_a \underline{\underline{H}}^{*T} + \frac{1}{\eta} \underline{\underline{\Phi}}_N^{-1} \right]^{-1} \underline{Y} \tag{3-50}$$

if the inverse of the singular matrix $\underline{\underline{H}}$ is interpreted as the pseudo-inverse, or Moore-Penrose generalized inverse,[1]

$$\underline{\underline{H}}^{\dagger} \triangleq \underline{\underline{H}}^{*T} [\underline{\underline{H}} \underline{\underline{H}}^{*T}]^{-1} \tag{3-51}$$

Then, if the k^{th} column of $\underline{\underline{\Phi}}_a$ is denoted by ϕ_k, and the noise is assumed to be bandlimited and white, the optimal estimate of the k^{th} message sample can be written

$$\hat{a}_k = \underline{c}^T \left[\underline{\underline{I}} + \frac{1}{\eta} \underline{c}^* \underline{c}^T \right]^{-1} \underline{Y} \quad , \tag{3-52}$$

where

$$\underline{c}^T \triangleq \phi_k^{*T} \underline{\underline{H}}^{*T} \underline{\underline{R}}^{-1} \quad , \tag{3-53}$$

and

$$\underline{\underline{R}} \triangleq \underline{\underline{H}} \, \underline{\underline{\Phi}}_a \underline{\underline{H}}^{*T} \quad . \tag{3-54}$$

---

[1] Deutsch, R., Estimation Theory, Prentice Hall, Englewood Cliffs, New Jersey, 1965, Ch. 7.

$\underline{c}$ may be interpreted as the set of tap gain coefficients for the optimal transversal equalizer (let $\eta \to \infty$ in (3-59)), and the matrix

$$\underline{\underline{F}} \triangleq \left[\underline{\underline{I}} + \frac{1}{\eta}\,\underline{c}^{*}\underline{c}^{T}\right]^{-1} = \left[\underline{\underline{I}} + \frac{1}{\eta}\,\underline{\underline{R}}^{-1}\right]^{-1} \tag{3-55}$$

as a filter analogous to that of Equations (3-6) and (3-8). The n^{th} order approximate filter would be

$$\underline{\underline{F}}_n = \sum_{k=0}^{n}\left[\frac{-1}{\eta}\right]^{k}\underline{\underline{R}}^{-k} = \left[\underline{\underline{I}} - \left(\frac{-1}{\eta}\right)^{n+1}\underline{\underline{R}}^{-(n+1)}\right]\left[\underline{\underline{I}} + \frac{1}{\eta}\,\underline{\underline{R}}^{-1}\right]^{-1}, \tag{3-56}$$

so that the n^{th} order approximate demodulator would be written

$$\hat{a}_k = \underline{c}^{T}\underline{\underline{F}}_n\underline{Y} \quad . \tag{3-57}$$

The performance of (3-64) is then given by

$$\begin{aligned}\frac{1}{\sigma_a^2}\,\mathrm{Var}(\hat{a}_k - a_k) &= 1 + \underline{\phi}_k^{*T}\underline{\underline{H}}^{*T}\underline{\underline{R}}^{-1}\underline{\underline{F}}_n\left(\underline{\underline{R}} + \frac{1}{\eta}\,\underline{\underline{I}}\right)\underline{\underline{F}}_n\underline{\underline{R}}^{-1}\underline{\underline{H}}\underline{\phi}_k \\ &\quad -2\underline{\phi}_k^{*T}\underline{\underline{H}}^{*T}\underline{\underline{R}}^{-1}\underline{\underline{F}}_n\underline{\underline{H}}\underline{\phi}_k \qquad (3\text{-}58) \\ &= 1 - \underline{\phi}_k^{*T}\underline{\underline{H}}^{*T}\left[\underline{\underline{I}} - \left(\frac{1}{\eta}\right)^{2(n+1)}\underline{\underline{R}}^{-2(n+1)}\right]\left(\underline{\underline{R}} + \frac{1}{\eta}\,\underline{\underline{I}}\right)^{-1}\underline{\underline{H}}\underline{\phi}_k .\end{aligned}$$

In this derivation use is made of the Hermitian symmetry of $\underline{\underline{R}}$ and $\underline{\underline{F}}_n$, and of the fact that they commute. It is not difficult to show that the performance of the exact demodulator (3-52), is given by

$$\frac{1}{\sigma_a^2}\,\mathrm{Var}(\hat{a}_k - a_k) = 1 - \underline{\phi}_k^{*T}\underline{\underline{H}}^{*T}\left(\underline{\underline{R}} + \frac{1}{\eta}\,\underline{\underline{I}}\right)^{-1}\underline{\underline{H}}\underline{\phi}_k \quad . \tag{3-59}$$

Thus the quantity,

$$\frac{1}{\eta^{2(n+1)}} \cdot \underline{\phi}_k^{*T}\underline{\underline{H}}^{*T}\underline{\underline{R}}^{-2(n+1)}\left(\underline{\underline{R}} + \frac{1}{\eta}\,\underline{\underline{I}}\right)^{-1}\underline{\underline{H}}\underline{\phi}_k \quad ,$$

which appears in (3-58) can be interpreted as the additional demodulation error caused by truncating the matrix filter approximation. This error goes to zero as the $2(n+1)^{th}$ power of the input SNR, η.

Now let us examine the performance of the various approximate demodulators given by Equations (3-46) - (3-48). Tables 3-1 to 3-3 give demodulator performance (the output SNR in decibels) for various channel configurations, input SNR's and observation intervals; the message source is Markov, and the noise is white. The columns labeled one through seven give the output SNR's for the following demodulator configurations:

1. The optimal, finite observation time demodulator.
2. The optimal transversal equalizer followed by the exact post-equalization filter.
3. The optimal transversal equalizer followed by the first-order post-equalization filter.
4. The optimal transversal equalizer alone.

Table 3-1. System Performance for Single-Notch, Band-Edge Fading.

D (dB)	T_0 (sec)	n (dB)	System Combination Number 1	2	3	4	5	6	7
7	10	10	9.7	9.7	8.4	7.8	9.7	8.4	7.8
		20	18.1	18.1	18.1	17.8	18.1	18.1	17.8
		30	27.8	27.8	28.8	27.8	27.8	27.8	27.8
		40	37.8	37.8	37.8	37.8	37.8	37.8	37.8
	20	10	9.7	9.7	8.4	7.8	9.7	8.4	7.8
		20	18.1	18.1	18.1	17.8	18.1	18.1	17.8
		30	27.8	27.8	27.8	27.8	27.8	27.8	27.8
		40	37.8	37.8	37.8	37.8	37.8	37.8	37.8
23	10	10	8.8	8.6	-9.9	2.2	6.2	-15.7	0.2
		20	13.6	13.2	12.9	11.6	7.9	7.4	6.9
		30	18.1	18.0	18.0	17.8	8.9	8.9	8.9
		40	19.5	19.5	19.5	19.5	9.1	9.1	9.1
	20	10	8.8	8.6	-16.6	0.6	8.2	-18.0	0.2
		20	14.1	13.0	11.1	10.6	11.9	9.8	9.6
		30	20.5	20.4	20.4	20.1	16.4	16.4	16.4
		40	27.0	27.0	27.0	27.0	18.1	18.1	18.0
	30	10	8.8	8.6	-18.0	0.3	8.6	-18.2	0.2
		20	14.1	13.0	10.4	10.3	12.8	10.2	10.1
		30	20.9	20.9	20.6	20.2	19.8	19.8	19.5
		40	29.9	29.7	29.7	29.7	25.6	25.6	25.6
44	10	10	8.8	8.4	-11.3	1.7	1.2	-26.8	-4.2
		20	13.0	11.9	12.1	10.1	1.0	-0.6	0.0
		30	14.5	14.3	14.3	14.1	1.0	0.9	0.8
		40	14.9	14.8	14.8	14.8	0.9	0.9	0.9
	20	10	8.8	8.5	-23.0	-1.2	1.7	-35.9	-6.0
		20	13.7	11.9	7.6	8.4	1.7	-6.2	0.0
		30	16.9	16.2	16.2	15.6	1.8	1.8	1.5
		40	18.6	18.0	18.0	18.0	1.8	1.8	1.7
	30	10	8.8	8.5	-29.0	-2.9	2.3	-40.4	-7.0
		20	13.7	11.6	2.0	6.9	2.4	-10.3	0.0
		30	17.9	16.4	16.5	15.5	2.6	2.6	2.3
		40	20.2	19.8	19.8	19.7	2.6	2.6	2.6

Table 3-2. System Performance for Single-Notch, Center-Band Fading.

D (dB)	T_0 (sec)	n (db)	System Combination Number 1	2	3	4	5	6	7
7	10	10	8.5	8.5	8.4	7.8	8.5	8.4	7.8
		20	17.9	17.9	17.9	17.8	17.9	17.9	17.8
		30	27.8	27.8	27.8	27.8	27.8	27.8	27.8
		40	37.8	37.8	37.8	37.8	37.8	37.8	37.8
	20	10	8.5	8.5	8.4	7.8	8.5	8.4	7.8
		20	17.9	17.9	17.9	17.8	17.9	17.9	17.9
		30	27.8	27.8	27.8	27.8	27.8	27.8	27.8
		40	37.8	37.8	37.8	37.8	37.8	37.8	37.8
23	10	10	4.6	4.5	2.7	1.9	3.7	-1.5	0.2
		20	9.5	9.5	9.5	9.2	7.5	7.5	6.9
		30	11.9	11.8	11.8	11.7	8.9	8.9	8.9
		40	12.1	12.1	12.1	12.1	9.1	9.1	9.1
	20	10	4.9	4.4	-2.1	0.6	4.2	-3.4	0.2
		20	10.9	10.9	10.9	10.3	10.3	10.3	9.6
		30	18.1	18.1	18.1	18.1	16.3	16.3	16.2
		40	21.0	21.0	21.0	21.0	18.0	18.0	18.0
	30	10	4.9	4.3	-3.4	0.3	4.3	-3.6	0.2
		20	11.2	10.9	10.9	10.3	10.8	10.8	10.2
		30	20.0	20.0	20.0	19.9	19.5	19.5	19.5
		40	27.5	27.5	27.5	27.5	25.6	25.6	25.6
44	10	10	4.2	3.6	2.5	0.7	1.3	-12.4	-4.2
		20	6.3	6.2	6.2	5.7	1.2	1.5	0.0
		30	7.0	6.8	6.8	6.8	0.9	0.9	0.8
		40	7.0	6.9	6.9	6.9	0.9	0.9	0.9
	20	10	4.5	3.6	-7.9	-1.5	1.3	-21.7	-6.0
		20	8.0	6.2	7.6	6.3	1.9	1.9	0.0
		30	9.6	6.8	9.5	9.4	1.8	1.8	1.5
		40	10.0	6.9	9.9	9.9	1.8	1.8	1.7
	30	10	4.6	3.6	-14.3	-3.0	1.5	-26.3	-7.0
		20	8.8	7.4	7.4	5.9	2.4	1.3	0.0
		30	11.1	11.1	11.1	10.9	2.6	2.6	2.3
		40	11.9	11.9	11.9	11.9	2.6	2.6	2.6

Table 3-3. System Performance For Five Tap Example Channels.

Channel No.	T_0 (sec)	n (db)	System Combination Number 1	2	3	4	5	6	7
1	10	10	8.5	8.5	6.6	6.0	8.5	6.6	6.0
		20	16.4	16.4	16.4	15.6	16.4	16.4	15.6
		30	26.0	26.0	26.0	26.0	26.0	26.0	26.0
		40	36.0	36.0	36.0	36.0	36.0	36.0	36.0
	20	10	8.5	8.5	6.6	6.0	8.5	6.6	6.0
		20	16.4	16.4	16.4	16.0	16.4	16.4	16.0
		30	26.0	26.0	26.0	26.0	26.0	26.0	26.0
		40	36.0	36.0	36.0	36.0	36.0	36.0	36.0
2	10	10	9.2	9.2	7.7	7.1	9.2	7.7	7.1
		20	17.4	17.4	17.4	17.1	17.4	17.4	17.1
		30	27.1	27.1	27.1	27.1	27.1	27.1	27.1
		40	37.1	37.1	37.1	37.1	37.1	37.1	37.1
	20	10	9.2	9.2	7.7	7.1	9.2	7.7	7.1
		20	17.4	17.4	17.4	17.1	17.4	17.4	17.1
		30	27.1	27.1	27.1	27.1	27.1	27.1	27.1
		40	37.1	37.1	37.1	37.1	37.1	37.1	37.1
3	10	10	8.2	8.2	6.2	5.7	7.5	2.4	4.1
		20	13.8	13.8	13.8	13.5	11.5	11.5	10.9
		30	16.6	16.6	16.5	16.5	13.0	13.0	12.9
		40	17.0	17.0	17.0	17.0	13.2	13.1	13.1
	20	10	8.2	8.2	2.7	4.7	7.5	1.1	3.9
		20	14.9	14.7	14.7	14.2	12.6	12.6	12.1
		30	21.1	21.1	21.1	21.0	15.7	15.7	15.7
		40	23.2	23.2	23.2	23.2	16.3	16.3	16.3
4	10	10	8.0	7.9	7.4	6.4	7.0	6.6	5.6
		20	14.9	14.6	14.6	14.5	11.6	11.6	11.5
		30	18.5	17.9	17.9	17.9	13.0	13.0	13.0
		40	18.9	18.4	18.4	18.4	13.2	13.2	13.2
	20	10	8.2	8.0	7.4	6.4	8.0	7.4	6.4
		20	16.5	16.5	16.5	16.3	16.5	16.5	16.3
		30	26.0	26.0	26.0	26.0	25.9	25.9	25.9
		40	33.4	33.4	33.4	33.4	32.9	32.9	32.9

Table 3-3. (Continued)

Channel No.	T_0 (sec)	n (db)	System Combination Number 1	2	3	4	5	6	7
5	10	10	6.6	6.3	-3.9	1.8	6.1	-4.5	1.6
		20	12.2	12.2	12.1	11.4	11.7	11.7	10.9
		30	18.6	18.5	18.5	18.4	17.1	17.1	17.1
		40	20.9	20.8	20.8	20.7	18.7	18.7	18.7
	20	10	6.7	6.2	-4.5	1.6	6.1	-4.6	1.6
		20	12.7	12.5	12.4	11.6	12.2	12.1	11.4
		30	21.5	21.4	21.4	21.3	19.9	19.9	19.9
		40	29.5	29.5	29.5	29.5	23.9	23.9	23.9
6	10	10	9.2	8.8	8.0	7.2	7.7	2.4	4.8
		20	14.9	14.8	14.8	14.5	11.0	11.0	10.3
		30	17.2	17.2	17.1	17.0	11.7	11.7	11.6
		40	17.7	17.4	17.4	17.4	11.7	11.7	11.7
	20	10	9.3	8.7	3.3	6.0	8.1	-1.7	4.5
		20	16.0	15.7	15.7	15.2	13.1	13.1	12.2
		30	21.1	21.1	21.1	21.0	15.3	15.3	15.2
		40	22.4	22.4	22.4	22.4	15.7	15.7	15.6

5. The Fourier series equalizer followed by the exact post-equalization filter.
6. The Fourier series equalizer followed by the first order post-equalization filter.
7. The Fourier series equalizer alone.

Careful examination of the data in these tables leads one to conclude that a low-order post-equalization filter is not a worthwhile addition to the system; improvement in performance is obtained only over a limited range of η, and the resultant improvement is slight. Also, if the equalization is poor (small T_0 and deep fading), the performance exhibits a severe threshold effect for low η, and the performance is worse than that of the equalizer alone (itself poor). Consequently, if optimal or near-optimal performance is required for low input SNR's, it is apparently necessary to use the optimal demodulating system with all its attendant complexity; simple equalizers are not sufficient.

For high input SNR ($\eta \geq 25$ dB) it is clear from the tables and also Figures 3-5 and 3-6, that the minimum mean-square transversal equalizer is nearly optimal, and that it is distinctly superior to the Fourier series (zero-forcing) equalizer. Since this optimal equalizer can be mechanized with only a modest increase in hardware as compared to the zero-forcing equalizer (see [26] through [28]), it is regarded as the most promising compromise between system complexity and system performance.

The observation interval (number of equalizer taps) should be chosen so that the equalization error is of the same order as the reciprocal of the input SNR (see Equation (3-45)). Additional observation time will only increase the noise output of the system, a reflection of the fact that the equalization has converted the channel from a dispersion-limited one to an additive-noise-limited one. The noise at the equalizer output is highly "colored," and only sophisticated filtering (i.e., the optimal demodulator) will improve the low SNR performance.

In the rest of this research we will consider only the two most promising systems.

1. The optimal demodulator, because it is the only system considered which works well for all SNR, and is of interest of its own right.
2. The optimal transversal equalizer, because it is much simpler to mechanize than the optimal demodulator, and its performance approaches that of the optimal demodulator for high SNR.

3.5 A Summary of Results for Known Dispersive Channel Demodulation

The optimal vector estimator for the message is given by Equation (3-2) to be (for white noise)

$$\hat{\underline{a}} = \left[\underline{\underline{H}}^{*T}\underline{\underline{H}} + \frac{1}{\eta}\,\underline{\underline{\phi}}_a^{-1}\right]^{-1}\underline{\underline{H}}^{*T}\underline{y} \quad , \tag{3-60}$$

and its performance given by (2-33),

$$\underline{\underline{\Lambda}} \triangleq \frac{1}{\sigma_a^2}\,\mathrm{Cov}(\hat{\underline{a}}-\underline{a}) = \frac{1}{\eta}\left[\underline{\underline{H}}^{*T}\underline{\underline{H}} + \frac{1}{\eta}\,\underline{\underline{\phi}}_a^{-1}\right]^{-1} \quad . \tag{3-61}$$

An alternative form given by Equation (3-50) permits the k^{th} element of $\hat{\underline{a}}$ to be written

$$\hat{a}_k = \underline{\phi}_k^{*T}\underline{\underline{H}}^{*T}\left[\underline{\underline{H}}\,\underline{\underline{\phi}}_a\underline{\underline{H}}^{*T} + \frac{1}{\eta}\,\underline{\underline{I}}\right]^{-1}\underline{y} \ , \tag{3-62}$$

with error variance given by (3-59):

$$\frac{1}{\sigma_a^2}\,\mathrm{Var}(\hat{a}_k - a_k) = 1 - \underline{\phi}_k^{*T}\underline{\underline{H}}^{*T}\left[\underline{\underline{H}}\,\underline{\underline{\phi}}_a\underline{\underline{H}}^{*T} + \frac{1}{\eta}\,\underline{\underline{I}}\right]^{-1}\underline{\underline{H}}\underline{\phi}_k \ ,$$

where $\underline{\phi}_k$ is the k^{th} column of $\underline{\underline{\phi}}_a$.

The estimate of the message obtained using the optimal transversal equalizer is the expression (3-62) in the limit as $\eta\to\infty$, i.e.

$$\hat{a}_k = \underline{\phi}_k^{*T}\underline{\underline{H}}^{*T}\left[\underline{\underline{H}}\,\underline{\underline{\phi}}_a\underline{\underline{H}}^{*T}\right]^{-1}\underline{y} \tag{3-64}$$

$$= \underline{c}^T\underline{y} \quad ,$$

where $\underline{c}$ is the set of equalizer tap gain coefficients. The performance, in the presence of noise, of this equalizer is given by (3-45), or by setting n=0 in (3-58).

$$\frac{1}{\sigma_a^2}\,\mathrm{Var}(\hat{a}_k - a_k) = \varepsilon^2(T_0) + \frac{1}{\eta}\,\underline{c}^T\underline{c}^* \qquad (3\text{-}65)$$

$$= 1 - \underline{\phi}_k^{*T}\underline{\underline{H}}^{*T}\left[\underline{\underline{H}}\,\underline{\underline{\phi}}_a\underline{\underline{H}}^{*T}\right]^{-1}\underline{\underline{H}}\underline{\phi}_k + \frac{1}{\eta}\,\underline{c}^T\underline{c}^* \quad .$$

$\varepsilon^2(T_0)$ is the equalization error, the residual error due to the finite observation interval as the noise goes to zero ($\eta \to \infty$). It can be seen from (3-63) that the performance of the optimal message estimator also approaches $\varepsilon^2(T_0)$ as $\eta \to \infty$.

These equations, (3-60) through (3-65), are the fundamental equations for predicting system performance. The optimal demodulator performance as calculated using (3-61) or (3-63) has the general form shown by curve 1 of Figure 3-7. As $\eta \to \infty$ the performance approaches the equalization error, $\varepsilon^2(T_0)$. The optimal equalizer performance, (3-65), is of the form shown by curve 2 of Figure 3-7. Its performance coincides with that of the optimal demodulator for large η, but for noisy systems the performance drops off linearly (in dB) as indicated by the second term of (3-65).

The height of the equalization error assymptote, curve 3, may be raised by increasing the observation interval T_0. If T_0 is made sufficiently large, then the bending toward this assymptote of the demodulator performance can be made to occur at values of η outside the range of interest for design purposes, and the system will be effectively noise-limited rather than limited by residual dispersion. Under this condition, the observation interval may be regarded as infinite,

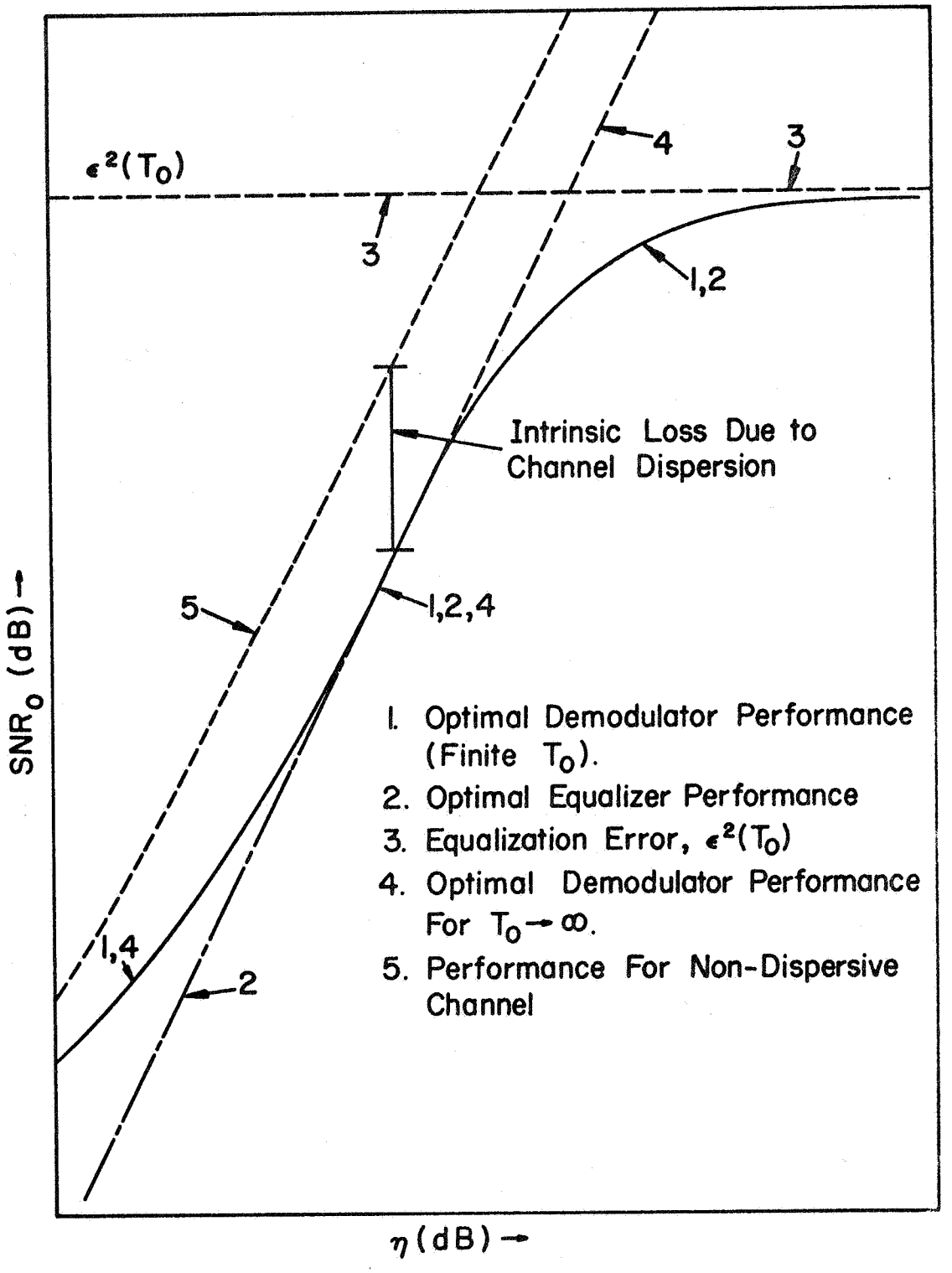

FIGURE 3-7. GENERALIZED PERFORMANCE OF DISPERSIVE CHANNEL DEMODULATORS.

and we may use the result for optimal demodulator performance given by (3-24), and rewritten here using z transforms:

$$\frac{1}{\sigma_a^2}\,\mathrm{Var}(\hat{a}(t)-a(t)) = \frac{1}{\eta}\cdot\frac{1}{2\pi j}\int \frac{1}{H(z^{-1})H^*(z)+\frac{1}{\eta}R_a^{-1}(z)}\,\frac{dz}{z} \tag{3-66}$$

This is shown as curve 4 in Figure 3-7. The performance is the same as for the finite T_0 optimal demodulator at low SNR, but continues to depend linearly upon η for large η, a consequence of the infinite observation time. Note that (3-66) requires only modest effort to evaluate (compared to (3-60) through (3-65)) and can often be performed analytically.

Note also from Figure 3-7 that an optimal equalizer with a sufficiently large observation interval has a performance curve of the same slope and intercept as the linear part of curve 4, so that the optimal equalizer has its performance under noise-limited conditions given by the assymptotic form of (3-66), i.e.,

$$\frac{1}{\sigma_a^2}\,\mathrm{Var}(\hat{a}(t)-a(t)) = \frac{1}{\eta}\cdot\frac{1}{2\pi j}\oint \frac{1}{H(z^{-1})H^*(z)}\,\frac{dz}{z}\ . \tag{3-67}$$

The constant

$$\frac{1}{2\pi j}\oint \frac{1}{H(z^{-1})H^*(z)}\,\frac{dz}{z}$$

is just the intrinsic loss in performance of a dispersive channel relative to a non-dispersive channel (see curve 5 of Figure 3-7) which was discussed in Section 2.5.

Examination of the assymptotic behavior shown in Figure 3-7 is reminiscent of the familiar Bode diagram[1] used in linear control theory to make rapid frequency response calculations, and suggests the following approximations for demodulator performance. The expression

$$\frac{1}{\sigma_a^2}\,\mathrm{Var}(\hat{a}(t)-a(t)) \doteq \frac{1}{\eta}\,\frac{1}{2\pi j}\oint \frac{1}{H(z^{-1})H^*(z) + \frac{1}{\eta}R_a^{-1}(z)}\,\frac{dz}{z} + \varepsilon^2(T_0) \tag{3-68}$$

could be used for optimal demodulator performance calculations, and the expression

$$\frac{1}{\sigma_a^2}\,\mathrm{Var}(\hat{a}(t)-a(t)) \doteq \frac{1}{\eta}\,\frac{1}{2\pi j}\oint \frac{1}{H(z^{-1})H^*(z)}\,\frac{dz}{z} + \varepsilon^2(T_0) \tag{3-69}$$

for the optimal transversal equalizer.

These expressions are excellent approximations to the exact performance equations, but are much easier to compute since the effect of the finite observation interval is isolated from the effects due to noise. The integrals of (3-68) and (3-69) may be evaluated using residue calculus, and the equalization error may be approximated using the method of an "equivalent" single-notch channel discussed at the end of Section 3.3. That is, we factor a high-order channel into a product of first order (single-notch) channels and compute

---

[1] Bower, J. L., and P. M. Schultheiss, Introduction to the Design of Servomechanisms, Wiley, N. Y., 1958, Ch. 6.

the equalization error for that single-notch channel with its root closest to the unit circle, using Equations (C-24) and (C-26) of Appendix C.

This technique requires only modest computations and permits rapid design calculations of reasonable accuracy.

CHAPTER 4: CHANNEL MEASUREMENT

4.1 Introduction

In this chapter techniques for the measurement of dispersive channels will be discussed. There are two basically different approaches to the problem of channel measurement: systems which measure the channel using the information-bearing signal alone; and systems which use a specially designed reference signal to measure the channel. It will be shown that the latter method leads to far simpler estimating systems than does the former, and that the difference in performance between the two is not very great. Optimal transmitted reference systems will be derived and analyzed, including the reference signal design, and some excellent suboptimal systems will be discussed as well.

4.2 Channel Estimation Using the Information-Bearing Signal Alone

The results of this section have been carried out using the sampled-data formulation of the dispersive channel demodulation problem as discussed in Section 2.4. The derivations are more straightforward and more easily interpreted using this formulation, and the resultant estimation scheme would probably have to be implemented on a digital computer anyway.

The observed channel output can be written in the form

$$\underline{y} = \underline{\underline{H}}\,\underline{a} + \underline{N} = \underline{\underline{A}}\,\underline{h} + \underline{N} \tag{4-1}$$

where $\underline{N}$, $\underline{\underline{H}}$, and $\underline{a}$ are as defined in Section 2.4, and

$$\underline{h} = \begin{bmatrix} h_1 \\ h_2 \\ \vdots \\ h_{n_c} \end{bmatrix}, \quad \underline{\underline{A}} = \begin{bmatrix} a_{n_c} & \cdots & a_1 \\ a_{n_c+1} & \cdots & a_2 \\ \vdots & & \\ a_{T_0+T_c} & \cdots & a_{T_0} \end{bmatrix}. \tag{4-2}$$

It is desired to estimate both the unknown vectors $\underline{a}$ and $\underline{h}$ on the basis of the observed channel output, $\underline{y}$, and prior knowledge of the statistics of the message $\underline{a}$. It will be assumed that $\underline{h}$ is an unknown, but non-random, parameter vector, so that no prior knowledge of $\underline{h}$ is available. The method of estimation will be to find the joint maximum likelihood estimate of the message and the channel state, i.e., maximize the probability density function $p(\underline{a},\underline{y}/\underline{h})$.[1] If the noise is assumed to be bandlimited and white, with variance σ_N^2, then this density function can be expressed in the following forms using (4-1) and (4-2).

---

[1]The joint probability density of the message $\underline{a}$ and observation $\underline{y}$ conditioned on a known channel, $\underline{h}$.

$$p(\underline{a},\underline{y}/\underline{h}) = K(\underline{y})\exp\left\{-\frac{1}{2\sigma_N^2}(\underline{y}-\underline{\underline{H}}\underline{a})^T(\underline{y}-\underline{\underline{H}}\underline{a}) - \frac{1}{2\sigma_a^2}\underline{a}^T\underline{\underline{\Phi}}_a^{-1}\underline{a}\right\}$$

$$= K(\underline{y})\exp\left\{-\frac{1}{2\sigma_N^2}(\underline{y}-\underline{\underline{A}}\underline{h})^T(\underline{y}-\underline{\underline{A}}\underline{h}) - \frac{1}{2\sigma_a^2}\underline{a}^T\underline{\underline{\Phi}}_a^{-1}\underline{a}\right\} \qquad (4\text{-}3)$$

K(y) is a constant not explicitly dependent upon $\underline{a}$ or $\underline{h}$. The optimization is carried out by setting the gradient of the logarithm of (4-3) equal to zero,[1] leading to the following set of simultaneous equations for the message and channel estimates, which are indicated by circumflex.

$$\hat{\underline{a}} = \left[\underline{\underline{H}}^T\underline{\underline{H}} + \frac{1}{\eta}\underline{\underline{\Phi}}_a^{-1}\right]^{-1}\hat{\underline{\underline{H}}}^T\underline{y} \qquad (4\text{-}4)$$

$$\hat{\underline{h}} = \left[\hat{\underline{\underline{A}}}^T\hat{\underline{\underline{A}}}\right]^{-1}\hat{\underline{\underline{A}}}^T\underline{y} \qquad (4\text{-}5)$$

This is a set of nonlinear equations, so there is no assurance that a solution exists, or is unique, but, even assuming such a solution could be found the indicated estimation procedure is a very complicated one indeed. It requires such extensive data storage and processing that a digital computer would surely be required to perform the estimation. An iterative solution seems the only practical method to solve such a system, so real-time data processing would require an extremely fast computer if the message bandwidth (sampling

---

[1] Deutsch, R., Estimation Theory, Prentice Hall, Englewood Cliffs, New Jersey, 1965, Ch. 3.

rate) is large. This rules the technique out for all but the largest, most specialized communications terminal applications.

The primary reason for considering this channel measurement technique at all is that it leads naturally to considerations of the Cramer-Rao lower bound [33] on the variance of unbiased estimators of the required parameters. This bound is useful for comparing with the performance of transmitted-reference channel measurement systems. It can be shown[1] that the error covariance matrix of any unbiased estimate of the parameter vector,

$$\underline{\theta} = \begin{bmatrix} \underline{a} \\ \underline{h} \end{bmatrix} \quad ,$$

must satisfy the matrix inequality,

$$\mathrm{Cov}(\underline{\hat{\theta}}-\underline{\theta}) - \underline{\underline{I}}^{-1} \geq 0 \quad , \tag{4-6}$$

where the inequality is taken in the sense that the matrix on the left side be positive semi-definite, and $\underline{\underline{I}}$ is the information matrix defined below. This is particular implies that[2]

---

[1] Rao, C. R., Linear Statistical Inference and Its Applications, Wiley, New York, 1965, p. 265. (The theorem as stated in this reference applies to conditional parameter estimates. It is easily extended to unconditional estimates by using the joint density function instead of the conditional, and interpreting expectations to be over the a-priori density of the message as well as the noise.)

[2] Hoffman and Kunze, Linear Algebra, Prentice Hall, Englewood Cliffs, New Jersey, 1961, p. 252.

$$\mathrm{Var}(\hat{\theta}_i - \theta_i) \geq \left[\underline{\underline{I}}^{-1}\right]_{ii} \tag{4-7}$$

That is, the diagonal elements of $\underline{\underline{I}}^{-1}$ give a lower bound on the error variance of any unbaised estimate of these parameters. The information matrix, $\underline{\underline{I}}$, is defined as follows.

$$[\underline{\underline{I}}]_{ij} = -E_{\underline{a},\underline{N}}\left[\frac{\partial^2 \ell n\ p(\underline{a},\underline{y}/\underline{h})}{\partial\theta_i \partial\theta_j}\right] \quad . \tag{4-8}$$

It is convenient to rewrite this using gradient notation.[1]

$$\underline{\underline{I}} = -E_{\underline{a},\underline{N}}\{\nabla_{\underline{\theta}}[\nabla_{\underline{\theta}} \ell n\ p)\underline{a},\underline{y}/\underline{h})]^T\} \quad . \tag{4-9}$$

This can be expressed in the partitioned form below.

$$\underline{\underline{I}} = -E_{\underline{a},\underline{N}}\begin{bmatrix} \nabla_{\underline{a}}[\nabla_{\underline{a}} \ell n\ p(\underline{a},\underline{y}/\underline{h})]^T & , & \nabla_{\underline{a}}[\nabla_{\underline{h}} \ell n\ p(\underline{a},\underline{y}/\underline{h})]^T \\ \nabla_{\underline{h}}[\nabla_{\underline{a}} \ell n\ p(\underline{a},\underline{y}/\underline{h})]^T & , & \nabla_{\underline{h}}[\nabla_{\underline{h}} \ell n\ p(\underline{a},\underline{y}/\underline{h})]^T \end{bmatrix} \tag{4-10}$$

Equation (4-3 may be used to show that

$$\nabla_{\underline{a}}\ \ell n\ p(\underline{a},\underline{y}/\underline{h}) = \frac{1}{\sigma_N^2}\underline{\underline{H}}^T\underline{y} - \left[\frac{1}{\sigma_N^2}\underline{\underline{H}}^T\underline{\underline{H}} + \frac{1}{\sigma_a^2}\underline{\underline{\phi}}_a^{-1}\right]^{-1}\underline{a} \tag{4-11}$$

$$\nabla_{\underline{h}}\ \ell n\ p(\underline{a},\underline{y}/\underline{h}) = \frac{1}{\sigma_N^2}\underline{\underline{A}}^T\underline{y} - \frac{1}{\sigma_N^2}\underline{\underline{A}}^T\underline{\underline{A}}\ \underline{h} \tag{4-12}$$

---

[1] See Deutsch, R., Estimation Theory, Prentice Hall, Englewood Cliffs, New Jersey, 1965, Ch. 3.

The off-diagonal partitions of (4-10) have zero expected value. This can be seen from (4-11) and (4-12) since the random vectors $\underline{a}$ and $\underline{y}$ appear linearly, and have zero mean. The diagonal partitions of (4-10) are gotten by taking the second gradients of (4-11) and (4-12).

$$\nabla_{\underline{a}}[\nabla_{\underline{a}} \ln p(\underline{a},\underline{y}/\underline{h})]^T = -\frac{1}{\sigma_N^2} \underline{\underline{H}}^T \underline{\underline{H}} - \frac{1}{\sigma_a^2} \underline{\underline{\Phi}}_a^{-1}, \quad (4\text{-}13)$$

$$\nabla_{\underline{h}}[\nabla_{\underline{h}} \ln p(\underline{a},\underline{y}/\underline{h})]^T = -\frac{1}{\sigma_N^2} \underline{\underline{A}}^T \underline{\underline{A}} \quad (4\text{-}14)$$

Thus the information matrix can be expressed in the form below.

$$\underline{\underline{I}} = \begin{bmatrix} \left[\frac{1}{\sigma_N^2} \underline{\underline{H}}^T \underline{\underline{H}} + \frac{1}{\sigma_a^2} \underline{\underline{\Phi}}_a^{-1}\right], & \underline{\underline{0}} \\ \underline{\underline{0}}, & E_{\underline{a}}\left[\frac{1}{\sigma_N^2} \underline{\underline{A}}^T \underline{\underline{A}}\right] \end{bmatrix} \quad (4\text{-}15)$$

Examination of the definition of the matrix $\underline{\underline{A}}$, Equation (4-2), indicates that

$$\frac{1}{\sigma_N^2} E_{\underline{a}}[\underline{\underline{A}}^T \underline{\underline{A}}] = \frac{\sigma_a^2}{\sigma_N^2} T_0 \underline{\underline{\Phi}}'_a$$

where T_0 is the number of observations of the channel output (observation time) and $\underline{\underline{\Phi}}'_a$ is the normalized covariance matrix

of an n_c-dimensional vector of message samples. If the ratio $\eta=\sigma_a^2/\sigma_N^2$ is interpreted as the input SNR, then, by (4-6),

$$\mathrm{Cov}\begin{bmatrix}\hat{\underline{a}}-\underline{a}\\ \hat{\underline{h}}-\underline{h}\end{bmatrix} \geq \underline{\underline{I}}^{-1} = \begin{bmatrix}\frac{\sigma_a^2}{\eta}\left[\underline{\underline{H}}^T\ \underline{\underline{H}} + \frac{1}{\eta}\ \underline{\underline{\Phi}}_a^{-1}\right] & \underline{\underline{0}}\\ \underline{\underline{0}} & \frac{1}{\eta T_0}\ \underline{\underline{\Phi}}_a'^{-1}\end{bmatrix}^{-1}, \qquad (4\text{-}16)$$

If the upper-diagonal partition of (4-16) (the message error-covariance) is compared with Equation (2-33), it can be seen that the lower bound on the error of the message portion of the joint estimation scheme is equal to the performance of the optimal message estimator for a known channel. It would, however, be impossible for the joint estimator to achieve this bound with a finite observation interval since the channel is not known perfectly.

The bound on the channel measurement,

$$\mathrm{Cov}(\hat{\underline{h}}-\underline{h}) = \frac{1}{\eta T_0}\ \underline{\underline{\Phi}}_a'^{-1}, \qquad (4\text{-}17)$$

is more realistic in that the error goes down in inverse proportion to the length of the measurement interval and the input SNR. If, in Equation (4-5) for the channel estimate, it were assumed that the message estimate, $\hat{\underline{\underline{A}}}$, were perfect, then it can be shown that (4-5) achieves the lower bound (4-17). In any non-ideal joint channel and message estimate there will always be some residual message estimation error, so the channel estimates will not be this good. However,

some crude, approximate calculations have indicated that the bound is unlikely to be more than an order of magnitude optimistic, and could quite conceivably be within a few decibels of actual performance if the input SNR is high.

The following observations concerning channel estimation using the information-bearing signal are in order.

1. This type of estimation is desirable in that all transmitter power goes into information transmission.
2. Joint estimation of channel and message is complicated. The estimate is nonlinear, requires an iterative or sequential solution, and could not be done in real time on large bandwidth channels with existing computer hardware.
3. The performance of this scheme is somewhat in doubt. There is no assurance that a solution will exist, or that a sequential procedure would converge to the solution if it did exist.
4. The drawbacks of such a scheme indicate that an investigation of simpler, transmitted-reference techniques is merited.

4.3 Channel Estimation Using Transmitted Reference Signals

The physical system required to measure the state of an unknown, dispersive channel may be greatly simplified if a

reference signal, known in advance at the receiver, is transmitted over the channel for the express purpose of making this measurement. Such a signal would be multiplexed with the information-bearing signal, and channel measurements made at time intervals consistent with the time variation of the channel. One method of performing this multiplexing is by time division. A short measurement signal could be periodically alternated with the message to keep the receiver informed of the true channel state. Another method of multiplexing is frequency division; single-sideband techniques could be used to transmit the reference signal on one sideband and the message on the other: the sidebands used would be periodically alternated. Longer measurements would be possible with the latter system without interrupting the information flow. (With a longer time interval it is possible to achieve larger signal signal energy for a given signal power.)

With either of the multiplexing schemes described it is possible to independently isolate the message and reference signals at the receiver, regardless of the channel state. The channel output due to the reference signal input can then be written

$$y(t) = h(t) \circledast s(t) + N(t), \qquad (4\text{-}18)$$

where s(t) is a known (possibly complex) reference waveform. When the tapped delay line channel model is assumed, (4-18) can be written in the following, more convenient form.

$$y(t) = \underline{h}^T \underline{s}(t) + N(t) = \underline{s}^T(t)\underline{h} + N(t), \qquad (4\text{-}19)$$

where

$$\underline{h} = \begin{bmatrix} h_1 \\ h_2 \\ \cdot \\ \cdot \\ \cdot \\ h_{n_c} \end{bmatrix}, \qquad \underline{s}(t) = \begin{bmatrix} s(t) \\ s(t-1) \\ \cdot \\ \cdot \\ \cdot \\ s(t-T_c) \end{bmatrix} \qquad (4\text{-}20)$$

The maximum likelihood technique for estimating a finite set of unknown parameters is well known[1] to be equivalent to the minimization of the functional

$$L(\underline{h}) = \int_0^{T_m} |\underline{y}(t) - \underline{h}^T\underline{s}(t)|^2 dt \quad . \qquad (4\text{-}21)$$

Equation (4-21) assumes that the channel output is observed over the time interval $0 \leq t \leq T_m$, and that the additive noise is essentially white. Here T_m denotes the measurement time. A necessary condition (it is also sufficient since $L(\underline{h})$ is convex) for the minimization of L requires that

$$\underline{0} = \nabla_{\underline{h}} L(\underline{h}) = \nabla_{\underline{h}} \int_0^{T_m} [y(t) - \underline{h}^T\underline{s}(t)][y(t) - \underline{h}^T\underline{s}(t)]^* dt$$

$$= -2\int_0^{T_m} [y(t) - \underline{h}^T\underline{s}(t)]^* \underline{s}(t)\, dt \quad . \qquad (4\text{-}22)$$

---

[1] Helstrom, Statistical Theory of Signal Detection, Pergamon Press, London, 1960, p. 199.

This equation may be solved for $\underline{h}$ to provide the following channel estimate.

$$\underline{\hat{h}} = \left[\int_0^{T_m} \underline{s}^*(t)\ \underline{s}^T(t)dt\right]^{-1} \int_0^{T_m} \underline{s}^*(t)\ y(t)dt \quad . \tag{4-23}$$

Suppose that s(t) satisfies either of the following conditions:

1. If s(t) is periodic, then T_m is a multiple of its period.
2. If s(t) is aperiodic, with duration T_s, then $T_m \geq T_s + T_c$, where T_c is the channel delay spread. (See Section 2.1)

Then the following identification is possible.

$$\int_0^{T_m} \underline{s}^*(t)\ \underline{s}^T(t)dt = E_s\ \underline{\underline{R}}_s \tag{4-24}$$

Here E_s denotes the total signal energy, and $\underline{\underline{R}}_s$ is the $(n_c x n_c)$ matrix of time samples of the normalized signal autocorrelation function. That is,

$$\left[\underline{\underline{R}}_s\right]_{ij} = \rho_s(j-i) \quad ,$$

where

$$\rho_s(\tau) = \frac{1}{E_s} \int_0^{T_m} s(t)s^*(t+\tau)dt \quad . \tag{4-25}$$

The optimal channel estimator then has the interpretation of a system which crosscorrelates the observed signal with various delayed replicas of the reference signal, and then performs a known linear combining operation on the correlator outputs to form the channel tap-gain estimates. This is a much simpler system than the joint channel and message estimator, and may be easily implemented with analog components.

The performance of the channel estimator is of great interest. Note that (4-23) can be rewritten in the form,

$$\hat{\underline{h}} = \frac{1}{E_s} \underline{\underline{R}}_s^{-1} \int_0^{T_m} \underline{s}^*(t) [\underline{s}^T(t)\ \underline{h} + N(t)]dt$$

$$= \underline{h} + \frac{1}{E_s} \underline{\underline{R}}_s^{-1} \int_0^{T_m} \underline{s}^*(t) N(t) dt \quad . \tag{4-26}$$

It then is easy to see that the estimator is unbiased,

$$E[\hat{\underline{h}}] = \underline{h} \quad , \tag{4-27}$$

and that

$$\mathrm{Cov}(\hat{\underline{h}}-\underline{h}) = \frac{1}{E_s^2} \underline{\underline{R}}_s^{-1} E\left\{ \int_0^{T_m} \int_0^{T_m} \underline{s}^*(t) \underline{s}^T(t) N(t) N^*(\tau) dt d\tau \right\} \underline{\underline{R}}_s^{-1}$$

$$= \frac{\sigma_N^2}{E_s} \underline{\underline{R}}_s^{-1} \tag{4-28}$$

Note that the measurement error decreases as the signal energy-to-noise power ratio (measurement SNR) increases, and that this error depends upon the choice of the reference signal through the correlation matrix $\underline{\underline{R}}_s$, given by Equation (4-25). This dependence upon the reference signal leads naturally to the investigation of the design of these signals to minimize the measurement error.

4.4 Optimal Choice of Reference Signals

Equation (4-27) shows that, for a given signal energy, the measurement error covariance depends upon the reference signal only through the signal autocorrelation function. Under the assumed normalization condition on $\underline{\underline{R}}_s$, Equation (4-24), the diagonal elements of $\underline{\underline{R}}_s$ must be unity. Also, since $\underline{\underline{R}}_s$ is the correlation matrix of a physical signal with positive power spectrum, it must be a positive semidefinite matrix.[1] It may thus be factored[2] in the following way,

$$\underline{\underline{R}}_s = \underline{\underline{R}}_s^{\frac{1}{2}} \cdot \underline{\underline{R}}_s^{\frac{1}{2}} \quad , \tag{4-29}$$

where the "square root" matrix, $R_s^{\frac{1}{2}}$, is Hermitian and positive semidefinite. With the assumed normalization, and with the factorization (4-29), the signal optimization problem is

---

[1] Papoulis, Probability, Random Variables, and Stochastic Processes, McGraw-Hill, New York, 1965, p. 349.

[2] Riesz, Sz.-Nagy, Functional Analysis, Ungar, New York, 1955, p. 265.

mathematically equivalent to the theorem of Rao[1] which states that

$$\left[\underline{\underline{R}}_s^{-1}\right]_{ii} \geq 1 \quad , \tag{4-30}$$

where the equality holds if

$$\underline{\underline{R}}_s = \underline{\underline{I}} \quad . \tag{4-31}$$

This implies that the measurement error variance is minimized by choosing $\underline{\underline{R}}_s$ as in Equation (4-31); and, under this condition, the measurement errors for different tap-gains are uncorrelated. That is,

$$\text{Cov}(\underline{\hat{h}}-\underline{h}) = \frac{\sigma_N^2}{E_s} \underline{\underline{I}} \tag{4-32}$$

The optimality condition on the reference signal thus reduces to the following restriction on its normalized autocorrelation function, $\rho_s(\tau)$.

$$\rho_s(\tau) = \begin{cases} 1; & \tau = 0 \\ 0; & |\tau| = 1,2, \ldots T_c \end{cases} \tag{4-33}$$

For pulse train signals of unit width this means that s(t) must have zero autocorrelation out to a value of delay equal to the channel delay spread, $T_c = n_c - 1$, and is arbitrary beyond that point. This is illustrated in Figure 4-1.

---

[1] Rao, Linear Statistical Inference and its Applications, Wiley, New York, 1965, p. 194.

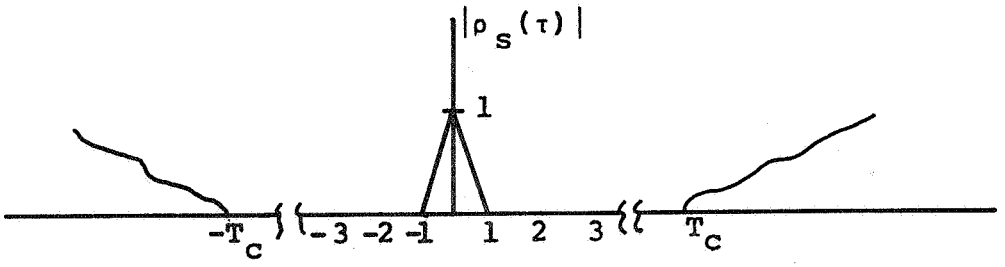

Figure 4-1. Autocorrelation Function of Optimal Reference Signal.

For signals which satisfy (4-31), the linear combining operation in the channel estimator, (4-23), is no longer required, so the estimating system reduces to a simple bank of crosscorrelators, as shown in Figure 4-2.

4.5 Design of Reference Signals

Condition (4-33) for the optimal reference signal defines classes of signals rather than the signals themselves. There is a consequent freedom of choice in picking the reference signal, and this freedom may be used to satisfy additional constraints imposed by practical systems. There are two broad classes of reference signals which can be considered:

1. Aperiodic, "one-shot" signals are useful for time-division multiplexing of the message and reference.
2. Periodic Signals are convenient when long, continuous measurements of the channel state

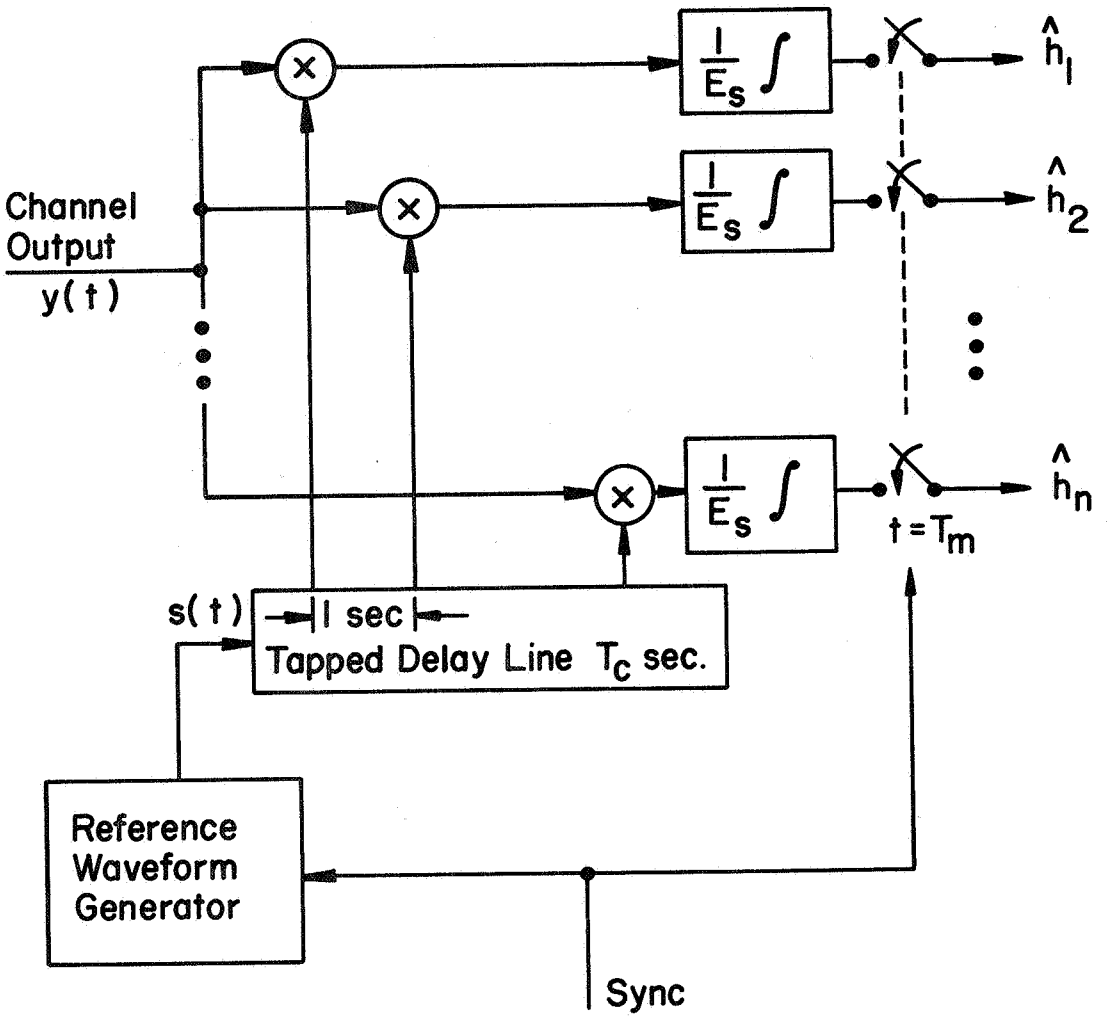

FIGURE 4-2. CHANNEL MEASUREMENT SYSTEM USING OPTIMAL TRANSMITTED-REFERENCE SIGNALS.

are possible, as in the case of the frequency-division multiplexing discussed in Section 4-3. In either of these cases it is convenient to use pulse-train signals for reference signals. The nominal signal bandwidth is easily controlled by the duration of an individual pulse in the train of pulses. (One second duration using the time-frequency normalization assumed in this research.) Also, pulse signals are easier to store, generate, and synchronize than more general waveforms; only a finite set of numbers are required to describe the signal. It will also be assumed in the discussion to follow that the reference signals are real. Real signals are a logical choice since the reference signal would normally be generated at baseband, where the representation must be real. An exception would be the case of SSB, where the baseband representation has an imaginary part which is the Hilbert transform of the real part. However, it is well known[1] that the autocorrelation function of the Hilbert transform of a signal equals the autocorrelation function of the signal itself, so the SSB version of a signal will be optimal if and only if its real part is optimal.

Aperiodic Signals

1. The simplest form of optimal reference signal is a single pulse (bandlimited impulse) with autocorrelation function of the form shown in

---

[1] Schwartz, Bennett, Stein, Communication Systems and Techniques, McGraw-Hill, New York, 1966, p. 34.

Figure 4-3. This signal is disadvantageous because it has low energy for a given peak power and measurement interval. Since, by (4-27), the measurement error is inversely proportional to the signal energy contained in the measurement interval, and since transmitters are normally limited in peak power, this is a serious drawback. If P_s denotes the maximum available peak power, then the total energy is given by

$$E_s = P_s \quad . \tag{4-34}$$

2. A better class of optimal signals is the set of "impulse equivalent pulse trains," or Huffman codes [47]. These are amplitude modulated pulse trains with autocorrelation functions as shown in Figure 4-4. If, for a given channel delay spread, the length of a Huffman code is at least one second longer, then these codes are optimal. Huffman codes up to length 14 have been investigated in this research to determine their energy distribution, and it has been found that average-to-peak power ratios on the order of 0.40 to 0.55 can be achieved. The achievable ratio tends downward as the codes get longer. For these

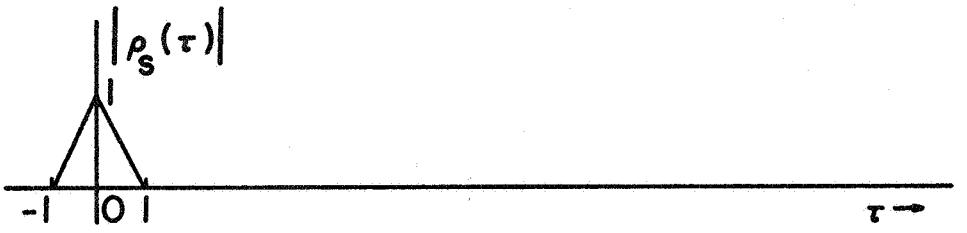

FIGURE 4-3. AUTOCORRELATION FUNCTION OF SINGLE PULSE

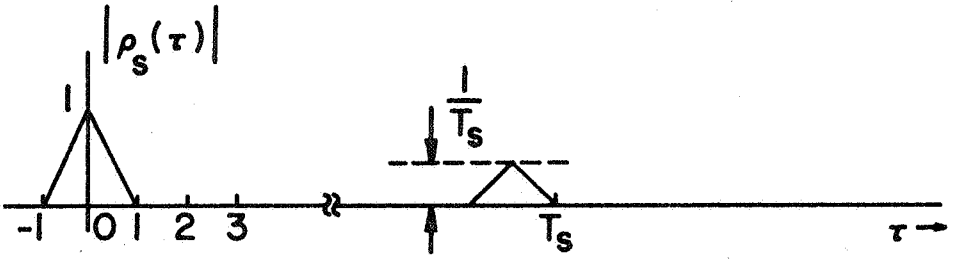

FIGURE 4-4. AUTOCORRELATION FUNCTION OF HUFFMAN CODE

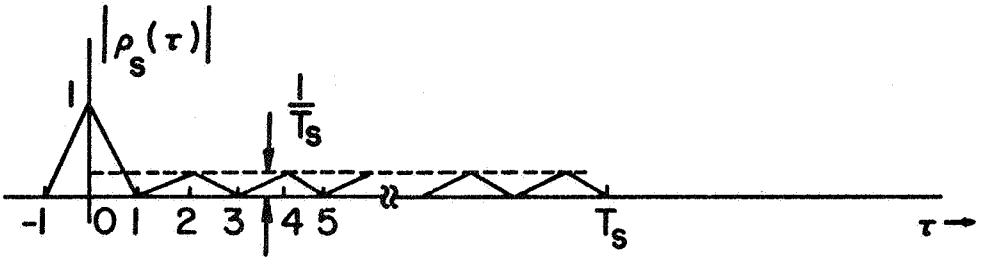

FIGURE 4-5. AUTOCORRELATION FUNCTION OF BARKER CODE

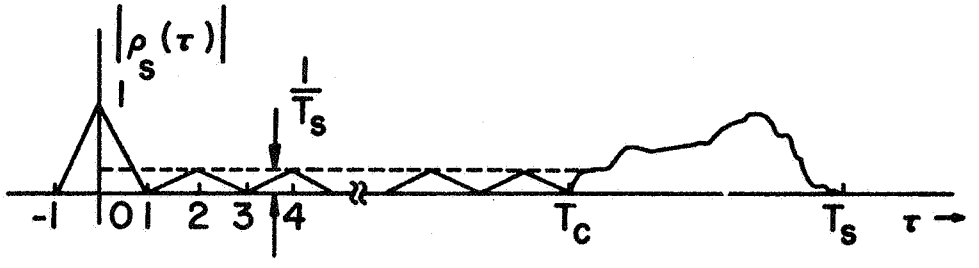

FIGURE 4-6. AUTOCORRELATION FUNCTION OF GENERALIZED BARKER CODE

signals the signal energy available with peak power P_s is

$$E_s = K \cdot T_s \cdot P_s \quad , \tag{4-35}$$

where T_s is the signal duration and K is the average-to-peak power ratio. Thus, with a modest increase in the measurement time, much lower measurement errors are possible than with single impulses.

3. A signal class which is suboptimal, but very good, is the set of Barker codes [48][49]. These are biphase (± 1), constant-envelope signals with autocorrelations shown in Figure 4-5. These codes exist only for certain lengths ($\leq$ 13 and odd), but the idea will be generalized to longer codes in the next paragraph. The fact that the out-of-phase correlation of these signals is not zero causes a degradation in the measurement error, (4-27) but this loss is slight. $\underline{\underline{R}}_s^{-1}$ has been computed for all signals with the Barker property up to length 13, and for all channel delay spreads, T_c, such that $T_c \leq T_s$. The worst case of degradation in measurement variance occurred when $T_c = 5$ and $T_s = 5$; a diagnal element of $\underline{\underline{R}}_s^{-1}$ with value 1.0714 occurred, corresponding to

a 0.3 dB loss in performance compared to the optimum. This is clearly a negligible effect when the average-to-peak power ratio of unity for these signals is considered. That is,

$$E_s \doteq T_s \cdot P_s \tag{4-36}$$

Thus, for a given signal duration, T_s, and a peak-power limitation, P_s, the suboptimal Barker code performs on the order of 3 dB better than the "optimal" Huffman codes.

4. The fact that the optimal autocorrelation function is restricted only for delays up to the channel delay spread, T_c, allows the Barker property to be extended to longer codes. That is, we can attempt to find bipolar binary sequences with the autocorrelation property shown in Figure 4-6. These would be "equivalent Barker codes" for the purpose of channel measurement. Such codes do indeed exist, and can even be generated by shift registers if PN sequences [44] are used in aperiodic fashion as the code words. Appendix D gives a listing of suitable cyclic permutations of PN sequences up to lengt 83, together with their aperiodic autocorrelation functions. It seems reasonable to assume that

a more general class exists for arbitrary code lengths.

Periodic Reference Signals

1. Tompkins [50] has investigated the existence of periodic ternary sequences (+1, 0, -1) up to length 26 which have zero out-of-phase correlation, as in Figure 4-4. These codes were found to have many zeros, resulting in poor average-to-peak power ratios. They are consequently unsuited for channel measurement. However, his investigation did show that there are no binary sequences with lengths between 4 and 26 whose periodic autocorrelation functions are of the form of Figure 4-7. One is thus led to remove part of the autocorrelation restriction and investigate the existence of "almost uncorrelated" periodic binary sequences with the property shown in Figure 4-8. This signal class has a single out-of-phase peak in its autocorrelation function, occurring at one-half the period, and its height was found to be $4/T_s$. Some elementary logical considerations show that any periodic binary sequence which has zero correlation at unit delay must be an integral multiple of 4 in length. An exhaustive search

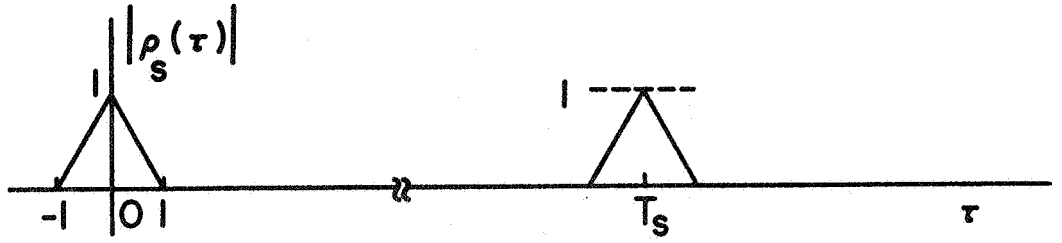

FIGURE 4-7. AUTOCORRELATION FUNCTION OF OPTIMAL, PERIODIC TERNARY SEQUENCE.

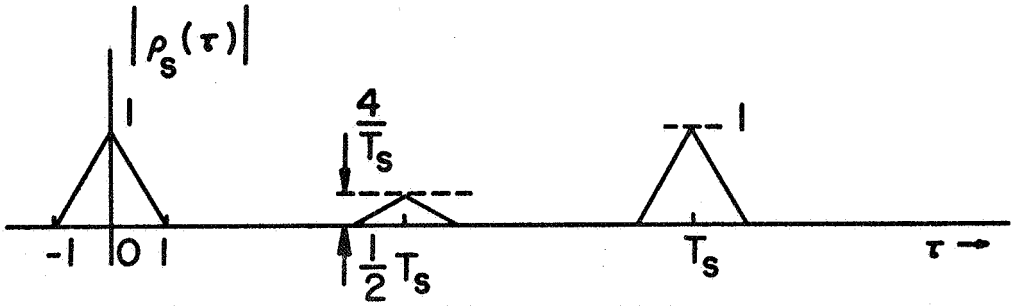

FIGURE 4-8. AUTOCORRELATION FUNCTION OF PERIODIC, ALMOST-UNCORRELATED BINARY SEQUENCE.

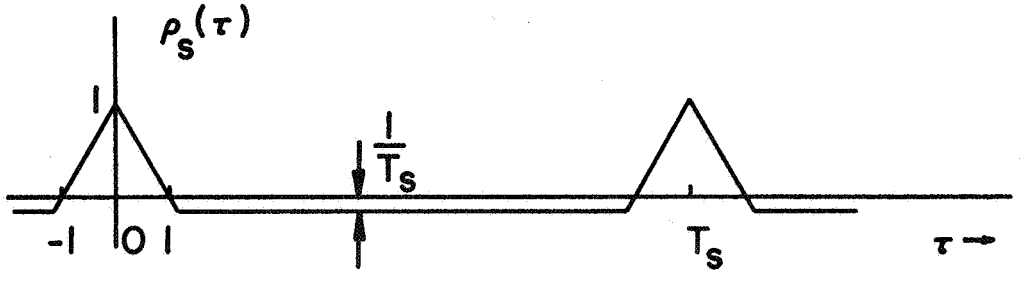

FIGURE 4-9. AUTOCORRELATION FUNCTION OF PERIODIC, PN SEQUENCE.

for such sequences was carried out for lengths of 4, 8, and 12, and they were found to exist. Table 4-1 gives one example of

Table 4-1. Listing of Almost Uncorrelated Periodic Sequences.

Code Length	Sequence
4	+1 +1 +1 -1
8	+1 -1 +1 +1 +1 +1 -1 -1
12	+1 -1 +1 -1 +1 +1 -1 -1 +1 +1 +1 +1

such sequences for each of the lengths investigated. (Any cyclic permutation or time reversal of these examples would also be in the class.) The search for these sequences was not carried out for longer codes because the exhaustive search is very wasteful of computer time, and because it was found that PN sequences perform nearly as well for channel measurements.

2. PN sequences [44] have autocorrelation functions of the form shown in Figure 4-9. These are not optimal signals, but their out-of-phase correlation is quite small if the sequence is long. The degradation due to the nonoptimality of the signals can be computed analytically using Rao's result.[1]

---

[1] Rao, Linear Statistical Inference and its Applications, Wiley, New York, 1965, p. 54.

$$\left[\underline{\underline{R}}_s^{-1}\right]_{ii} = \frac{1 - \frac{T_c - 1}{T_s}}{\left[1 - \frac{T_c}{T_s}\right]\left[1 + \frac{1}{T_s}\right]} \qquad (4\text{-}37)$$

T_s is the signal period, and T_c is the channel delay spread. This expression can be seen to rapidly approach unity for $T_s >> T_c \geq 1$. Thus PN sequences differ negligibly in performance from optimal signals is the measurement period is much longer than the channel delay spread. The ease of generation of these signals, together with their near-optimal performance, makes them the most likely candidates for reference signals in any practical communication system.

Both the periodic signal classes discussed have constant envelopes, so their total energy is just

$$E_s = T_m \cdot P_s \quad . \qquad (4\text{-}38)$$

T_m denotes the total measurement time. (A multiple of the signal period.) It is thus possible to trade signal power for measurement time and simultaneously keep the measurement error fixed. Since, in a frequency-division multiplexing scheme, the only limitation on measurement time is the rate of channel time variation (the information flow is continuous), it is possible that only a negligible amount of

transmitter power need be devoted to channel measurement if the channel is slowly varying. This will be shown to be the case in the next chapter.

4.6 Summary

In this chapter the general problem of channel measurement has been investigated. It was shown that channel estimators which make use of only the information-bearing signal require an exceedingly complex, impractical physical mechanization. This technique does however lead to the investigation of lower bounds on the variance of any channel estimation scheme, for fixed transmitted power.

Great simplifications in the measurement system can be obtained if a known reference signal is transmitted for the express purpose of measuring the channel. The optimal estimate of channel state for systems of this type was derived and analyzed, and a criterion for the joint optimality of both the channel estimator and reference signal was found. Signals optimal with respect to this criterion were found, and they were compared on the basis of fixed peak transmitter power. Near optimal signals were also considered, and their performance analyzed.

These investigations lead to the conclusion that the channel measurement system which best combines performance with simplicity is, in all probability, a frequency-division multiplexed, transmitted-reference system which used periodic PN sequences for reference signals.

CHAPTER 5: DEMODULATOR PERFORMANCE FOR UNKNOWN DISPERSIVE CHANNELS

The performance of adaptive demodulators using transmitted reference channel measurements is considered. Exact equations for the overall performance of the communication systems are developed, and they are evaluated numerically for several examples of interest. A study of the optimal division of transmitter power between reference signal and message is included as well. The results of these calculations point the way to a vastly simpler set of approximate performance quations which give results in good agreement with the exact results.

This approximate analysis provides analytical formulas for overall system performance which are the basis of a simplified design procedure, using assymptotic forms, for predicting the operation of dispersive channel communications systems in terms of fundamental design parameters of the system.

5.1 Assumptions

In this chapter we will consider only the two most promising demodulation systems for dispersive channels - the optimal demodulator, and the high-SNR approximation to it,

the minimum mean-square equalizer.[1] For white additive noise, which will be assumed throughout the chapter, the optimal demodulator is given by

$$\hat{\underline{a}} = \left[\underline{\underline{H}}^{*T}\underline{\underline{H}} + \frac{1}{\eta}\,\underline{\underline{\phi}}_a^{-1}\right]^{-1} \underline{\underline{H}}^{*T}\underline{y} = \underline{\underline{Q}}^{-1}\underline{\underline{H}}^{*T}\underline{y} \quad , \qquad (5\text{-}1)$$

the vector estimate of the message. An alternate way of writing the k^{th} component of (5-1) was developed in Section 3.4 using the pseudo-inverse.

$$\hat{a}_k = \underline{\phi}_k^{*T}\,\underline{\underline{H}}^{*T}\left[\underline{\underline{H}}\,\underline{\underline{\phi}}_a\,\underline{\underline{H}}^{*T} + \frac{1}{\eta}\,\underline{\underline{I}}\right]^{-1} \underline{y} \quad . \qquad (5\text{-}2)$$

The vector $\underline{\phi}_k$ denotes the k^{th} column of the normalized message covariance matrix, $\underline{\underline{\phi}}_a$.

The optimal equalizer is just the zero-noise version of (5-2), i.e.,

$$\hat{a}_k = \underline{\phi}_k^{*T}\,\underline{\underline{H}}^{*T}\left[\underline{\underline{H}}\,\underline{\underline{\phi}}_a\,\underline{\underline{H}}^{*T}\right]^{-1} \underline{y} = \underline{c}^T\underline{y} \quad , \qquad (5\text{-}3)$$

where $\underline{c}$ is the vector of equalizer tap-gains.

In this chapter we will be concerned with systems for which the true state of the channel is not known to the receiver, but only an estimate, say $\hat{\underline{\underline{H}}}$, of the true channel $\underline{\underline{H}}$ is available. Thus in (5-1) through (5-3) the channel-dependent quantities must be replaced by their estimates.

---

[1] These systems are optimal for known channels; for unknown channels the strategy will be to use the same structure as for known channels, but substitute estimates of the channel parameters for the channel dependent quantities. The terminology "optimal" will, however, be retained.

The channel estimates will be assumed to have been obtained by an optimal transmitted reference measurement system discussed in Chapter 4. Then the measurement errors of the individual channel tap gains are statistically independent of each other, and will be independent of the message and noise as well, for either time-division or frequency-division multiplexing of the message and reference signals. The measurement error covariance was given by (4-32),

$$\mathrm{Cov}(\underline{\hat{h}}-\underline{h}) = \frac{\sigma_N^2}{E_s}\,\underline{\underline{I}} \quad , \tag{5-4}$$

where E_s is the energy of the reference signal within the measurement interval, T_m. For a power-limited transmitter, with power P_s available for channel measurement, the best choice of reference signals was found to be the class of constant-envelope signals, for which

$$E_s = P_s \times T_m \quad . \tag{5-5}$$

Thus we can write

$$\mathrm{Cov}(\underline{\hat{h}}-\underline{h}) = \frac{\sigma_N^2}{P_s T_m}\,\underline{\underline{I}} = \frac{1}{\eta_m T_m}\,\underline{\underline{I}} \quad , \tag{5-6}$$

where η_m is defined to be the input SNR of the measurement system.

One last assumption which will be made is that the first (or, in general, the largest) channel tap gain is known.

This is done to account for the fact that any constant multiple of the message is an error-free message estimate for purposes of communication. The assumption of one known tap gain mathematically fixes the overall gain level of the channel, and, in effect, simulates automatic gain control.

5.2 Exact Calculations of System Performance

The method used to determine the effect of noisy channel measurements on system performance is to find the error variance as a function of the true channel state and the receivers estimate of that state, and then average with respect to the estimation error, or "mismatch." For a channel $\hat{\underline{\underline{H}}}$, the optimal demodulator becomes

$$\hat{\underline{a}} = \left[\hat{\underline{\underline{H}}}^{*T}\hat{\underline{\underline{H}}} + \frac{1}{\eta_a}\underline{\underline{\phi}}_a^{-1}\right]^{-1} \hat{\underline{\underline{H}}}^{*T}\underline{y} = \hat{\underline{\underline{Q}}}^{-1}\hat{\underline{\underline{H}}}^{*T}\underline{y} \ , \qquad (5\text{-}7)$$

where the message SNR, η_a is defined to be

$$\eta_a = \frac{\sigma_a^2}{\sigma_N^2} = \frac{P_a}{\sigma_N^2} \ , \qquad (5\text{-}8)$$

and P_a is the power devoted to transmitting the message. The normalized error covariance, conditioned on the channel estimate, is defined to be

$$\underline{\underline{\Lambda}}(\hat{\underline{h}}) \triangleq \frac{1}{\sigma_a^2} E_{\underline{a},\underline{N}}\left[(\hat{\underline{a}}-\underline{a})(\hat{\underline{a}}-\underline{a})^{*T}\right] \ . \qquad (5\text{-}9)$$

This will be called the channel mismatch function. Then the overall performance of the system is obtained by averaging with respect to $\underline{\hat{h}}$.

$$\underline{\underline{\Lambda}} \triangleq E_{\underline{\hat{h}}}[\underline{\underline{\Lambda}}(\underline{\hat{h}})] \tag{5-10}$$

Defining a measurement error matrix, or mismatch matrix, to be

$$\underline{\underline{E}} \triangleq (\underline{\underline{\hat{H}}} - \underline{\underline{H}}) \tag{5-11}$$

we may write, for the optimal demodulator,

$$\begin{aligned}(\underline{\hat{a}}-\underline{a}) &= \underline{\underline{\hat{Q}}}^{-1}\ \underline{\underline{\hat{H}}}^{*T}\ \underline{y} - \underline{a} \\ &= \underline{\underline{\hat{Q}}}^{-1}\left[\underline{\underline{\hat{H}}}^{*T}(\underline{\underline{H}}\underline{a} + N) - \underline{\underline{\hat{Q}}}\ \underline{a}\right] \\ &= \underline{\underline{\hat{Q}}}^{-1}\left[\underline{\underline{\hat{H}}}^{*T}\ \underline{N} - (\underline{\underline{\hat{H}}}^{*T}\ \underline{\underline{E}} + \frac{1}{\eta}\underline{\underline{\Phi}}_a^{-1})\underline{a}\right] \quad .\end{aligned} \tag{5-12}$$

Performing the operations indicated by (5-9) we obtain the channel mismatch function for the optimal demodulator.

$$\begin{aligned}\underline{\underline{\Lambda}}(\underline{\hat{h}}) &= \underline{\underline{\hat{Q}}}^{-1}\left[\frac{1}{\eta_a}\underline{\underline{\hat{H}}}^{*T}\underline{\underline{\hat{H}}} + (\underline{\underline{\hat{H}}}^{*T}\underline{\underline{E}} + \frac{1}{\eta_a}\underline{\underline{\Phi}}_a^{-1})\ \underline{\underline{\Phi}}_a(\underline{\underline{E}}^{*T}\underline{\underline{\hat{H}}} + \frac{1}{\eta_a}\underline{\underline{\Phi}}_a^{-1})\right]\underline{\underline{\hat{Q}}}^{-1} \\ &= \frac{1}{\eta_a}\underline{\underline{\hat{Q}}}^{-1} + \underline{\underline{\hat{Q}}}^{-1}\left[\underline{\underline{\hat{H}}}^{*T}\ \underline{\underline{E}}\ \underline{\underline{\Phi}}_a\ \underline{\underline{E}}^{*T}\ \underline{\underline{\hat{H}}} + \frac{1}{\eta_a}(\underline{\underline{\hat{H}}}^{*T}\ \underline{\underline{E}} + \underline{\underline{E}}^{*T}\ \underline{\underline{\hat{H}}})\right]\underline{\underline{\hat{Q}}}^{-1}\end{aligned} \tag{5-13}$$

A similar procedure is used to obtain a channel mismatch function, $\lambda_k(\underline{\hat{h}})$, for the optimal equalizer, (5-3).

$$\hat{a}_k - a_k = \underline{\phi}_k^{*T} \hat{\underline{\underline{H}}}^{*T} \left[\hat{\underline{\underline{H}}} \underline{\underline{\phi}}_a \hat{\underline{\underline{H}}}^{*T} \right]^{-1} (\underline{\underline{H}}\, \underline{a} + \underline{N}) - a_k$$

$$= \hat{\underline{c}}^T [\underline{\underline{H}}\, \underline{a} + \underline{N}] - a_k \qquad (5\text{-}14)$$

$$\lambda_k(\hat{\underline{h}}) \triangleq \frac{1}{\sigma_a^2} E_{\underline{a},\underline{N}} \left| \hat{a}_k - a_k \right|^2$$

$$= 1 + \hat{\underline{c}}^T \left[\underline{\underline{H}}\, \underline{\underline{\phi}}_a \underline{\underline{H}}^{*T} + \frac{1}{\eta_a} \underline{\underline{I}} \right] \hat{\underline{c}}^* - 2\mathrm{Re}\left[\hat{\underline{c}}^T \underline{\underline{H}}\, \underline{\phi}_k \right] \qquad (5\text{-}15)$$

This mismatch function is then averaged over measurement errors to obtain the overall equalizer performance, λ_k.

$$\lambda_k = E_{\hat{\underline{h}}} \left[\lambda_k(\hat{\underline{h}}) \right] \qquad (5\text{-}16)$$

Equations (5-13) and (5-15) are the basic formulas for the investigation of the effects of channel measurement error. Note that this error appears in a complicated, non-linear fashion involving matrix inverses, so that the analytical evaluation of the expectation with respect to $\hat{\underline{h}}$ of these mismatch functions is an intractable problem. Instead, numerical methods were used initially to perform the averages of (5-10) and (5-16) in order to observe trends and parameter dependencies. These calculations provided enough insight into the problem to suggest a much simpler approximate performance calculation which will be described in a later section. However, let us first describe the numerical procedure used to perform the "exact" calculations.

It should first of all be noted that (5-13) and (5-15) are not the most efficient formulations for numerical purposes because of the special nature of the matrices involved. (See Equations (2-26) and (2-35).) These matrices have many zeroes in the "corners," and identical elements along diagonals, so that it is possible to develop special formulas for the matrix products which take advantage of these properties to substantially reduce the number of multiplications required. However, the details of these simplifications will not be discussed here.

The numerical technique uses the integral form of the expectation operation of (5-10) or (5-16). (Actually only the diagonal elements of (5-10) were computed).

$$\underline{\underline{\Lambda}} = E_{\hat{\underline{h}}}[\underline{\underline{\Lambda}}(\hat{h})] = \int \underline{\underline{\Lambda}}(\hat{\underline{h}})\ p(\hat{h})\ d\hat{\underline{h}} \qquad (5\text{-}17)$$

$p(\hat{\underline{h}})$ is the joint probability density function of the channel tap-gain measurements, known from Chapter 4 to be Gaussian and uncorrelated, with mean values equal to the true values of the channel tap-gains. This integral is over the $T_c=n_c-1$ unknown channel tap gains (recall from the preceding section that h_1 was assumed known), so that it in general implies a multiple integration. It was found that the complicated form of the integrund, $\underline{\underline{\Lambda}}(\hat{\underline{h}})$, caused even double integral calculations to be of astronomical dimensionality, so that this "brute-force" approach was restricted to the case of

single-notch fading (T_c=1), for which $\underline{\underline{\Lambda}}(\underline{\hat{h}})$ is a function only of a scalar variable, $\hat{h}_2$.

If the input SNR, η_a, and the true channel state are fixed, then any diagonal element, $\lambda_k(\hat{h}_2)$, of the mismatch functions (5-13) or (5-15) is a function of $\hat{h}_2$ alone. A piecewise-linear approximation to this function was generated by the following algorithm.

1. For the largest measurement error variance to be considered (-8dB), the 95 percent confidence interval for $\hat{h}_2$ was computed.
2. The value of $\lambda_k(\hat{h}_2)$ was computed at the endpoints of this interval and also at the midpoint ($\hat{h}_2 = h_2$), dividing the interval into two subintervals.
3. For each of these subintervals the value of $\lambda_k(\hat{h}_2)$ was computed at the midpoint and compared to the midpoint of the straight line connecting the values of $\lambda_k(\hat{h}_2)$ at the endpoints.
4. If the resultant difference was more than 2 percent of the true value of $\lambda_k(\hat{h}_2)$, then step 3 was repeated for each of the new subintervals.

Since the mismatch function turns out to be reasonably smooth, this nested-interval iteration procedure produces a predictably accurate piecewise linear approximation to $\lambda_k(\hat{h}_2)$. Once this approximation is obtained the actual integration in

(5-17) is a straightforward calculation for any value of measurement error variance smaller than the worst case indicated in step 1.

5.3 Results of the Exact Calculations of System Performance

Some examples of the results of these calculations of the "exact" performance equations are given in Figures 5-1 through 5-4. The performance criterion is the reciprocal of the average error variance, or output SNR, for that component of the vector message estimate which the receiver would regard as the best on the basis of the noisy channel measurement. This is plotted as a function of the message SNR, η_a, for various values of the measurement SNR, $\eta_m T_m$. The curve with $\eta_m T_m = \infty$ is the limiting case of known channel state, and the curve labeled "dispersion bound" gives the ultimate performance for any system operating over the same channel, that of the optimal demodulator with infinite observation interval when the channel is known.

The examples of Figures 5-1 and 5-3 were chosen to illustrate the situation in which the length of the observation interval, T_0, is not a limiting factor over the ranges of parameters considered, and may be regarded as infinite. This is evidenced by the fact that SNR_0 is assymptotically proportional to η_a for the known channel, the sign of a system limited by additive noise. Conversely, Figures 5-2 and 5-4 illustrate the situation where insufficient observation time causes the system to be dispersion-limited as η_a gets large.

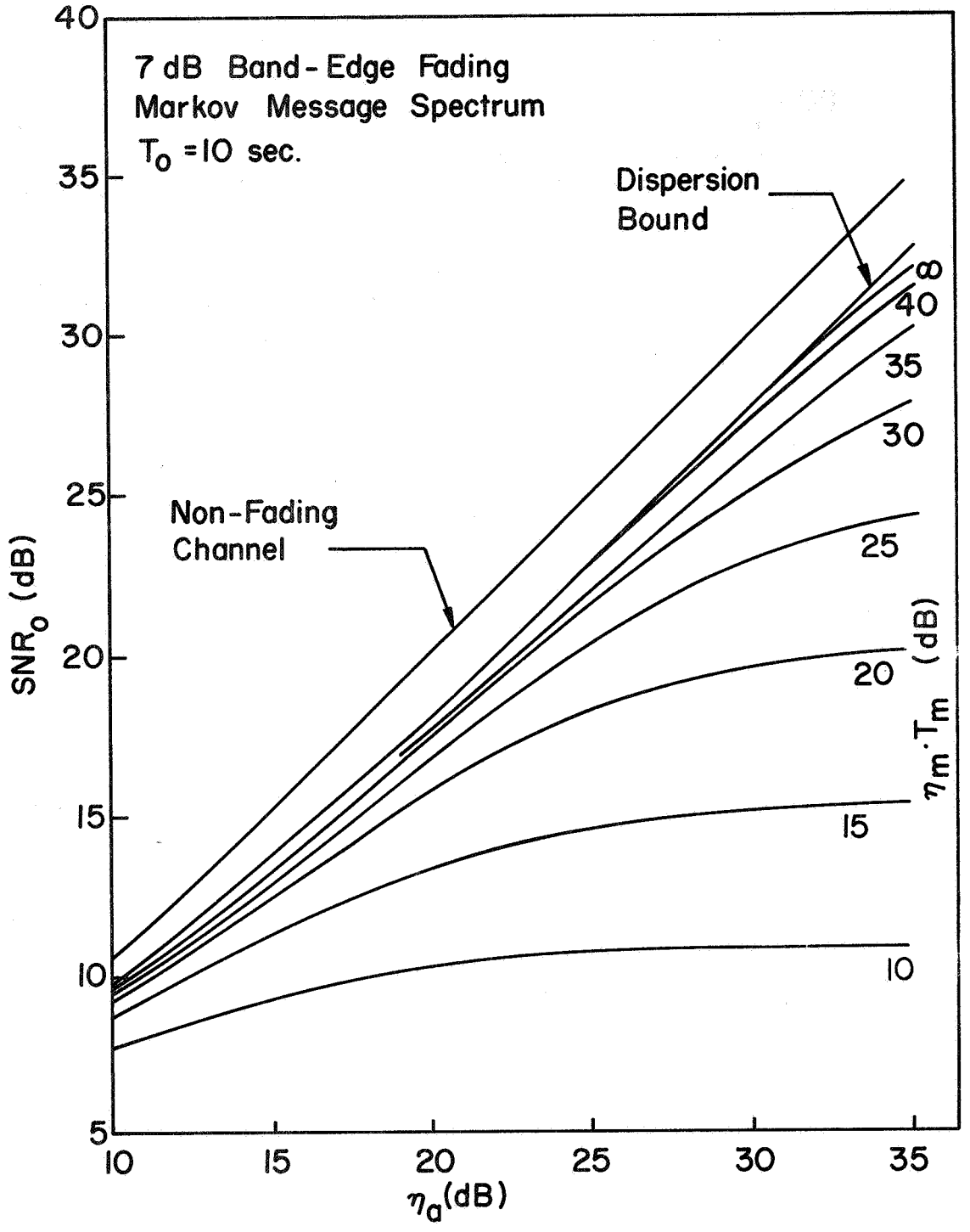

FIGURE 5-1. OPTIMAL DEMODULATOR PERFORMANCE FOR 7 dB BAND-EDGE FADING.

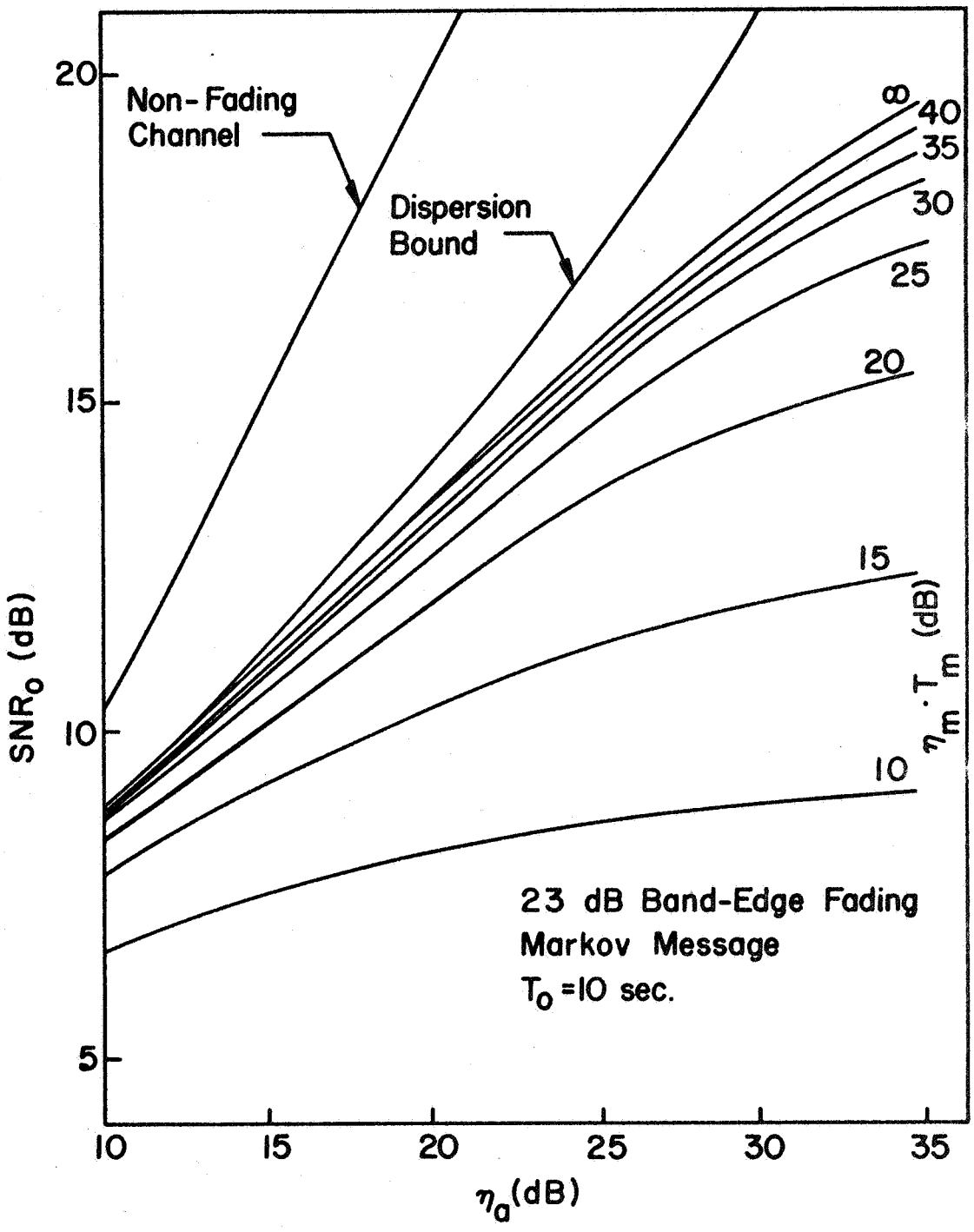

FIGURE 5-2. OPTIMAL DEMODULATOR PERFORMANCE FOR 23 dB BAND-EDGE FADING.

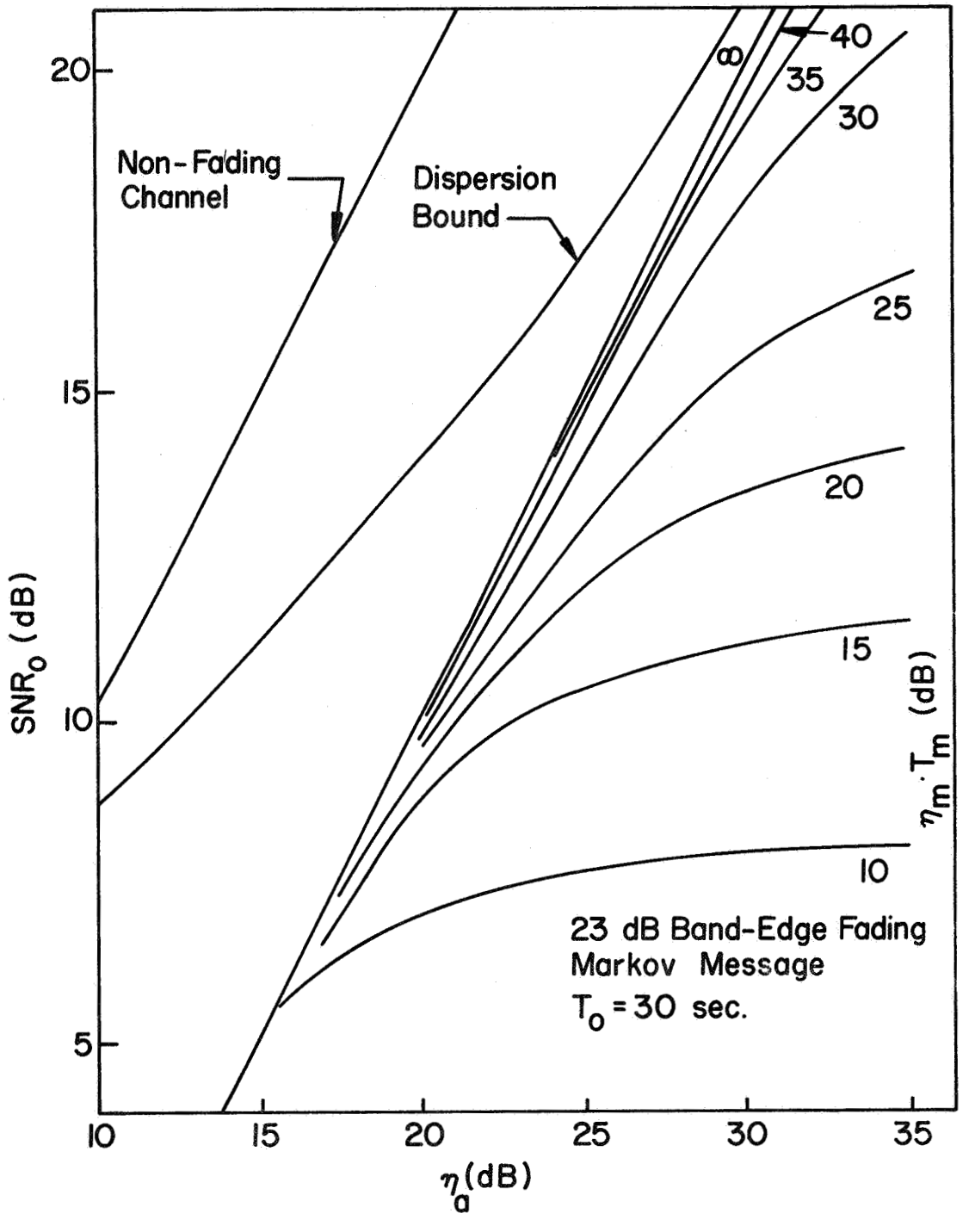

FIGURE 5-3. OPTIMAL EQUALIZER PERFORMANCE FOR 23 dB BAND-EDGE FADING (T_0 = 30 sec.)

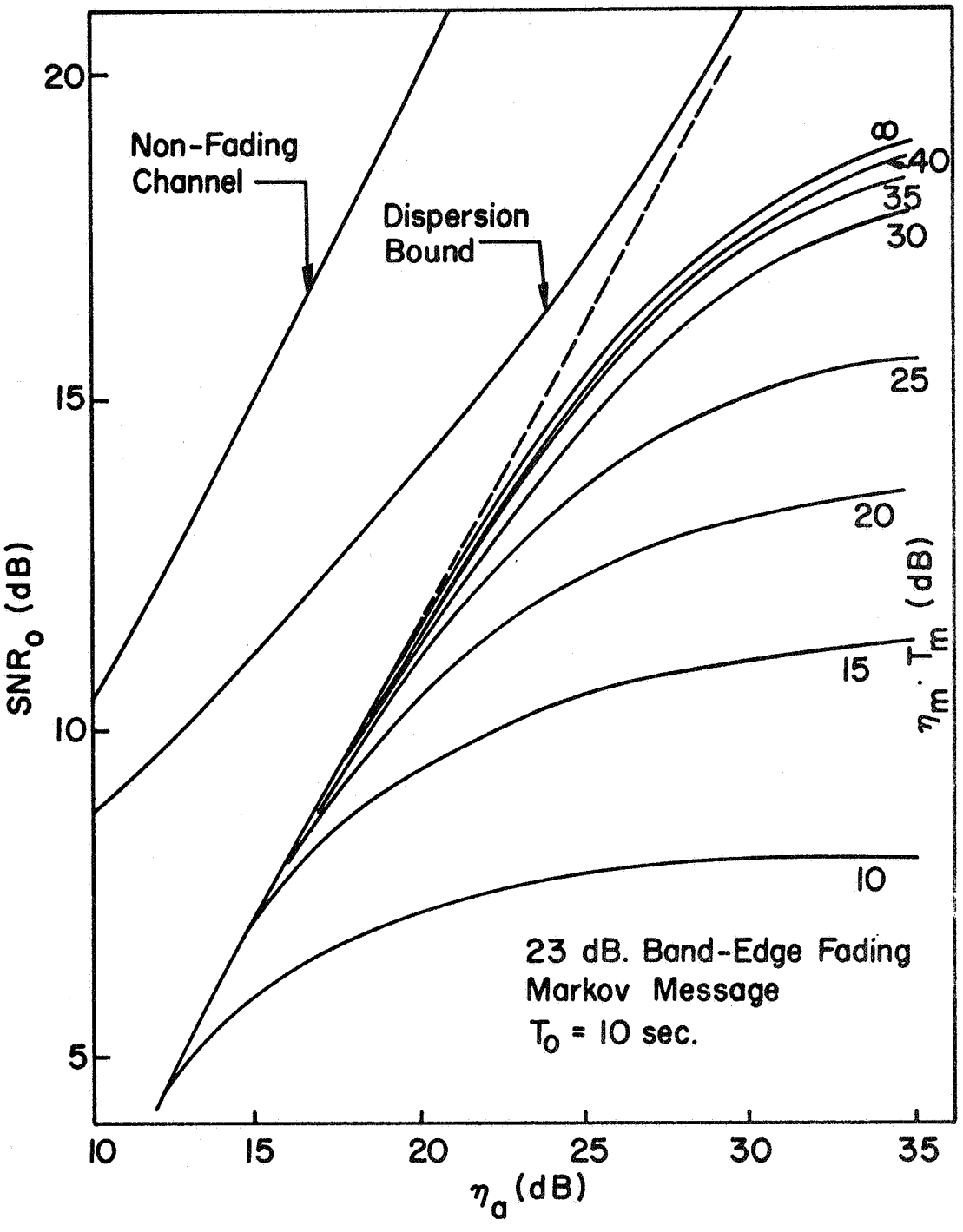

FIGURE 5-4. OPTIMAL EQUALIZER PERFORMANCE FOR 23 dB BAND-EDGE FADING (T_0 = 10 sec.)

In all these figures the curves tend to level-off and approach an assymptote as $\eta_a \to \infty$, so that the gross effect of channel measurement errors is seen to be another ultimate performance limitation to be added to those caused by additive noise, incomplete equalization, and channel dispersion itself. The dependence of the numerical values of these new assymptotes upon the various design parameters of the system is not at all obvious from the theory so far developed, but the approximate analysis of the next section provides good estimates.

Another feature common to all the Figures 5-1 through 5-4 is the monotonic improvement in performance with respect to both η_a and $\eta_m T_m$, but with decreasing rates of improvement in each variable. Since η_a and η_m are not independent, but are constrained by the power limitation on the transmitter, this behavior suggests the possibility of an optimal division of transmitter power. Suppose the available power is P, that δ represents the fraction of this power devoted to channel measurement, and that η denotes the total input SNR available. That is,

$$\eta \triangleq \frac{P}{\sigma_N^2} \tag{5-18}$$

Then we can express η_a and η_m in terms of the power division parameter δ.

$$\eta_a = \frac{P_a}{\sigma_N^2} = (1-\delta)\eta \tag{5-19}$$

$$\eta_m = \frac{P_s}{\sigma_N^2} = \delta\eta \qquad (5\text{-}20)$$

Then the optimal power division, δ_{opt}, is that choice of δ which maximizes SNR_0.

A typical example of the dependence of performance on δ is given by Figure 5-5, for the same system and channel illustrated by Figure 5-1. When the measurement interval T_m is reasonably long, the system performance is remarkably insensitive to power division; it is possible to devote only a few percent of the transmitter power to channel measurement and still achieve performance within 1dB of the optimum. Note also the substantial improvement in maximum performance as T_m goes from 1 second (a single pulse measurement) to 100 seconds (a long measurement sequence). Since, as pointed out in Chapter 4, measurement time is quite cheap compared to observation time, the measurement should be made as long as possible, consistent with the fading rate of the channel.

A search procedure was used to optimize the power division for many examples of single-notch selective fading, and the optimal performance is tabulated in Tables 5-1 through 5-4. The numbered columns in these tables correspond to the following system configurations.

1. The optimal demodulator with infinite observation interval and known channel state. (The dispersion bound.)

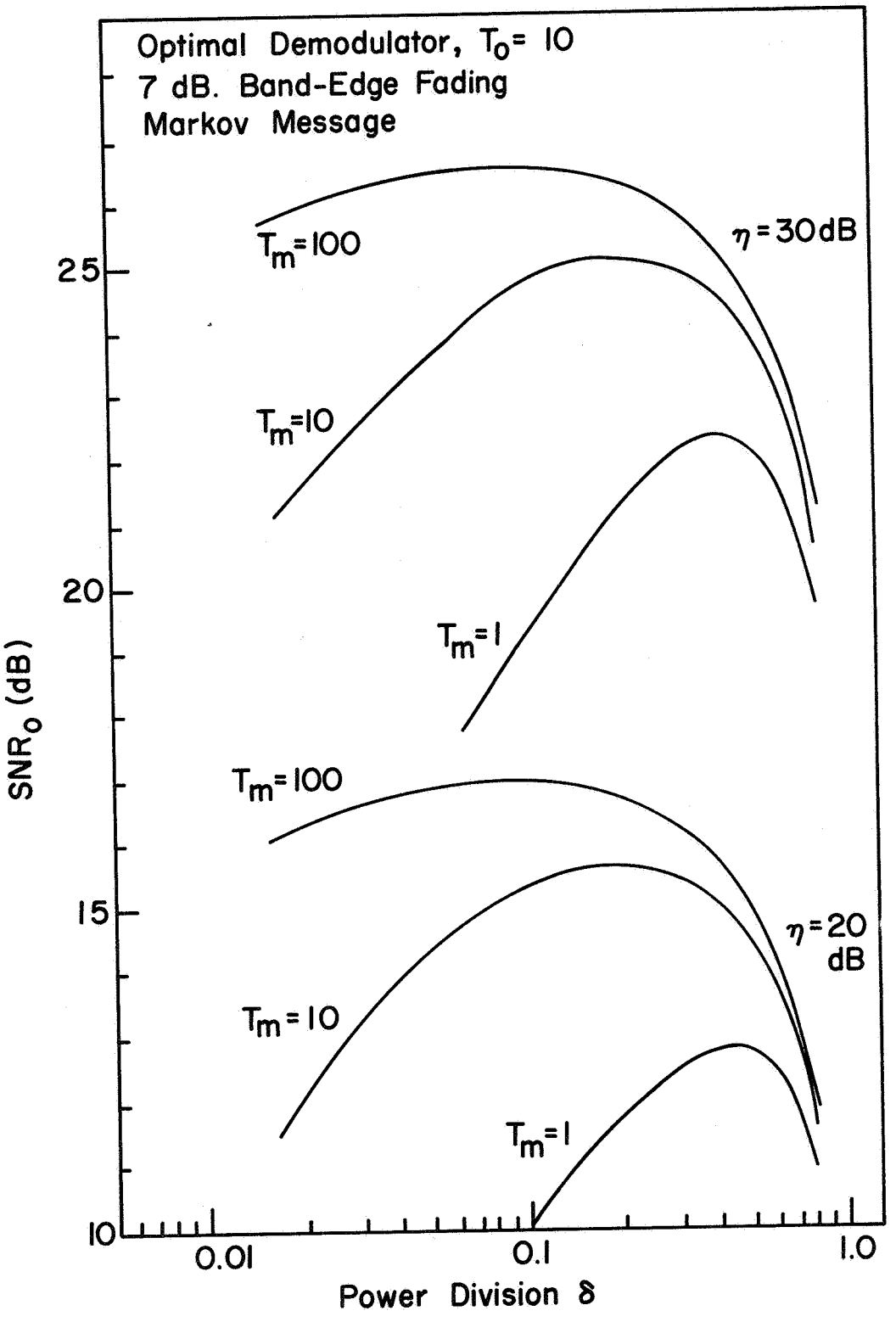

FIGURE 5-5. AN EXAMPLE OF TRANSMITTER POWER DIVISION.

Table 5-1. System Performance Comparison for 7 dB Band-Edge Fading.

n	1	T_m	2	3	4	5	T_m	2	3	4	5
10	9.7	1	....	....	....	....	10	7.8	5.4	4.2	4.0
12	11.2	1	6.9	4.3	3.2	2.9	10	9.2	6.8	6.7	6.6
14	12.8	1	8.3	5.4	4.9	4.6	10	10.6	8.6	9.1	9.1
16	14.5	1	9.6	6.8	6.4	6.0	10	12.2	10.7	11.3	11.3
18	16.2	1	11.2	8.9	8.8	8.7	10	13.9	12.8	13.5	13.5
20	18.1	1	12.9	11.3	11.5	11.5	10	15.7	14.9	15.5	15.5
22	19.9	1	14.9	13.6	13.9	13.9	10	17.6	16.9	17.6	17.6
24	21.9	1	16.7	15.7	16.2	16.2	10	19.4	19.0	19.6	19.6
26	23.8	1	18.7	18.1	18.4	18.4	10	21.3	21.1	21.6	21.7
28	25.8	1	20.5	20.0	20.4	20.4	10	23.3	23.1	23.6	23.7
30	27.8	1	22.5	22.2	22.5	22.5	10	25.2	25.1	25.6	25.7
32	29.8	1	24.3	24.1	24.4	24.4	10	27.2	27.2	27.7	27.7
34	31.8	1	26.3	26.2	26.6	26.6	10	29.2	29.1	29.7	29.7
36	33.8	1	28.2	28.1	28.5	28.5	10	31.2	31.2	31.7	31.7
10	9.7	100	8.9	6.7	6.7	6.7	∞	....	....	....	....
12	11.2	100	10.2	8.4	8.9	8.9	∞	11.2	9.8	9.8	9.8
14	12.8	100	11.8	10.4	10.9	10.9	∞	....	....	....	....
16	14.5	100	13.4	12.4	13.0	13.0	∞	14.4	13.8	13.8	13.8
18	16.2	100	15.2	14.4	14.9	14.9	∞	....	....	....	....
20	18.1	100	17.0	16.5	17.0	17.0	∞	18.0	17.8	17.8	17.8
22	19.9	100	18.8	18.5	19.0	19.0	∞	....	....	....	....
24	21.9	100	20.8	20.5	21.0	21.0	∞	21.9	21.8	21.8	21.8
26	23.8	100	22.7	22.5	23.0	23.0	∞	....	....	....	....
28	25.8	100	24.7	24.6	25.0	25.0	∞	25.8	25.8	25.8	25.8
30	27.8	100	26.6	26.5	27.0	27.0	∞	....	....	....	....
32	29.8	100	28.5	28.5	29.0	29.0	∞	29.8	29.8	29.8	29.8

Table 5-2. System Performance Comparison for 23 dB Band-Edge Fading.

n	1	T_m	2	3	4	5	T_m	2	3	4	5
10	8.7	1	....	....	....	....	10	7.1	2.3	2.3	1.9
12	9.8	1	6.0	2.1	2.1	1.9	10	8.0	4.0	3.8	3.5
14	10.8	1	7.1	3.9	3.8	3.6	10	9.0	5.7	5.1	4.8
16	11.9	1	8.1	5.7	5.4	5.1	10	10.0	7.4	6.6	6.3
18	12.9	1	9.0	7.4	6.8	6.6	10	10.9	8.8	7.9	7.6
20	14.0	1	10.1	8.8	8.2	7.9	10	11.9	10.2	9.4	9.0
22	15.2	1	11.2	10.1	9.6	9.3	10	13.0	11.5	10.8	10.3
24	16.5	1	12.4	11.2	10.9	10.5	10	14.0	12.8	12.6	11.9
26	18.0	1	13.6	12.6	12.3	11.9	10	15.0	14.3	14.6	13.9
28	19.6	1	14.7	13.6	13.7	13.3	10	16.0	15.7	16.6	16.0
30	21.2	1	15.8	14.8	15.5	14.8	10	17.0	16.8	18.5	18.1
32	22.9	1	16.7	16.1	17.5	16.9	10	17.8	17.6	20.2	20.1
34	24.6	1	17.5	17.3	19.7	19.2	10	18.5	18.2	21.9	22.0
36	26.5	1	18.3	18.0	21.4	21.1	10	19.1	18.6	23.4	24.0
10	8.7	100	8.0	2.7	2.6	2.2	∞	....	....	....	....
12	9.8	100	9.0	4.4	4.1	3.7	∞	9.8	4.2	2.6	2.3
14	10.8	100	9.9	6.1	5.4	5.0	∞	....	....	....	....
16	11.9	100	10.9	7.9	6.9	6.5	∞	11.8	8.0	6.6	6.3
18	12.9	100	11.8	9.3	8.2	7.7	∞	....	....	....	....
20	14.0	100	12.8	10.9	9.9	9.3	∞	13.5	11.6	10.6	10.3
22	15.2	100	13.8	12.4	11.9	11.2	∞	....	....	....	....
24	16.5	100	14.7	13.9	14.0	13.4	∞	15.3	14.7	14.5	14.3
26	18.0	100	15.7	15.2	15.9	15.4	∞	....	....	....	....
28	19.6	100	16.7	16.4	17.6	17.4	∞	17.3	17.0	18.0	18.2
30	21.2	100	17.5	17.3	19.4	19.4	∞	....	....	....	....
32	22.9	100	18.3	18.0	21.3	21.4	∞	18.8	18.4	21.8	22.2

Table 5-3. System Performance Comparison for 7 dB Center-Band Fading.

n	1	T_m	2	3	4	5	T_m	2	3	4	5
10	8.5	1	....	....	....	....	10	6.3	3.6	2.3	1.9
12	10.2	1	4.9	1.1	0.3	0.1	10	7.7	5.6	5.6	5.6
14	12.0	1	6.3	2.2	1.0	0.6	10	9.3	7.6	8.0	8.0
16	13.9	1	7.8	3.9	2.6	2.3	10	11.2	9.6	10.1	10.1
18	15.8	1	9.7	6.3	6.1	5.9	10	13.0	11.8	12.4	12.4
20	17.8	1	11.7	9.0	9.0	9.0	10	14.9	13.9	14.5	14.5
22	19.8	1	13.6	11.3	11.8	11.6	10	16.8	16.0	16.6	16.6
24	21.8	1	15.5	13.8	14.0	14.0	10	18.8	18.0	18.6	18.5
26	23.8	1	17.5	15.8	16.1	16.1	10	20.6	20.1	20.6	20.6
28	25.8	1	19.1	18.0	18.3	18.3	10	22.4	22.1	22.6	22.6
30	27.8	1	20.6	20.0	20.3	20.3	10	24.2	24.2	24.7	24.8
32	29.8	1	22.3	22.1	22.4	22.7	10	26.2	26.1	26.7	27.1
34	31.8	1	24.2	24.1	24.4	25.4	10	28.2	28.2	28.7	29.1
36	33.8	1	26.2	26.2	26.4	27.2	10	....	30.0	....	30.5
10	8.5	100	7.4	5.9	6.3	6.3	∞	....	....	....	....
12	10.2	100	9.0	7.8	8.4	8.4	∞	10.2	9.8	9.8	9.8
14	12.0	100	10.8	9.8	10.5	10.5	∞	....	....	....	....
16	13.9	100	12.7	11.9	12.5	12.5	∞	13.9	13.8	13.8	13.8
18	15.8	100	14.6	13.9	14.5	14.5	∞	....	....	....	....
20	17.8	100	16.5	16.0	16.6	16.6	∞	17.8	17.8	17.8	17.8
22	19.8	100	18.4	18.0	18.6	18.6	∞	....	....	....	....
24	21.8	100	20.4	20.0	20.6	20.6	∞	21.8	21.8	21.8	21.8
26	23.8	100	22.3	22.0	22.6	22.6	∞	....	....	....	....
28	25.8	100	24.2	24.0	24.6	24.6	∞	25.8	25.8	25.8	25.8
30	27.8	100	....	26.0	26.5	26.6	∞	....	....	....	....
32	29.8	100	....	27.8	....	....	∞	29.8	29.8	29.8	29.8

Table 5-4. System Performance Comparison for 23 dB Center-Band Fading.

n	1	T_m	2	3	4	5	T_m	2	3	4	5
10	4.9	1	....	....	....	....	10	3.4	1.3	0.8	0.7
12	6.0	1	2.9	1.2	0.8	0.7	10	4.1	2.8	1.9	1.6
14	7.2	1	3.4	2.7	1.9	1.7	10	4.8	3.8	2.7	2.5
16	8.6	1	4.1	3.5	2.8	2.6	10	5.6	5.0	3.8	3.5
18	10.2	1	4.6	4.4	3.6	3.4	10	6.5	6.1	5.0	4.5
20	11.6	1	5.5	5.3	4.5	4.2	10	7.5	6.7	6.5	5.9
22	12.2	1	6.6	5.8	5.4	5.2	10	8.6	8.1	8.6	7.8
24	14.8	1	7.7	6.3	6.5	6.1	10	9.4	9.3	10.7	10.0
26	16.5	1	8.8	7.2	7.7	7.3	10	10.2	10.3	12.7	12.1
28	18.5	1	9.5	8.3	9.4	8.8	10	10.8	10.9	14.4	14.0
30	20.4	1	10.4	9.8	11.8	11.0	10	11.3	11.2	15.9	16.0
32	22.3	1	10.9	10.7	14.0	13.3	10	11.5	11.5	17.1	17.9
34	24.3	1	11.2	11.2	15.7	15.2	10	11.7	11.7	18.2	19.7
36	26.3	1	11.5	11.5	17.0	17.2	10	11.9	11.8	....	....
10	4.9	100	4.0	1.7	1.0	0.9	∞	....	....	....	....
12	6.0	100	4.8	3.3	2.1	1.8	∞	5.5	3.6	2.6	2.3
14	7.2	100	5.6	4.5	3.2	2.7	∞	....	....	....	....
16	8.6	100	6.5	6.0	5.0	4.3	∞	7.4	6.8	6.5	6.3
18	10.2	100	7.5	7.1	7.1	6.4	∞	....	....	....	....
20	11.6	100	8.5	8.4	9.1	8.5	∞	9.4	9.2	10.3	10.3
22	13.2	100	9.4	9.5	11.0	10.5	∞	....	....	....	....
24	14.8	100	10.2	10.3	12.7	12.5	∞	10.9	10.7	13.8	14.2
26	16.5	100	11.8	10.8	14.3	14.5	∞	....	....	....	....
28	18.5	100	11.2	11.2	15.9	16.5	∞	11.7	11.5	16.8	18.0
30	20.4	100	11.5	11.4	17.1	....	∞	....	....	....	....
32	22.3	100	11.7	11.7	....	....	∞	12.0	11.9	19.0	21.7

2. The optimal demodulator, T_0 = 10 seconds

3. The optimal equalizer, T_0 = 10 seconds

4. The optimal equalizer, T_0 = 20 seconds

5. The optimal equalizer, T_0 = 30 seconds

The value of the optimal power division was found to lie in the ranges below, for all entries in the tables.

$$0.38 \leq \delta_{opt} \leq 0.58 \quad , \quad T_m = 1$$

$$0.21 \leq \delta_{opt} \leq 0.32 \quad , \quad T_m = 10 \qquad (5\text{-}21)$$

$$0.08 \leq \delta_{opt} \leq 0.12 \quad , \quad T_m = 100$$

However, these optimal values were not at all critical, as evidenced by Figure 5-5, which is quite typical of all the cases considered in the tables.

Some examples taken from these tables illustrate the general behavior of complete demodulating systems for unknown dispersive channels. Figure 5-6 is a comparison of the optimal demodulator and optimal equalizer under conditions such that the length of the observation interval is not a limiting factor. The optimal equalizer performance approaches that of the optimal demodulator when the input SNR is high, but the lack of post-equalization filtering causes significant degradation for η small, the same behavior observed for known channels. Note the crucial importance of the length of the channel measurement, T_m, on overall system performance. For T_m=1 (single pulse measurement) there is severe degradation in performance relative to the case of known channel state (T_m=∞). However, if the fading rate of the channel is

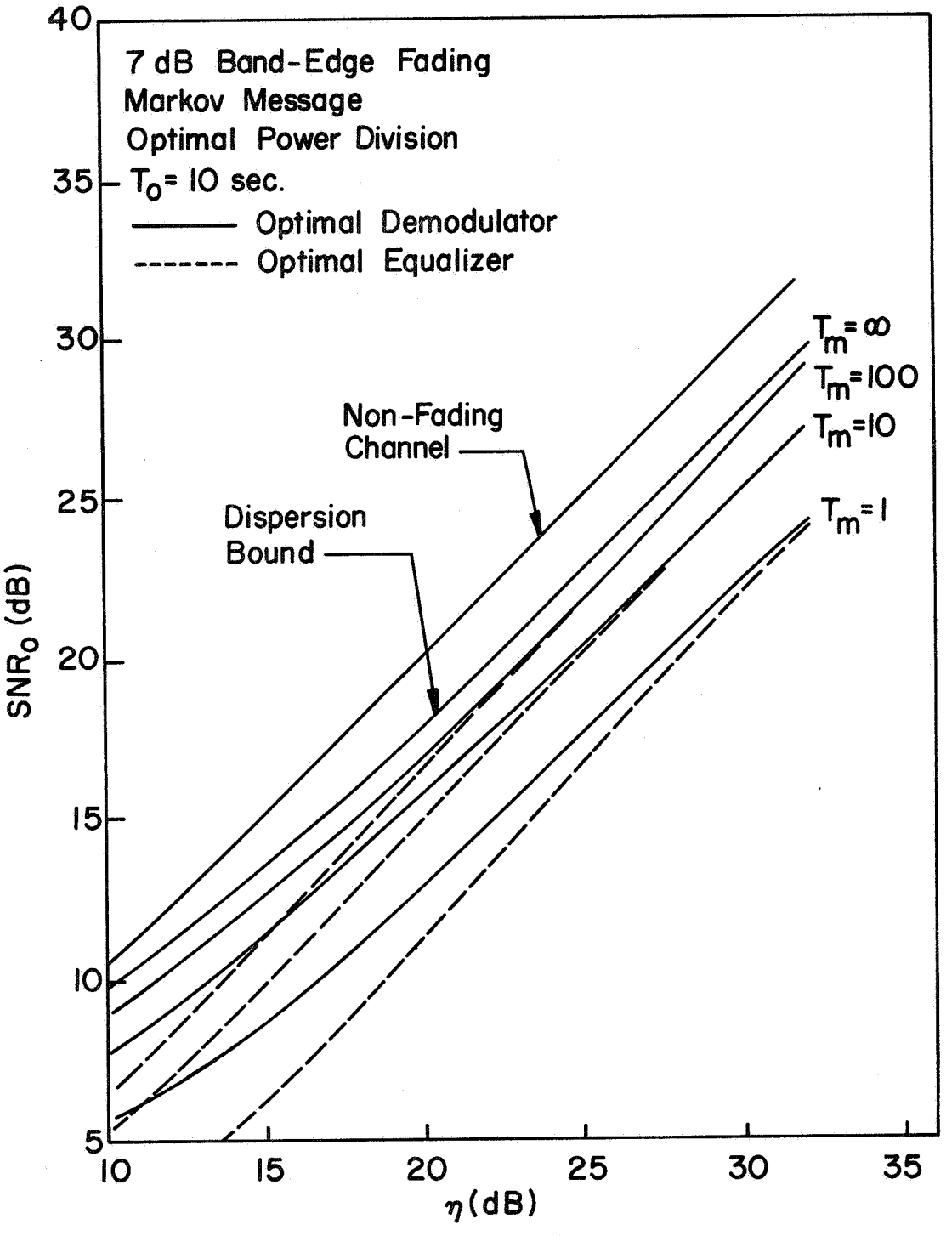

FIGURE 5-6. OVERALL DEMODULATOR PERFORMANCE COMPARISON FOR 7dB BAND-EDGE FADING.

sufficiently slow that the measurement can be performed over an interval of 100 seconds, then the optimal demodulator can be made to perform within 1dB of the performance for a known channel. But this known-channel case is just the Cramer-Rao bound on performance of any technique for communicating over dispersive channels (Section 4.2), so that the transmitted-reference technique results in very nearly fully-optimal systems for demodulation if the fading rate is reasonably slow (one hundredth of the channel bandwidth).

Figure 5-7 illustrates the case where performance is limited due to insufficient observation time. The remarks made in reference to Figure 5-6 hold here as well, but there is the usual flattening of the curves for large n caused by incomplete equalization.

Figure 5-8 compares the optimal equalizer performance for two different values of observation interval. The T_0=10 case is identical to the dashed curves of Figure 2-7, for which T_0 was a limiting factor. However, for T_0=30 the system is fundamentally noise-limited, as evidenced by the linear improvement with n. Notice that increasing T_0 when the system is not limited by incomplete equalization (before the T_0=10 curves flatten out) causes some loss in performance, an effect noted and explained at the end of Section 3.4.

Examination of many examples of these "exact" calculations of demodulator performance leads to the conclusion that nothing startling happens for the case of unknown channels. That is, the system's non-linear dependence on channel

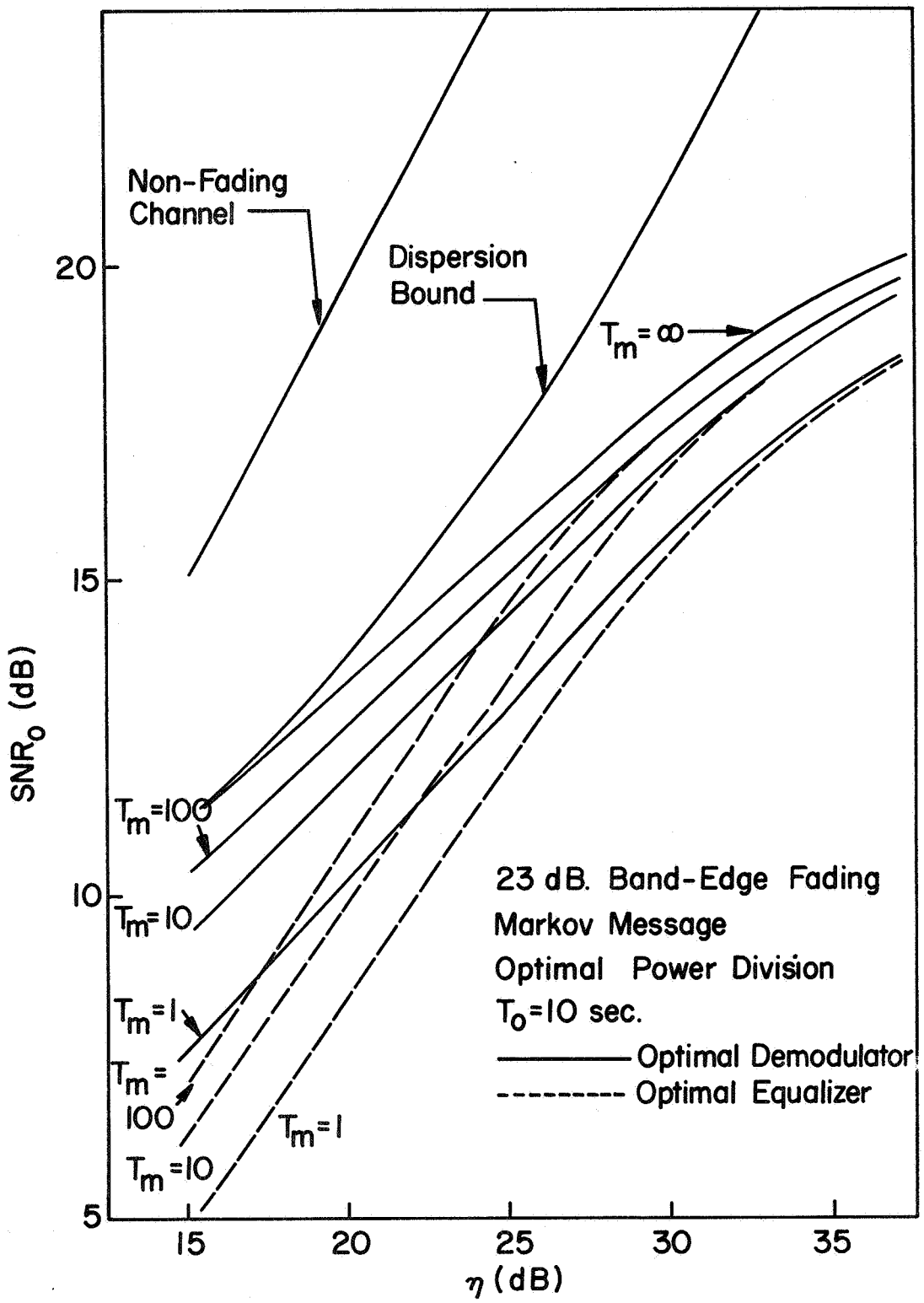

FIGURE 5-7. OVERALL DEMODULATOR PERFORMANCE COMPARISON FOR 23 dB BAND-EDGE FADING.

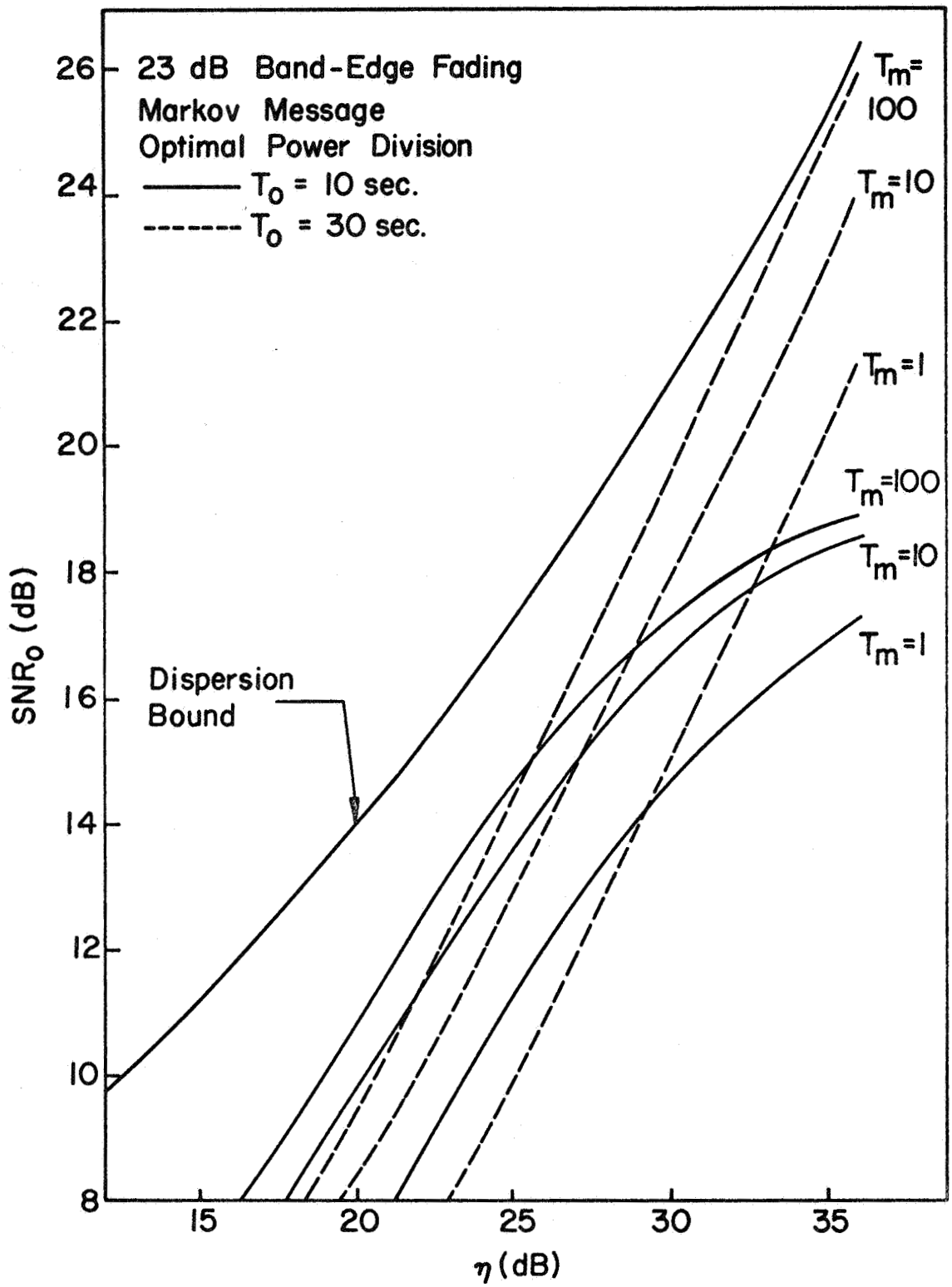

FIGURE 5-8. OVERALL PERFORMANCE OF OPTIMAL EQUALIZERS FOR 23 dB BAND-EDGE FADING.

measurement errors does not appear to cause any threshold effects or catastrophic breakdowns in performance, at least for the reasonably small measurement errors considered. The degradation due to channel measurement error is graceful, and examining Figures 5-6 through 5-8 carefully, it can be seen that increasing the measurement error (reducing T_m) merely tends to push down the entire performance curve. (This is not exactly true, but very nearly so.) Since this approximate behavior of adding a mere constant to the estimation error is a fundamentally linear effect, one is led to attempt the linearization of the exact performance equations with respect to channel measurement errors, and extend the analytical results by approximation.

5.4 An Approximate Analysis of the Effect of Noisy Channel Measurements

For the optimal demodulator the mismatch function was given by (5-13):

$$\underline{\underline{\Lambda}}(\hat{\underline{h}}) = \frac{1}{\eta_a}\hat{\underline{\underline{Q}}}^{-1} + \hat{\underline{\underline{Q}}}^{-1}\left[\hat{\underline{\underline{H}}}^{*T}\underline{\underline{E}}\,\underline{\underline{\phi}}_a\underline{\underline{E}}^{*T}\hat{\underline{\underline{H}}} + \frac{1}{\eta_a}\left(\hat{\underline{\underline{H}}}^{*T}\underline{\underline{E}} + \hat{\underline{\underline{E}}}^{*T}\hat{\underline{\underline{H}}}\right)\right]\hat{\underline{\underline{Q}}}^{-1} \tag{5-22}$$

$$\hat{\underline{\underline{Q}}} = \left[\hat{\underline{\underline{H}}}^{*T}\hat{\underline{\underline{H}}} + \frac{1}{\eta_a}\underline{\underline{\phi}}_a^{-1}\right] \tag{5-23}$$

The difficulty in averaging (5-22) with respect to $\hat{\underline{h}}$ is caused by the matrix inverses. Suppose that we take the linear variation of $\hat{\underline{\underline{Q}}}^{-1}$ with respect to the measurement error matrix E. That is, if $\hat{\underline{\underline{H}}} = \underline{\underline{H}} + \varepsilon\underline{\underline{E}}$, then the first variation

of $\hat{\underline{\underline{Q}}}^{-1}$ with respect to $\underline{\underline{E}}$ is $\frac{d}{d\varepsilon}\hat{\underline{\underline{Q}}}^{-1}\Big|_{\varepsilon=0}$.

$$\frac{d}{d\varepsilon}\hat{\underline{\underline{Q}}}^{-1}\Big|_{\varepsilon=0} = -\hat{\underline{\underline{Q}}}^{-1}\left[\frac{d}{d\varepsilon}\hat{\underline{\underline{Q}}}\right]\hat{\underline{\underline{Q}}}^{-1}\Big|_{\varepsilon=0} = -\underline{\underline{Q}}^{-1}\left[\frac{d}{d\varepsilon}\hat{\underline{\underline{Q}}}\Big|_{\varepsilon=0}\right]\underline{\underline{Q}}^{-1}$$

$$= -\underline{\underline{Q}}^{-1}\left[\underline{\underline{H}}^{*T}\,\underline{\underline{E}} + \underline{\underline{E}}^{*T}\,\underline{\underline{H}}\right]\underline{\underline{Q}}^{-1} \qquad (5\text{-}24)$$

Thus, to a first approximation,

$$\hat{\underline{\underline{Q}}}^{-1} \doteq \underline{\underline{Q}}^{-1} - \underline{\underline{Q}}^{-1}\left[\underline{\underline{H}}^{*T}\,\underline{\underline{E}} + \underline{\underline{E}}^{*T}\,\underline{\underline{H}}\right]\underline{\underline{Q}}^{-1} \quad . \qquad (5\text{-}25)$$

If (5-25) is then substituted into (5-22) and all terms higher than second order in $\underline{\underline{E}}$ and $\frac{1}{\eta}$ are neglected (both are presumed small) we obtain

$$\underline{\underline{\Lambda}}(\hat{\underline{h}}) \doteq \frac{1}{\eta_a}\left[\underline{\underline{Q}}^{-1} - \underline{\underline{Q}}^{-1}\left(\underline{\underline{H}}^{*T}\,\underline{\underline{E}} + \underline{\underline{E}}^{*T}\,\underline{\underline{H}}\right)\underline{\underline{Q}}^{-1}\right]$$

$$+ \underline{\underline{Q}}^{-1}\left[\underline{\underline{H}}^{*T}\,\underline{\underline{E}}\,\underline{\underline{\Phi}}_a\,\underline{\underline{E}}^{*T}\,\underline{\underline{H}} + \frac{1}{\eta_a}\left(\underline{\underline{H}}^{*T}\,\underline{\underline{E}} + \underline{\underline{E}}^{*T}\,\underline{\underline{H}}\right)\right]\underline{\underline{Q}}^{-1}$$

$$= \frac{1}{\eta_a}\underline{\underline{Q}}^{-1} + \underline{\underline{Q}}^{-1}\,\underline{\underline{H}}^{*T}\,\underline{\underline{E}}\,\underline{\underline{\Phi}}_a\,\underline{\underline{E}}^{*T}\,\underline{\underline{H}}\,\underline{\underline{Q}}^{-1} \quad . \qquad (5\text{-}26)$$

Now the measurement error appears in a simple way, and the average of $\underline{\underline{\Lambda}}(\hat{\underline{h}})$ with respect to $\hat{\underline{h}}$ may be carried out analytically.

$$\underline{\underline{\Lambda}} = E_{\hat{\underline{h}}}[\underline{\underline{\Lambda}}(\hat{\underline{h}})] = \frac{1}{\eta_a}\underline{\underline{Q}}^{-1} + \underline{\underline{Q}}^{-1}\,\underline{\underline{H}}^{*T}\,\overline{(\underline{\underline{E}}\,\underline{\underline{\Phi}}_a\underline{\underline{E}}^{*T})}\,\underline{\underline{H}}\,\underline{\underline{Q}}^{-1} \qquad (5\text{-}27)$$

This same result can be obtained by a different approach to linearization - assuming that the mismatch occurs in the actual channel. That is, fix the demodulator and average over an ensemble of mismatched channels rather than fix the channel and average over an ensemble of mismatched demodulators. In this alternate approach the mismatch matrix $\underline{\underline{E}}$ appears linearly at the outset.

To illustrate the second method consider the optimal equalizer, (5-3).

$$\hat{a}_k = \underline{\phi}_k^{*T}\, \underline{\underline{H}}^{*T}\left[\underline{\underline{H}}\, \underline{\underline{\phi}}_a\, \underline{\underline{H}}^{*T}\right]^{-1} \underline{y} = \underline{c}^T\, \underline{y} \tag{5-28}$$

Putting the mismatch in the channel we have

$$\underline{y} = \underline{\underline{\hat{H}}}\underline{a} + N = (\underline{\underline{H}} + \underline{\underline{E}})\,\underline{a} + \underline{N} \tag{5-29}$$

so that

$$\lambda_k(\underline{\hat{h}}) = \frac{1}{\sigma_a^2} E_{\underline{a},\underline{N}} \left|\hat{a}_k - a_k\right|^2$$

$$= 1 + \underline{\phi}_k^{*T}\, \underline{\underline{H}}^{*T}\left[\underline{\underline{H}}\, \underline{\underline{\phi}}_a \underline{\underline{H}}^{*T}\right]^{-1}\left[\underline{\underline{\hat{H}}}\, \underline{\underline{\phi}}_a\, \underline{\underline{\hat{H}}}^{*T} + \frac{1}{n}\, \underline{\underline{I}}\right]\left[\underline{\underline{H}}\, \underline{\underline{\phi}}_a \underline{\underline{H}}^{*T}\right]^{-1} \underline{\underline{H}}\, \underline{\phi}_k$$

$$- \underline{\phi}_k^{*T}\, \underline{\underline{H}}^{*T}\left[\underline{\underline{H}}\, \underline{\underline{\phi}}_a \underline{\underline{H}}^{*T}\right]^{-1} \underline{\underline{\hat{H}}}\underline{\phi}_k - \underline{\phi}_k^{*T}\, \underline{\underline{\hat{H}}}^{*T}\left[\underline{\underline{H}}\, \underline{\underline{\phi}}_a\, \underline{\underline{H}}^{*T}\right]^{-1} \underline{\underline{H}}\, \underline{\phi}_k \quad . \tag{5-30}$$

Taking the average of (5-30 with respect to $\underline{\hat{h}}$, and noting that the measurement errors have zero mean, we obtain the average error variance for the optimal equalizer.

$$\lambda_k = E_{\hat{\underline{h}}}\left[\lambda_k(\hat{\underline{h}})\right] = 1 - \underline{\phi}_k^{*T}\,\underline{\underline{H}}^{*T}\left[\underline{\underline{H}}\,\underline{\underline{\phi}}_a\,\underline{\underline{H}}^{*T}\right]^{-1}\underline{\underline{H}}\underline{\phi}_k$$

$$+ \frac{1}{\eta_a}\,\underline{\phi}_k^{*T}\,\underline{\underline{H}}^{*T}\left[\underline{\underline{H}}\,\underline{\underline{\phi}}_a\,\underline{\underline{H}}^{*T}\right]^{-2}\underline{\underline{H}}\,\underline{\phi}_k \qquad (5\text{-}31)$$

$$+ \underline{\phi}_k^{*T}\,\underline{\underline{H}}^{*T}\left[\underline{\underline{H}}\,\underline{\underline{\phi}}_a\,\underline{\underline{H}}^{*T}\right]^{-1}\overline{\left[\underline{\underline{E}}\,\underline{\underline{\phi}}_a\underline{\underline{E}}^{*T}\right]}\left[\underline{\underline{H}}\,\underline{\underline{\phi}}_a\underline{\underline{H}}^{*T}\right]^{-1}\underline{\underline{H}}\underline{\phi}_k$$

This unwieldy expression is considerably simplified by using (5-28) to identify $\underline{c}$, and (3-65) to identify the equalization error, $\varepsilon^2(T_0)$.

$$\lambda_k = \varepsilon^2(T_0) + \frac{1}{\eta_a}\,\underline{c}^T\,\underline{c}^* + \underline{c}^T\overline{\left[\underline{\underline{E}}\,\underline{\underline{\phi}}_a\underline{\underline{E}}^{*T}\right]}\underline{c}^* \qquad (5\text{-}32)$$

Both the optimal demodulator performance, (5-27), and the optimal equalizer performance, (5-32), require the matrix $\overline{\left[\underline{\underline{E}}\,\underline{\underline{\phi}}_a\underline{\underline{E}}^{*T}\right]}$. For uncorrelated, zero-mean measurement errors with variances $(\eta_m T_m)^{-1}$, and assuming $\underline{a}$ has stationary covariance,[1] it can be shown using the matrix definitions (5-11) and (2-26) that

$$\overline{\left[\underline{\underline{E}}\,\underline{\underline{\phi}}_a\,\underline{\underline{E}}^{*T}\right]} = \frac{T_c}{\eta_m T_m}\,\underline{\underline{\phi}}_a \quad . \qquad (5\text{-}33)$$

Thus the approximate performance of the optimal demodulator is

---

[1] All elements of each diagonal of $\underline{\underline{\phi}}_a$ are identical. ($\underline{\underline{\phi}}_a$ is a Toeplitz matrix).

$$\underline{\underline{A}} = \frac{1}{\eta_a} \underline{\underline{Q}}^{-1} + \frac{T_c}{\eta_m T_m} \underline{\underline{Q}}^{-1} \underline{\underline{H}}^{*T} \underline{\underline{\Phi}}_a \underline{\underline{H}} \underline{\underline{Q}}^{-1} \quad , \tag{5-34}$$

and the performance of the optimal equalizer is

$$\lambda_k = \varepsilon^2(T_0) + \frac{1}{\eta_a} \underline{c}^T \underline{c}^* + \frac{T_c}{\eta_m T_m} \underline{c}^T \underline{\underline{\Phi}}_a \underline{c}^* . \tag{5-35}$$

Comparing these equations with the corresponding expressions for the case of known channels in Section 3.5 shows that the noisy channel measurements are accounted for by an additional term,

$$\frac{T_c}{\eta_m T_m} \underline{\underline{Q}}^{-1} \underline{\underline{H}}^{*T} \underline{\underline{\Phi}}_a \underline{\underline{H}} \underline{\underline{Q}}^{-1} \tag{5-36}$$

for the optimal demodulator, and

$$\frac{T_c}{\eta_m T_m} \underline{c}^T \underline{\underline{\Phi}}_a \underline{c}^* \tag{5-37}$$

for the optimal equalizer. Both go to zero as the measurement error, $(\eta_m T_m)^{-1}$, goes to zero.

Equations (5-34) and (5-35), obtained by linearizing the dependence upon measurement error, have been found to be in good agreement (within 1 dB) with the results of the "exact" performance calculations of Section 5.3 for reasonably small measurement errors ($\eta_m T_m \geq$ 10dB). Although, because of the extreme dimensionality of the exact performance equations, the two methods could be compared only for the case of

single-notch fading, (T_c=1), it is felt that (5-34) and (5-35) are valid for higher-order channels as well; the degradation due to imperfect channel measurements is simply proportional to the number of unknown channel tap gains, a perfectly logical result.

5.5 The Infinite-Interval Approximation

Equations (5-34) and (5-35), although vastly easier to evaluate than the exact performance equations, nonetheless require matrix inversion because they still retain the "exact" dependence upon observation interval. Yet more simplification is possible if we assume, in the manner of Section 3.5, that the observation interval merely puts an upper limit on system performance through the equalization error, $\varepsilon^2(T_0)$, and that below this limit the observation interval may be regarded as infinite since the system is fundamentally noise-limited.

For $T_0=\infty$ the optimal demodulator is a filter, f(t), satisfying Equation (2-21).

$$\int_{-\infty}^{\infty} R_y(\lambda_1-\lambda_2)\ f(t-\lambda_2)\ d\lambda_2 = R_{ax}(\lambda_1-t)\ . \qquad (5\text{-}38)$$

Then, putting the measurement error dependence into the channel state, the message estimate is

$$\hat{a}(t) = f(t) \circledast [\hat{h}(t) \circledast a(t) + N(t)]\ , \qquad (5\text{-}39)$$

for which the average estimation error can be shown to be

$$E\,|\hat{a}(t) - a(t)|^2 = R_a(0) - \int_{-\infty}^{-\infty}\int_{-\infty}^{-\infty} f(\lambda_1)\, f^*(\lambda_2) R_y(\lambda_1-\lambda_2)\,d\lambda_1 d\lambda_2$$

$$+ \frac{T_c}{\eta_m T_m} \int_{-\infty}^{\infty}\int_{-\infty}^{\infty} f(\lambda_1)\, f^*(\lambda_2) R_a(\lambda_1-\lambda_2)\,d\lambda_1 d\lambda_2, \tag{5-40}$$

and where the expectation has been carried out over message, noise, and measurement error. Rewriting (5-40) in terms of Fourier transforms with the aid of Parseval's formula and Equation (2-23) for the Fourier transform of f(t) we obtain

$$E\left[|\hat{a}(t) - a(t)|^2\right] = \frac{1}{2\pi}\int_{\pi}^{\pi} \frac{S_a(\omega) S_N(\omega)}{S_a(\omega)\,|H(-j\omega)|^2 + S_N(\omega)}\,d\omega$$

$$+ \frac{T_c}{\eta_m T_m}\,\frac{1}{2\pi}\int_{-\pi}^{\pi} \frac{S_a{}^3(\omega)\,|H(-j\omega)|^2}{\left[S_a(\omega)\,|H(-j\omega)|^2 + S_N(\omega)\right]^2}\,d\omega. \tag{5-41}$$

Recognizing that integrals of this type are most easily carried out in the z domain using residue calculus, we replace (5-41) by its z transform analog, letting $R_a(z)$ denote the z transform of the <u>normalized</u> message autocorrelation. If, at the same time, we include the effect of finite T_0 by adding in the equalization error $\varepsilon^2(T_0)$, the following approximation to the optimal demodulation performance is obtained.

$$\frac{1}{\sigma_a^2} E\left[\left|\hat{a}(t) - a(t)\right|^2\right] = \frac{1}{\eta_a} \frac{1}{2\pi j} \oint \frac{1}{H(z^{-1})\, H^*(z) + \frac{1}{\eta_a} R_a^{-1}(z)} \frac{dz}{z}$$

(5-42)

$$+ \frac{T_c}{\eta_m T_m} \frac{1}{2\pi j} \oint \frac{R_a(z) H(z^{-1}) H^*(z)}{\left[H(z^{-1}) H^*(z) + \frac{1}{\eta_a} R_a^{-1}(z)\right]^2} \frac{dz}{z} + \varepsilon^2(T_0)$$

This expression, although it may not look simple, requires only algebraic manipulations if $\varepsilon^2(T_0)$ is estimated by the method of "equivalent single-notch channels" described in Section 3.5.

Recalling that the optimal equalizer is just the assymptotic form of the optimal demodulator as $\eta_a \to \infty$, its performance is given by the assymptotic form of (5-42).

$$\frac{1}{\sigma_a^2} E\left[\left|\hat{a}(t) - a(t)\right|^2\right] = \frac{1}{\eta_a} \frac{1}{2\pi j} \oint \frac{1}{H(z^{-1}) H^*(z)} \frac{dz}{z}$$

(5-43)

$$\frac{T_c}{\eta_m T_m} \frac{1}{2\pi j} \oint \frac{R_a(z)}{H(z^{-1}) H^*(z)} \frac{dz}{z} + \varepsilon^2(T_0)$$

Comparing these last two equations for unknown channels with (3-68) and (3-69), for known channels, the effect of noisy measurements is seen to be accounted for by the middle term in (5-42) and (5-43). Since the performance curves are known to flatten out as $\eta_a \to \infty$ (see Figures 5-1 through 5-4), an estimate of the resultant assymptote is now known to be

$$\frac{T_c}{\eta_m T_m} \frac{1}{2\pi j} \oint \frac{R_a(z)}{H(z^{-1})\ H^*(z)} \frac{dz}{z} \quad , \qquad (5\text{-}44)$$

so that families of measurement error assymptotes can easily be drawn for design purposes in the manner of Figures 5-1 through 5-4. The other required assymptotes were already known from Section 3.5. Thus we have a complete quick-design procedure based on assymptotic forms, similar in nature to the Bode plots of control theory.

5.6 Optimal Power Division

Equations (5-42) and (5-43) may be used to obtain a simple approximate formula for optimal power division, discussed first in Section 5.3. In principle, all one has to do is substitute (5-19) and (5-20) for η_a and η_m respectively into (5-42) and (5-43) and minimize with respect to δ. The optimal δ will then be a rather complicated function of the channel state, message spectrum, total SNR, η, T_c, and T_m. This is undesirable since a feedback link would be required to inform the transmitter of the state of the channel. However, as was pointed out in Section 5.3, the optimal power division is not at all critical (Figure 5-5), especially if $\frac{T_m}{T_c} >> 1$. A simple "rule of thumb" for optimal power division which lies within the ranges given by (5-21) and is independent of channel state, message spectrum, and η is obtained by assuming a white message spectrum in (5-43) (i.e. $R_a(z)=1$). The

resultant division of power, if not precisely optimal, is at least very good.

Substituting (5-19) and (5-20) into (5-43) with $R_a(z)=1$ we obtain

$$\frac{1}{\sigma_a^2} E\left[|\hat{a}(t)-a(t)|^2\right] = \frac{1}{\eta}\left[\frac{1}{(1-\delta)} + \frac{T_c}{\delta T_m}\right] \cdot \frac{1}{2\pi j}\oint \frac{1}{H(z^{-1})H^*(z)} \frac{dz}{z}$$

$$+ \varepsilon^2(T_0) \qquad (5\text{-}45)$$

Minimizing with respect to δ we easily obtain

$$\delta_{opt} = \frac{1}{1 + \sqrt{T_m \cdot T_c^{-1}}} \quad , \qquad (5\text{-}46)$$

a simple formula agreeing well with (5-21) for $T_c=1$.

Assuming that this expression gives a "good" division of power we substitute for η_a and η_m in (5-42) and (5-43) to obtain formulas for overall system performance. For the optimal demodulator the performance is

$$\frac{1}{\sigma_a^2} \mathrm{Var}(\hat{a}(t) - a(t)) =$$

$$\frac{(1+\sqrt{T_c \cdot T_m^{-1}})}{\eta} \frac{1}{2\pi j}\oint \frac{1}{H(z^{-1})H^*(z) + \frac{(1+\sqrt{T_c \cdot T_m^{-1}})}{\eta} R_a^{-1}(z)} \frac{dz}{z} +$$

$$+\frac{\sqrt{T_c \cdot T_m^{-1}}\,(1+\sqrt{T_c \cdot T_m^{-1}})}{\eta}\,\frac{1}{2\pi j}\oint \frac{H(z^{-1})H^*(z)R_a(z)}{H(z^{-1})H^*(z)+\frac{(1+\sqrt{T_c \cdot T_m^{-1}})}{\eta}R_a^{-1}(z)}\,\frac{dz}{z}$$

$$+\varepsilon^2(T_0) \quad , \tag{5-47}$$

while for the optimal equalizer we have

$$\frac{1}{\sigma_a^2}\,\mathrm{Var}(\hat{a}(t)-a(t)) = \frac{(1+\sqrt{T_c \cdot T_m^{-1}})}{\eta}\,\frac{1}{2\pi j}\oint \frac{1}{H(z^{-1})H^*(z)}\,\frac{dz}{z}$$

$$+\frac{\sqrt{T_c \cdot T_m^{-1}}\,(1+\sqrt{T_c \cdot T_m^{-1}})}{\eta}\cdot\frac{1}{2\pi j}\oint \frac{R_a(z)}{H(z^{-1})H^*(z)}\,\frac{dz}{z}+\varepsilon^2(T_0)\ . \tag{5-48}$$

These equations for the overall performance of demodulators for unknown dispersive channels are known to be reasonable approximations to the actual performance for single-notch selective fading, the only case for which exact results were available, and they appear to be reasonable for higher-order channels as well. They are simple to evaluate given the gross design parameters of the system: demodulator observation interval, T_0, which determines system complexity; total SNR η, determined by the available transmitter power, receiver noise figure, and channel attenuation; measurement time, T_m, limited by the channel fading rate; and channel delay-spread, T_c, dependent upon the transmission medium and signalling bandwidth. For purposes of design, a worst-case analysis could be performed, the worst case taken to be a

single notch fade at the peak of the signal spectrum. This approximation procedure provides a starting point for the practical design of dispersive channel communication systems.

CHAPTER 6: CONCLUDING REMARKS

6.1 Summary and Conclusions

In Chapter 1 several questions about the demodulation of signals passed through selective-fading channels were posed. An appropriate summary of this research is an attempt to answer these questions.

1. First of all, the channel is assumed to be a bandlimited, slowly time-varying, selective fading channel described by a tapped delay-line channel model whose parameters are stationary over time intervals consistent with the rate of fading.
2. The optimal demodulator for analog communication over this type of channel is developed using the technique of maximizing a-posteriori probability. The receiver structure obtained for non-linear modulation is found to defy practical implementation (and analysis as well) in its derived form, so the research is restricted to consideration of linear passband recovery of the transmitted signal, an operation both practical and amenable to analysis. Wiener-Hopf methods are used to obtain the

minimum mean-square-error demodulator, using an integral formulation to study idealized systems which are assumed to observe the entire past and future of the channel output, and a sampled-data formulation to investigate more realistic systems having finite observation time.

It is found that channel dispersion produces an intrinsic loss in performance relative to non-fading channels. That is, no amount of sophisticated signal processing can completely overcome the effects of dispersion. It is also found that the length of the observation interval limits the performance of the demodulator for high SNR whenever fading is severe.

The optimal dispersive channel demodulator turns out to require some rather sophisticated filtering operations which are not easily adapted to different channel states, hence expensive to mechanize. Consequently, effort is devoted to the consideration of suboptimal approximations to the optimal demodulator which use transversal equalizers based on a zero-noise assumption. Such equalizers were known to be practical from the literature. A novel approach to the

performance analysis of zero-forcing and minimum mean-square error equalizers leads to the conclusion that the latter equalization algorithm works significantly better than the former for severe fading channels. In addition, it is found that the dependence of equalizer performance upon its observation interval or length (hence cost) is basically governed by that zero of the selective-fading channel which is closest to the unit circle in the complex Z plane. Thus, for purposes of approximating the equalization error, high order dispersive channels can be reduced to an equivalent single-notch channel.

An investigation of the performance of equalizers in the presence of noise shows that the optimal equalizer is a near-optimal demodulator under low-noise conditions, but that there is serious degradation when there is much noise; the zero-forcing equalizer works considerably less well. A study of post-equalization filtering techniques to improve the low SNR performance leads to the negative conclusion that they are not worthwhile: only the exact optimal demodulator works well for low SNR.

Finally, putting together all the results for known-channel demodulation, it is found that the general performance of the optimal demodulator and optimal equalizer may be approximately described if the assymptotes of the performance as the noise goes to zero, and as the observation interval goes to infinity, are known, which they are from previous results of this research. This makes possible a graphical design procedure similar to the Bode diagram of control theory.

3. When the channel is unknown, it must in some way be estimated in order to effectively demodulate the message. Two different channel measurement techniques are considered: channel estimation using the message alone to probe the channel, along with its a-priori statistics; channel estimation making use of a special reference signal known in advance to the receiver. The former technique is desirable in that all transmitter power is devoted to information transfer, but it is found to be impractical for analog communication. However, its ultimate performance is given by the Cramer-Rao bound, a useful theoretical result for judging the actual performance of transmitted-reference

measurement systems, systems which are quite easy to build.

Joint optimization of the channel state estimate and reference signal, subject to a power constraint, gives a reference signal optimality criterion which is exactly satisfied by certain classes of pulse signals and approximately by many other classes. Consideration of transmitter peak-power limitations and ease of generation indicates that PN sequences although suboptimal, make admirable reference signals, for either periodic or aperiodic measurements.

4. Imperfect channel measurements affect the performance of transmitted-reference communications systems of the estimator-correlator type in a complicated, non-linear way. Numerical methods are used to investigate system performance for single-notch selective fading channels, the only computationally feasible case; the results show that the basic effect of noisy channel measurements is to increase the effective equalization error, the assymptotic demodulator performance as the additive noise goes to zero. Optimal division of transmitter power between reference signal and message is studied as well. It is discovered

that this optimum is not at all critical, and that if the fading rate of the channel permits long channel measurements, only a small fraction of the transmitter power need be devoted to channel measurement, making the transmitted reference technique very nearly fully optimal in the sense of the Cramer-Rao bound on performance. In addition, the overall system performance curves (optimized with respect to power division) are, for different values of measurement error, found to be very nearly mere translations of one another along the performance axis. This suggests a linearized performance analysis to find the appropriate constant of translation.

5. Equivalent linearization of the system dependence upon channel measurement errors provides a reasonably accurate estimate of the effect of these errors on system performance which is far simpler than the exact performance computations. An additional approximation which isolates the effects due to finite observation interval from the effects of additive noise and channel measurement errors permits the description of overall system performance in terms of easily-computed integrals which determine the assymptotes of the performance curves.

These assymptotes may be used for a graphical design procedure to provide quick estimates of the performance of dispersive-channel communications systems suitable for "first-cut" design or parametric studies. Only fundamental system parameters are retained: observation interval (equalizer length); receiver noise figure (noise power); channel delay spread; measurement interval (fading rate); transmitter power; signal power spectrum; channel state (could be accounted for on a worst-case basis).

Finally, a "rule of thumb" for transmitter pwoer division is developed which depends only upon the gross channel parameters of delay apread and fading rate; this division of power provides nearly optimal performance without requiring a feedback link from receiver to transmitter.

6.2 Some Areas for Further Research

In the course of this research three topics for future research suggested themselves, but were not actively pursued.

1. There must be a better optimality criterion for non-linear, bandwidth-expanding modulation systems operating over dispersive channels than either MAP or minimum mean-square passband equalization. Both these criteria require

passband delay lines with bandwidths much wider than that required by the message itself. It would be eminently desirable from a practical viewpoint to perform the equalization on the message estimate at baseband, perhaps in a non-linear way, or preceded by a non-linear device. A new criterion which somehow constrained the delay line to operate at baseband would be of great interest.

2. The fact that equalizaer performance is governed by that channel root closest to the unit circle in the Z plane suggests an investigation of the distribution of channel roots for a statistically described channel. In testing this principle by random examples some feel was obtained for the problem, but was purely qualitative and empirical. It would be interesting to find the effect of the channel correlation bandwidth and multipath intensity profile [1] on this distribution.

3. This research assumed that the channel was stationary over a given time-interval. A direct extension would be to assume a first-order time variation (that is, assume a channel impulse response of the form $h(t)=h_0(t) + t\,h_1(t)$ and find the optimal

demodulators and channel estimators based on this assumption. Although rate estimators are as a rule inaccurate, perhaps the overall system dependence is relatively insensitive to this type of error. In any event, the unpalatable fact of channel time-variation would be explicitly accounted for, and some fears about the effects of non-stationarity could possibly be laid to rest.

LIST OF REFERENCES

1. Schwartz, M., W. R. Bennett, S. Stein. Communication Systems and Techniques, McGraw Hill, New York, 1966.

2. Hancock, J. C., P. A. Wintz. Signal Detection Theory, McGraw Hill, New York, 1966.

3. Durrani, S. H. "Rejection of Multipath Interference in Satellite Communications by Use of Narrow-Band Filters," I. E. E. E. Transactions on Aerospace and Electronic Systems, Vol. AES-4, No. 1, Jan., 1968.

4. Anderson, R. E. "Sideband Correlation of Lunar and Echo Satellite Reflection Signals in the 900 Mc. Range," Proceedings of the IEEE, Vol. 49, No. 6, June, 1961.

5. Middleton, D. Statistical Communication Theory, McGraw Hill, New York, 1960.

6. Kailath, T. "Channel Characterization: Time-Variant Dispersive Channels," Lectures on Communication System Theory, E. J. Baghdady, ed., McGraw Hill, New York, 1961.

7. Lebow, I., et al. "The West Ford Belt as a Communication Medium," Proceedings of the IEEE, Vol. 52, No. 5, May, 1964.

8. Root, W. L. "On the Measurement and Use of Time-Varying Communications Channels," Information and Control, Vol. 8, August, 1965.

9. Kailath, T. "Sampling Models for Linear, Time-Variant Filters," MIT Research Lab. of Electronics, Cambridge, Mass., Report No. 352, May, 1959.

10. Clarke, K. "Random Channel Simulation and Instrumentation," Convention Record, First Annual IEEE Communication Convention, Boulder, Colo., June, 1965.

11. Stein, S. "Theory of a Tapped Delay Line Fading Simulator," Convention Record, First Annual IEEE Communication Convention, Boulder, Colo., June, 1965.

12. Walker, W. "A Simple Baseband Fading Multipath Channel Simulator," Convention Record, First Annual IEEE Communication Convention, Boulder, Colo., June, 1965.

13. Stein, S. "Statistical Characterization of Fading Multipath Channels," Sylvania Applied Research Lab., Waltham, Mass., Report No. 321, Jan., 1963.

14. Youla, D. C. "The Use of Maximum Likelihood in Estimating Continuously Modulated Intelligence Which Has Been Corroupted By Noise," IRE Transactions on Information Theory, Vol. IT-3, March, 1954.

15. Thomas, J. B., T. Wong. "On the Statistical Theory of Optimal Demodulation," IRE Transactions on Information Theory, Vol. IT-6, No. 3, Sept., 1960.

16. Williams, T. R. "Optimum Receivers," IEEE Transactions on Communication Systems, Vol. COM-12, Sept., 1964.

17. Parzen, E. J. "Extraction and Detection Problems and Reproducing Kernel Hilbert Spaces," J. SIAM on Control, Ser. A., Vol. 1, 1962.

18. Davenport, W. B., W. L. Root. An Introduction to the Theory of Random Signals and Noise, McGraw Hill, New York, 1958, Chapter 11.

19. Tufts, D. W. "Matched Filters and Intersymbol Interference," Cruft Lab., Harvard U., Cambridge, Mass., Report No. 345, July, 1961.

20. Tufts, D. W. "Certain Results in Pulse Transmission Theory," Cruft Lab., Harvard U., Cambridge, Mass., Report No. 355, Feb., 1962.

21. Tufts, D. W. "Nyquist's Problem in Pulse Transmission Theory," Cruft Lab., Harvard U., Cambridge Mass., Report No. 425, Sept.,1963.

22. Tufts, D. W. "Summary of Certain Intersymbol Results," IEEE Transactions on Information Theory, Vol. IT-10, Oct., 1964.

23. George, D. A., D. C. Coll. "The Reception of Time-Dispersed Pulses," Convention Record, First Annual IEEE Communication Convention, Boulder, Colo., June, 1965.

24. George, D. A. "Matched Filters For Interfering Signals," IEEE Transactions on Information Theory, Vol. IT-11, Jan., 1965.

25. Niesson, C. W., P. R. Drouilhet. "Adaptive Equalizer for Pulse Transmission," Third Annual IEEE Communication Convention, Minneapolis, Minn., June, 1967.

26. Lucky, R. w., H. R. Rudin. "An Automatic Equalizer for General Purpose Communications Channels," Bell System Technical Journal, Vol. 46, No. 9, Nov., 1967.

27. Lucky, R. W. "Automatic Equalization for Digital Communications," Bell System Technical Journal, Vol. 44, April, 1965.

28. Lucky, R. W. "Techniques for the Adaptive Equalization of Digital Communications Systems," Bell System Technical Journal, Vol. 45, Feb., 1966.

29. Ditoro, M. J. "A New Method of High-Speed Adaptive Serial Communication Through any Time-Variable and Dispersive Transmission Medium," Convention Record, First Annual IEEE Communication Convention, Boulder, Colo., June, 1965.

30. Ditoro, M. J., et al. "H. F. Anti-Multipath Device (ADAPTICOM)," Final Report, Cardion Electronics Inc., AD-451765, Dec., 1965.

31. Schreiver, K. E., H. L. Funk, E. Hopner. "Automatic Distortion Correction for Efficient Pulse Transmission," IBM Journal of Research and Development, Vol. 9, Jan., 1965.

32. Van Trees, H. L. "Analog Communications Over Randomly Time-Varying Channels," IEEE Transactions on Information Theory, Vol. IT-12, Jan., 1966.

33. Rao, C. R. Linear Statistical Inference and Its Applications. John Wiley & Sons, New York, 1965, Chapter 5.

34. Middleton, D. Statistical Communication Theory, McGraw Hill, New York, 1960, Chapter 21.

35. Van Trees, H. L. "Bounds on the Accuracy Attainable in the Estimation of Continuous Random Processes," IEEE Transactions on Information Theory, Vol. IT-12, July, 1966.

36. Kailath, T. "Correlation Detection of Signals Perturbed by a Random Channel," IRE Transactions on Information Theory, Vol. IT-6, June, 1960.

37. Price, R., P. E. Green. "A Communication Technique for Multipath Channels," Proceedings of the IRE, Vol. 46, March, 1958.

38. Rushforth, C. R. "Transmitted Reference Techniques for Random or Unknown Channels," IEEE Transactions on Information Theory, Vol. IT-10, Jan., 1964.

39. Hingorani, G. P., J. C. Hancock. "A Transmitted Reference System for Communication in Random or Unknown Channels," IEEE Transactions on Communication Technology, Vol. COM-13, Sept., 1965.

40. Chesler, D. A. "A Simple Adaptable Receiver with Pilot Tones for Analog Communication Through Selective Fading Channels," Eighth National Communications Symposium, Utica, New York, Oct., 1962.

41. Kailath, T. "Estimating Filters for Linear, Time-Variant Channels," MIT Research Lab. of Electronics. Cambridge, Mass., Report No. 58, July, 1960.

42. Kailath, T. "Measurements on Time-Variant Communication Channels," IRE Transactions on Information Theory, Vol. IT-8, Sept., 1962.

43. Turin, G. L. "On the Estimation in the Presence of Noise of the Impulse Response of a Random Linear Filter," IRE Transactions on Information Theory, Vol. IT-3, March, 1957.

44. Golomb, S. W. Digital Communications, Prentice Hall Inc., Englewood Cliffs, New Jersey, 1964.

45. Weiner, N. Extrapolation, Interpolation, and Smoothing of Stationary Time Series, John Wiley and Sons, New York, 1949.

46. Courant, R., D. Hilbert. Methods of Mathematical Physics, Interscience Publishers, Inc., New York, 1953, Chapter III.

47. Huffman, D. A. "The Generation of Impulse Equivalent Pulse Trains," IEEE Transactions on Information Theory, Vol. IT-8, Sept., 1962.

48. Barker, R. H. "Group Synchronizing of Binary Digital Systems," Communication Theory, W. Jackson, ed., Academic Press, New York, 1953.

49. Turyn, R., J. Storer. "On Binary Sequences," Proceedings of The American Mathematical Society, Vol. 12, June, 1961.

50. Tompkins, F. N. Codes with Zero Correlation, Ph. D. Thesis, Purdue University, W. Lafayette, Ind., 1960.

APPENDIX A

DERIVATION OF THE MAP ESTIMATE

In Section 2.2 the generalized MAP optimality criterion was defined to be the minimum of the functional ε^2 given by (2-11).

$$\varepsilon^2 = \int_T \int_T R_N^{-1}(u-\tau)[y(u) - x(u)][y(\tau) - x(\tau)]^* du d\tau$$

$$+ \int_{T_a} \int_{T_a} R_a^{-1}(\lambda-\tau) a(\lambda) a^*(\tau) d\lambda d\tau \qquad \text{(A-1)}$$

This functional is optimized by a variational procedure. Let $a(t) = \hat{a}(t) + \sigma\eta(t)$, where $\hat{a}(t)$ is the optimal estimate of $a(t)$, and $\eta(t)$ is an arbitrary complex perturbation. Then $\hat{a}(t)$ is the solution to the variational equation[1]

$$\frac{d}{d\sigma} \varepsilon^2(\sigma) \Big|_{\sigma=0} = 0 \qquad \text{(A-2)}$$

Noting that

$$\frac{dx(t)}{d\sigma}\Big|_{\sigma=0} = \frac{d}{d\sigma} \int_{T_a} h(\tau-\lambda) s(a,\lambda) d\lambda$$

$$= \int_{T_a} h(\tau-\lambda) \frac{\partial s(a,\lambda)}{\partial a}\Big|_{a=\hat{a}} \eta(\lambda) d\lambda \quad , \qquad \text{(A-3)}$$

[1] See reference 46, Chapter 4.

and making use of the Hermitian symmetry of the covariance operators, we obtain

$$0 = \frac{d\varepsilon^2}{d\sigma}\bigg|_{\sigma=0} = 2\mathrm{Re}\int_{T_a} \eta(\lambda)d\lambda\Bigg\{\int_{T_a} R_a^{-1}(\lambda-\tau)\hat{a}^*(\tau)d\tau \tag{A-4}$$

$$- \int_T R_N^{-1}(u-\tau)\,[y(\tau)-\hat{x}(\tau)]^*d\tau\int_T h(u-\lambda)\,\frac{\partial s(a,\lambda)}{\partial a}\bigg|_{a=\hat{a}} du\Bigg\},$$

where

$$\hat{x}(t) = h(t) \circledast s(a,t).$$

Equation (A-4) must be satisfied for any arbitrary complex perturbation $\eta(\lambda)$; since both the real and imaginary parts of $\eta(\lambda)$ can be chosen independently, then <u>both</u> the real and imaginary parts of the term in braces in (A-4) must be identically zero. That is,

$$\int_{T_a} R_a^{-1}(\lambda-\tau)\hat{a}^*(\tau)d\tau \tag{A-6}$$

$$= \int_T \int_T h(u-\lambda)\frac{\partial s(a,\lambda)}{\partial a}\bigg|_{a=\hat{a}} R_N^{-1}(u-\tau)\,[y(\tau)-x(\tau)]^*d\tau du$$

for all $\lambda\varepsilon T_a$. Convolving (A-6) with the positive definite operator R_a and noting the resultant identity on the left-hand side we obtain

$$\hat{a}^*(t) = \int_{T_a} \int_{T} \int_{T} R_a(t-\lambda) h(u-\lambda) \left.\frac{\partial s(a,\lambda)}{\partial a}\right|_{a=\hat{a}}$$

$$\cdot R_N^{-1}(u-\tau)\,[y(\tau)-\hat{x}(\tau)]^* du\,d\lambda\,d\tau \quad , \qquad \text{(A-7)}$$

$$t \in T_a \quad .$$

This can be written more conveniently as

$$\hat{a}(t) = \int_{T} \left\{ h^*(\tau) \circledast \left[\left.\frac{\partial s^*(a,\tau)}{\partial a}\right|_{a=\hat{a}} R_a^*(t-\tau) \right] \right\} d\tau$$

$$\cdot \int_{T} R_N^{-1}(u-\tau)\,[y(u)-\hat{x}(u)]\,du \quad , \qquad \text{(A-8)}$$

$$t \in T_a \quad .$$

This integral equation, (A-8), is a necessary condition for the MAP estimate.

APPENDIX B

THE EQUIVALENCE OF THE MAP AND MEAN SQUARE ERROR CRITERIA FOR LINEAR MODULATION

For linear modulation the MAP estimate of a message transmitted over a known dispersive channel is given by (2-12) to be

$$\hat{a}(t) = \int_T \left[h^*(\tau) \circledast R_a^*(t-\tau) \right] d\tau \int_T R_N^{*-1}(\tau-u)\,[y(u)-\hat{x}(u)]\,du \qquad \text{(B-1)}$$

$$= \int_T R_{ax}(\tau-t)\,d\tau \int_T R_N^{-1}(u-\tau)\,[y(u)-\hat{x}(u)]\,du \qquad \text{(B-2)}$$

for $t \in T_a$. Defining the function $g(\tau)$ to be

$$g(\tau) = \int_T R_N^{-1}(u-\tau)\,[y(u)-\hat{x}(u)]\,du \qquad \text{(B-3)}$$

and operating on (B-3) with the noise covariance function, R_N, we find

$$\int_T g(\tau)\, R_N(\tau-t)\,d\tau = y(t)-\hat{x}(t) \qquad \text{(B-4)}$$

Then (B-2) can be written

$$\hat{a}(t) = \int_T g(\tau)\ R_{ax}(\tau-t)\ d\tau \qquad \text{(B-5)}$$

Operating on both sides of (B-5) with the channel impulse response, h(t), we obtain

$$\hat{x}(t) = h(t) \circledast \hat{a}(t) = \int_{T_a} h(t-\lambda)\ \hat{a}(\lambda)d\lambda$$

$$= \int_{T_a} h(t-\lambda)d\lambda \int_T g(\tau)\ R_{ax}(\tau-\lambda)\ d\tau$$

$$= \int_T g(\tau)\ d\tau \int_{T_a} h(t-\tau)\ R_{ax}(\tau-\lambda)\ \lambda$$

$$= \int_T g(\tau)\ R_x(\tau-t)\ dt \qquad \text{(B-6)}$$

The last equality above comes from the general properties of random signals passed through linear systems. Substitution of (B-6) into (B-4) gives

$$y(t) = \hat{x}(t) + \int_T g(\tau)\ R_N(\tau-t)\ d\tau$$

$$= \int_T g(\tau)\ \left[R_x(\tau-t) + R_N(\tau-t)\right]d\tau$$

$$= \int_T g(\tau)\ R_y(\tau-t)\ d\tau \qquad \text{(B-7)}$$

Equations (B-5) and (B-7) together define the MAP estimate.

Now suppose that $\tilde{a}(t)$ is the minimum mean-square error estimate of a(t) given by (2-20) and (2-21). That is,

$$\tilde{a}(t) = \int_T f(t-\lambda)\, y(\lambda)\, d\lambda, \tag{B-8}$$

where

$$\int_T R_y(\lambda_1-\lambda_2)\, f(t-\lambda_2)\, d\lambda_2 = R_{ax}(\lambda_1-t), \quad \lambda_1 \varepsilon T \quad . \tag{B-9}$$

Then, using (B-7) in Equation (B-8),

$$\tilde{a}(t) = \int_T f(t-\lambda)y(\lambda)d\lambda = \int_T f(t-\lambda)d\lambda \int_T g(\tau)R_y(\tau-\lambda)d\tau$$

$$= \int_T g(\tau)d\tau \int_T f(t-\lambda)R_y(\tau-\lambda)d\lambda \quad . \tag{B-10}$$

Making use of (B-9) and then (B-5) we find

$$\tilde{a}(t) = \int_T g(\tau)\, R_{ax}(\tau-t)d\tau = \hat{a}(t). \tag{B-11}$$

Thus the minimum mean-square error estimator and the MAP estimator are the same.

APPENDIX C

EVALUATION OF THE OPTIMAL DEMODULATOR PERFORMANCE FOR SINGLE-NOTCH SELECTIVE FADING

The performance of the finite observation interval optimal demodulator was given by the error covariance matrix, (2-33).

$$\underline{\underline{\Lambda}} = \frac{1}{\sigma_a^2} \mathrm{Cov}(\underline{\hat{a}}-\underline{a}) = \frac{1}{n} \underline{\underline{\Omega}}^{-1} = \frac{1}{n} \left[\underline{\underline{H}}^{*T} \underline{\underline{\Phi}}_N^{-1} \underline{\underline{H}} + \frac{1}{n} \underline{\underline{\Phi}}_a^{-1} \right]^{-1} . \qquad \text{(C-1)}$$

For single-notch fading the channel is given by

$$H(j\omega) = h_1 + h_2 e^{-j\omega} = \frac{1 - re^{+j\omega_0} e^{-j\omega}}{\sqrt{1+r^2}} . \qquad \text{(C-2)}$$

Note that the following identities hold if we make the definition

$$\rho \triangleq |h_1 h_2^*| = \frac{-r}{1+r^2} . \qquad \text{(C-3)}$$

$$|h_1|^2 = \frac{1+\sqrt{1-4\rho^2}}{2} , \quad |h_2|^2 = \frac{1-\sqrt{1-4\rho^2}}{2} \qquad \text{(C-4)}$$

$$\left| \frac{h_2}{h_1} \right|^2 = r^2 , \qquad \text{(C-5)}$$

$$|h_1|^2 + |h_2|^2 = 1 \quad . \tag{C-6}$$

If the additive noise is assumed to be bandlimited and white, $\underline{\underline{\Phi}}_N = \underline{\underline{I}}$, it is possible to develop an analytical expression for the diagonal elements (error variances) of $\underline{\underline{\Lambda}}$. For a white message spectrum we have $\underline{\underline{\Phi}}_a^{-1} = \underline{\underline{I}}$, while for the Markov message source of Section 2.5, $\underline{\underline{\Phi}}_a^{-1}$ is the tri-diagonal matrix of Equation (2-35). In either case the matrix $\underline{\underline{Q}}$ of (C-1) is a tri-diagonal matrix of the form

$$\underline{\underline{Q}} = K \begin{bmatrix} a & c^* & \cdot & \cdot & \cdot & 0 \\ c & 1 & \cdot & & & \cdot \\ \cdot & \cdot & \cdot & \cdot & & \cdot \\ \cdot & & \cdot & \cdot & \cdot & \cdot \\ \cdot & & & \cdot & 1 & c^* \\ 0 & \cdot & \cdot & \cdot & c & b \end{bmatrix} , \tag{C-7}$$

where the parameters a, b, c, and K are identified in Table C-1.

Let us now suppose that the observation interval is of length T_0=m seconds, so that $\underline{\underline{Q}}$ is of order m+1, and is a function of m.

$$\underline{\underline{Q}} = \underline{\underline{Q}}(m) \tag{C-8}$$

Now define the following determinants of arbitrary order n.

Table C-1. Parameter Definitions for the Matrix $\underline{Q}$.

Message Source	$\underline{K}$	$\underline{a}$	$\underline{b}$	$\underline{c}$
White	$1 + \frac{1}{\eta}$	$\frac{\lvert h_2 \rvert^2 + \frac{1}{\eta}}{K}$	$\frac{\lvert h_1 \rvert^2 + \frac{1}{\eta}}{K}$	$\frac{\rho e^{j\omega_0}}{K}$
Markov ($x = e^{-\alpha}$)	$1 + \frac{1}{\eta}\frac{1+x^2}{1+x^2}$	$\frac{\lvert h_2 \rvert^2 + \frac{1}{\eta} \cdot \frac{1}{1-x^2}}{K}$	$\frac{\lvert h_1 \rvert^2 + \frac{1}{\eta}\frac{1}{1-x^2}}{K}$	$\frac{\rho e^{j\omega_0} - \frac{1}{\eta}\frac{X}{1-x^2}}{K}$

$$A(n) = \det\begin{bmatrix} a & c^* & & & 0 \\ c & 1 & \ddots & & \\ & \ddots & \ddots & \ddots & \\ & & \ddots & 1 & c^* \\ 0 & & & c & 1 \end{bmatrix} \tag{C-9}$$

$$B(n) = \det\begin{bmatrix} 1 & c^* & & & 0 \\ c & 1 & \ddots & & \\ & \ddots & \ddots & \ddots & \\ & & \ddots & 1 & c^* \\ 0 & & & c & b \end{bmatrix} \tag{C-10}$$

$$D(n) = \det\begin{bmatrix} 1 & c^* & & & 0 \\ c & 1 & \ddots & & \\ & \ddots & \ddots & \ddots & \\ & & \ddots & 1 & c^* \\ 0 & & & c & 1 \end{bmatrix} \tag{C-11}$$

Then, using elementary row operations, the following recursion formulas involving these determinants may be derived.

$$\begin{aligned} \det \underline{Q}(m) &= K^{m+1}[a\, B(m) - |c|^2\, B(m-1)] \\ &= K^{m+1}[b\, A(m) - |c|^2\, A(m-1)] \end{aligned} \tag{C-12}$$

$$A(n) = a\, D(n-1) - |c|^2\, D(n-2), \quad A(0) = 1, \quad A(1) = a. \tag{C-13}$$

$$B(n) = b\, D(n-1) - |c|^2\, D(n-2), \quad B(0) = 1, \quad B(1) = b. \tag{C-14}$$

$$D(n) = D(n-1) - |c|^2\, D(n-2), \quad D(0) = 1, \quad D(1) = 1. \tag{C-15}$$

Also, the i^{th} diagonal cofactor of the matrix $\underline{Q}(m)$ can be seen to be

$$K^m \, A(i-1) \, B(m-i+1), \tag{C-16}$$

so that Cramer's rule may be applied to evaluate the diagonal elements of $\underline{\underline{\Lambda}}$.

$$[\underline{\underline{\Lambda}}]_{ii} = \frac{1}{\eta} \cdot \frac{K^m \, A(i-1) \, B(m-i+1)}{\det \underline{\underline{Q}}(m)}$$

$$= \frac{1}{K\eta} \cdot \frac{A(i-1) \, B(m-i+1)}{a \, B(m) - |c|^2 \, B(m-1)} \tag{C-17}$$

Both A(n) and B(n) in (C-17) are given in terms of D(n), so we seek a closed-form solution for D(n). Examination of (C-15) reveals that D(n) is the solution to a second order, linear, homogeneous difference equation which may be solved by standard techniques[1] subject to the initial conditions which are given.

$$D(n) = \frac{(1+\sqrt{1-4|c|^2})^{n+1} - (1-\sqrt{1-4|c|^2})^{n+1}}{2^{n+1}\sqrt{1-4\,c^2}} \tag{C-18}$$

Thus the error variances for the optimal demodulator are explicitly determined as functions of the observation interval.

In Chapter 3 it is desirable to find the performance of the optimal demodulator as the noise goes to zero ($\eta \to \infty$).

---

[1] Van Der Pol, B., H. Bremmer, Operational Calculus, Cambridge University Press, London, 1964, Chapter 13.

In particular, we are interested in the $(m+1)^{st}$ diagonal element of $\underline{\underline{\Lambda}}$, which, by (C-17), can be written

$$[\underline{\underline{\Lambda}}(m)]_{m+1,\ m+1} = \frac{1}{K\eta} \cdot \frac{A(m)}{a\ B(m) - |c|^2 B(m-1)}$$

$$= \frac{1}{K\eta} \cdot \frac{a\ D(m-1) - |c|^2\ D(m-2)}{ab\ D(m-1) - (a+b)|c|^2 D(m-2) + |c|^4 D(m-3)} \qquad \text{(C-19)}$$

After considerable manipulation, and using (C-15), it can be shown that

$$[\underline{\underline{\Lambda}}(m)]_{m+1,\ m+1} = \frac{1}{K\eta} \cdot \frac{D(m) - K_1(\eta)\ D(m-1)}{\frac{1}{K\eta} \cdot [D(m) - K_2(\eta)\ D(m-1)]}$$

$$= \frac{1 - K_1(\eta)\ \frac{D(m-1)}{D(m)}}{1 - K_2(\eta)\ \frac{D(m-1)}{D(m)}} \ , \qquad \text{(C-20)}$$

where $K_1(\eta)$ and $K_2(\eta)$ are functions of η with the assymptotic forms below.

$$\lim_{\eta\to\infty} K_1(\eta) = |h_1|^2 \qquad \text{(C-21)}$$

$$\lim_{\eta\to\infty} K_2(\eta) = \begin{cases} 0 \ , \text{ White message} \\ \frac{x}{1-x^2}\left[x+2\rho\,\text{Cos}\omega_0\right], \text{ Markov Message} \end{cases} \qquad \text{(C-22)}$$

Using (C-18), (C-3) through (C-5), and Table C-1 we obtain the following:

$$\lim_{\eta\to\infty} \frac{D(m-1)}{D(m)} = 2 \cdot \frac{(1+\sqrt{1-4\rho^2})^m - (1-\sqrt{1-4\rho^2})^m}{(1+\sqrt{1-4\rho^2})^{m+1} - (1-\sqrt{1-4\rho^2})^{m+1}} \tag{C-23}$$

$$= \frac{1}{|h_1|^2} \cdot \frac{1 - \left|\frac{h_2}{h_1}\right|^{2m}}{1 - \left|\frac{h_2}{h_1}\right|^{2(m+1)}} = \frac{1}{|h_1|^2} \frac{1 - r^{2m}}{1 - r^{2(m+1)}}$$

Thus, for the white message source we have

$$\varepsilon_w^2(m) \triangleq \lim_{\eta\to\infty} [\underline{\underline{\Lambda}}]_{m+1,m+1} = 1 - \frac{1 - r^{2m}}{1-r^{2(m+1)}} \tag{C-24}$$

$$= (r^2)^m \frac{1 - r^2}{1 - (r^2)^{m+1}}$$

while, for the Markov message source, the mean square error is

$$\varepsilon_M^2(m) \triangleq \lim_{\eta\to\infty} [\underline{\underline{\Lambda}}]_{m+1,m+1} = \frac{\varepsilon_w^2(m)}{1 + \frac{x}{1-x^2}\left[x+2\rho\cos\omega_0\right]\left[1-\varepsilon_w^2(m)\right]} . \tag{C-25}$$

The subscripts w and M stand for white and Markov message sources respectively. If the observation interval, $T_0 = m$, is sufficiently large, then the mean square error for the white message, $\varepsilon_w^2(m)$, will be small,

$$\varepsilon_w^2(m) << 1 \quad ,$$

so that the error for the Markov message is approximately

$$\varepsilon_M^2(m) \doteq \frac{\varepsilon_W^2(m)}{1 + \frac{x}{1-x^2}\left[x + 2\rho \cos\omega_0\right]} \qquad \text{(C-26)}$$

Thus there is an improvement or degradation in the Markov message case relative to the case of a white message: this factor is seen to depend upon the fading depth (through ρ), and upon the placement of the fading notch, ω_0, but is independent of the observation interval.

APPENDIX D

PN SEQUENCES WITH SMALL APERIODIC AUTOCORRELATION

Table D-1 is a listing of that cyclic permutation of a PN sequence of length T_s (given in the left-hand column) which has the smallest possible out-of-phase autocorrelation in the vicinity of the origin of the delay axis. Table D-2 gives the corresponding autocorrelation values. Note that for the longer sequences the autocorrelation is essentially zero (relative to the peak, hence near-optimal for channel measurement. Consequently, it is possible to make long, aperiodic channel measurements with easily-generated constant envelope signals and achieve very nearly optimal performance.

Table D-1. List of Aperiodic Pseudo-Noise (PN) Sequences.

7	++--	+-										
11	+-++-	+++--	-									
15	++++-	--+--	++-+-									
19	++-++	--+++	+-+-+	----								
23	-+-++	--++-	-+-+-	---++	+++							
31	--++-	+--+-	---+-	+-+++	-++--	-++++	+					
35	+++--	-++++	+-+++	--+--	--+-+	-++--	+--+-					
43	++-+-	++-++	--+-+	--+++	-++++	+---+	-+++-	----+	---			
47	--+-+	-+++-	-+---+	+-++-	--+-+	-++--	--+--	---++	++-++	++		
59	++-++	-+-+-	--+--	+-+++	-+-+-	-+--+	++-++	++--+	++++-	----+	+----	+---
63	++++- -+-	-+-+-	--++-	---+-	----+	+++++	-+-+-	++--+	+-+++	-++-+	--+--	+++--
67	----- -+++-	-+-+- ++	---++	+--++	-+-++	--+--	+-+--	++---	++++-	+-+++	+++--	+---+
71	---++ --++-	+-+-- +-++-	+-+-- +	+++--	-+--+	+-+--	-+---	----+	+++++	-+++-	+--++	-+++-
79	+++++ --++-	+-++- ++--+	---++ +++-+	---+- --+-	+-+-+	-+++-	-++++	--+--	----+	-++-+	----+	+--+-
83	+++++ -++--	++-+- +-+++	-+++- +---+	++--+ +---+	---++ -+-	-+---	----+	-+-++	+--++	+----	+-++-	-+--+

Table D-2. Aperiodic Autocorrelation Functions for PN Sequences.

T_s	$R_s(0)$	$R_s(1)$	$R_s(2)$	$R_s(3)$	$R_s(4)$	$R_s(5)$	$R_s(6)$	$R_s(7)$	$R_s(8)$	$R_s(9)$	$R_s(10)$
7	+7	+0	-1	+0	-1	+0	-1				
11	+11	0	-1	0	-1	0	-1	0	-1	0	-1
15	+15	0	-1	0	-1	-4	-1	-2	+1	0	+3
17	+17	0	+1	0	+1	0	-1	0	-3	0	-1
23	+23	0	-1	0	-1	-2	-3	0	-3	-2	+3
31	+31	0	+1	0	-1	0	-3	-4	-1	+2	+3
35	+35	0	-1	0	-1	0	-1	0	-1	-2	-1
43	+43	0	+1	0	-1	-2	+3	0	+3	0	-1
47	+47	0	+1	0	+1	-2	-1	+2	-3	0	-5
59	+59	0	+1	0	-1	0	+3	0	-1	+2	-5
63	+63	0	-1	0	+1	0	+1	0	-7	-2	-3
67	+67	0	+1	0	+1	+2	+3	0	+1	+2	-3
71	+71	0	-1	0	-1	0	-1	-2	-3	+2	+1
79	+79	0	-1	0	+1	0	+1	-2	+1	-4	-7
83	+83	0	-1	0	-1	0	+1	+2	-1	+2	-3